MULTIPLE EXPRESSED ISOFORMS OF TIN2 COOPERATE WITH TPP1/POT1 TO STIMULATE TELOMERASE PROCESSIVITY IN HUMAN CELLS

by
Alexandra Mims Pike

A dissertation submitted to Johns Hopkins University in conformity with the requirements for the degree of Doctor of Philosophy

Baltimore, Maryland

September 2017

ABSTRACT

Telomere length maintenance is critical for cells that divide many times. Disrupting telomere length equilibrium causes short telomere syndromes, characterized by stem cell failure causing age-related degenerative disease, or cancer, a disease characterized by unregulated cell growth. Mammalian telomeres are bound by a six-membered shelterin complex. Mutations in the gene encoding shelterin protein TIN2 have been identified in patients with short telomere syndromes. Understanding the mechanism of disease these patients has been challenged by incomplete understanding of how TIN2 regulates telomere length in normal cells.

Because TIN2 has two known isoforms, we asked whether the isoforms have different roles in the cell. Using CRISPR/Cas9 genomic editing, we incorporated an epitope tag at the endogenous TIN2 gene and found a new isoform. Using 3'RACE and PacBio SMRT-sequencing we identified this third isoform, TIN2M, that retains the last intron and is expressed across human cell types. We found that all three TIN2 isoforms localize to telomeres, but have different effects on telomere length as measured by Southern blot.

Then, we asked whether TIN2 could regulate telomere length through interactions with TPP1, which is part of the TPP1/POT1 telomerase processivity complex. We adapted a cell-based system to test TIN2's effects on telomerase using a direct telomerase activity assay. Surprisingly, we found that TIN2 cooperates with TPP1/POT1 to stimulate telomerase processivity. All three TIN2 isoforms were able to stimulate telomerase processivity above previously observed TPP1/POT1 stimulation. TIN2 did not stimulate

telomerase in the absence of TPP1/POT1 or in the presence of TPP1 TEL-patch mutants that do not stimulate telomerase, suggesting TIN2 functions with TPP1/POT1. Preliminary data also suggests that the patient with TIN2 mutations do not stimulate telomerase.

We conclude that TIN2 is part of a heterotrimeric shelterin subcomplex with TPP1/POT1, and that TIN2/TPP1/POT1 plays an important role in binding single-stranded telomeric DNA and stimulating telomerase. We discuss these findings in the context of recent advances in understanding the telomerase holoenzyme, including a possible mechanism for coupling telomerase with lagging strand DNA replication. We propose that uncoupling these two activities causes telomere shortening independent of that observed in the absence of telomerase activity.

Thesis Advisor: Carol W. Greider, Ph.D.
Daniel Nathans Professor and Director
Department of Molecular Biology and Genetics
Johns Hopkins University School of Medicine

Thesis Reader: Andrew Holland, Ph.D.
Assistant Professor
Department of Molecular Biology and Genetics
Johns Hopkins University School of Medicine

ACKNOWLEDGEMENTS

This work described here would not have been possible without the academic support, camaraderie, motivation, and overall positive energy in the "Blue, Yellow, & Red" labs. I would specifically like to thank Dr. Carol Greider for her unparalleled mentorship throughout this journey. Carol, in her calm leadership, guided me through technical challenges and unexpected results and did not let me lose sight of my goals. Carol has a unique scientific intuition and methodical approach to answering scientific questions that I hope to have absorbed during this time.

I would also like to thank Margaret Strong for her help with cell culture, TIN2 immunofluoresence experiments, lab management, jokes and sarcasm, cupcakes, and raspberry tarts. I would like to thank Carla Connelly for countless isotope orders, helping me piece together protocols, watching out for me like a daughter, and cupcakes and candy.

Several other key players helped with the experiments described here: Jon Alder, who initiated the CRISPR tagging of TIN2 among many other thoughtful conversations; Dr. Sarah Wheelan and John Paul Ouyang for help with the PacBio experiments; our collaborators Dr. Debbie Wuttke and Leslie Glustrom who provided the recombinant TIN2L and helpful discussions about telomeric single-stranded binding proteins; Cate Kiefe who taught me useful scientific graphic design guidelines.

I would like to acknowledge my baymate Becca Keener for the time spent sharing stories, troubleshooting experiments, planning weddings, etc. She certainly has motivated me to work harder, and has helped me through the melon-collie times. I still do not think people realize how serious we are about starting our own lab across the hall. Also a

special thanks to Stella and Stevie, the true OG's of my time in the Greider Lab, for many coffee breaks and KBBQ outings and great friendship. And of course to Kiki and Calliekins, for keeping us young and social.

Our tight-knit "sixth floor family" of the Armanios and Holland labs fostered an idealized community to conduct research and grow as a graduate student. Between joint group meetings, social gatherings, and late night conversations in the hallway, I could not have asked for a better group to brainstorm and troubleshoot with. I would also like to thank the administrative staff of the MBG department for all of their work and friendship over the years. I would like to thank the graduate program in Cellular and Molecular Medicine and the close friends that I made during my time at Johns Hopkins.

I would like to thank my family for their support of the past six years, especially my parents especially for encouraging curiosity and creativity in my approach to the world and my Yiayia for the inspiration, encouragement, and shipments of koulourakia. Finally, I would like to thank my husband Pike for the support and motivation throughout this journey.

Table of Contents

List of Figures

Chapter 1. Introduction

1.1 Telomeres

Telomeres are protective nucleoprotein structures at the ends of linear chromosomes. They are named from the Greek words *τελος* (end) and *μερος* (part) (Muller 1938). Telomeres were first described as the end parts of chromosomes that serve a protective function distinct from broken or otherwise non-natural DNA ends (Muller 1938; McClintock 1941). They also serve to counteract sequence loss due to the end replication problem, which is the inability of the DNA replication machinery to fully replicate linear DNA all the way to the end (Watson 1972; Olovnikov 1973)

Different organisms have evolved different methods for protecting and maintaining the linear ends of DNA ends. Viruses with linear genomes use special secondary structures or end-terminal DNA binding proteins to achieve full replication of their genomic DNA. Most eukaryotes, such as *Tetrahymena,* budding and fission yeast, and vertebrates, have repetitive G-rich telomeres that are maintained by a unique reverse transcriptase enzyme called telomerase (Blackburn 1990). Some insects, such as *Drosophila,* use transposons to maintain and elongate telomeres (Casacuberta 2017)

Human telomeres consist of roughly 8 kilobases of double-stranded TTAGGG repeats, with a single-stranded 3' overhang of approximately 100 nucleotides. The telomere is bound by six telomere specific proteins, known collectively as shelterin: TRF1, TRF2, POT1, TIN2, TPP1, and Rap1 (Figure 1.1). Telomeric repeat-binding factor 1 (TRF1) and Telomeric repeat-binding factor 2 (TRF2) bind double-stranded telomeric DNA (Zhong et al. 1992; Bilaud et al. 1997; Bianchi et al. 1997; Broccoli et al. 1997). TRF1 and TRF2 are both homodimers that specifically bind two adjacent

telomeric sequence motifs. Protection of telomeres protein 1 (POT1) specifically binds to telomeric single-stranded DNA (Baumann & Cech 2001; Baumann et al. 2002). The proteins TPP1 (previously TINT1/PTOP/PIP1), TRF1-interacting factor 2 (TIN2), and Repressor/Activator protein 1 (Rap1) bind telomeres specifically through interactions with TRF1, TRF2, or POT1 (Ye, Donigian, et al. 2004; Liu, Safari, et al. 2004; Ye, Hockemeyer, et al. 2004). TPP1 has been shown to form a heterodimer with POT1 (Wang et al. 2007; Li & de Lange 2003), and Rap1 interacts with the TRFH domain of TRF2. TIN2 binds directly to TRF1 and TRF2 as well as TPP1.

The shelterin proteins have been shown to have roles in both telomere end protection by suppressing the DNA damage response and in telomere length regulation by both positively and negatively regulating telomerase activity at the telomere (Palm & de Lange 2008).

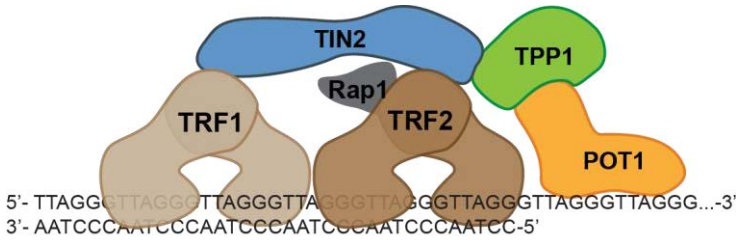

Figure 1.1 Shelterin
Mammalian telomeres are TTAGGG repeats bound by the six-membered shelterin complex, consisting of TRF1, TRF2, POT1, TPP1, TIN2, and Rap1.

1.2 Telomere Length Equilibrium

Telomere length is maintained around a median equilibrium length. The median telomere length is specific for the organism. For example, while human telomeres are distributed around 8 kilobases, *Saccharomyces cerevisiae* telomeres have a median length

of about 300 base pairs. Telomere shortening during cell division is counteracted by the enzyme telomerase in a regulated process that maintains the telomere length distribution.

Telomeres shorten by approximately 50bp each time a cell divides due to the end replication problem (Harley et al. 1990) (Figure 1.2A). While this is typically described as the inability to copy the last bit of DNA after the RNA primer is removed from the lagging strand, further sequence loss could result from the placement of the last Okazaki fragment or from replication fork collapse. Because the telomeric sequence is repetitive and noncoding, this sequence loss is likely tolerated. However, if telomeres get too short, they lose their protective function and trigger a DNA damage response. Ultimately, without a way to restore telomere length, cells undergo senescence or apoptosis.

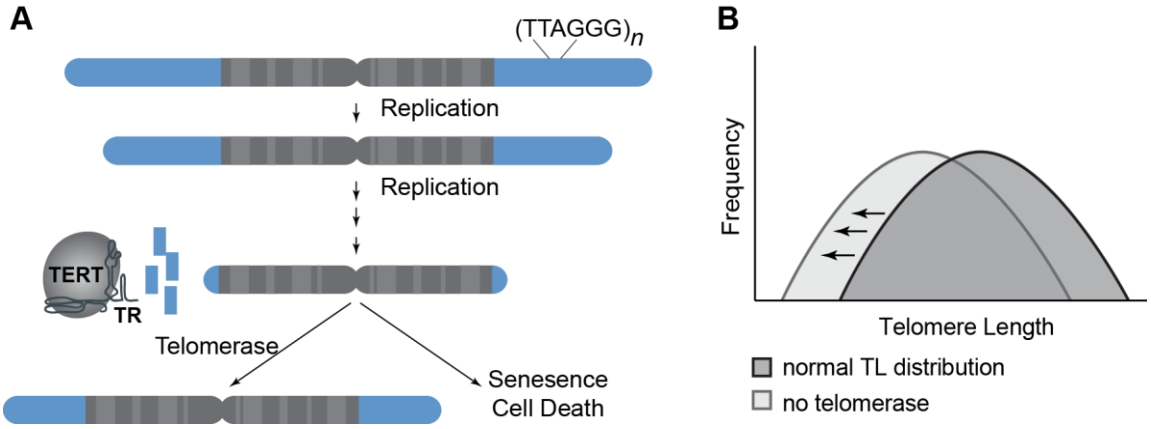

Figure 1.2. Telomere Length Equilibrium.
(**A**) Telomeres shorten with every round of cell division. Telomerase adds telomere repeats to maintain telomere length and allow for further cell division. (**B**) Absence of functional telomerase shifts the telomere length equilibrium leading to an increase in critically short telomeres that contribute to pathogenesis.

The enzyme telomerase contains a reverse transcriptase, TERT, and an RNA component, TR (Greider & Blackburn 1985; Greider & Blackburn 1989). Telomerase counters the telomere shortening in dividing cells by adding telomere repeats to the 3' end using a template region of the TR component to align and copy telomere repeats.

Telomerase levels are highly regulated, with expression restricted to about 100-250 copies per cell (Xi & Cech 2014). Telomere proteins both positively and negatively regulate access of telomerase to the telomere and modulate its activity. Telomere elongation occurs in late S-phase, and telomerase recruitment and activity are regulated by many different post-translational modifications (Vogan & Collins 2015). Finally, telomerase shows a slight preference for adding to shorter telomeres over longer telomeres (Hemann et al. 2001; IJpma & Greider 2003).

There are still many unanswered questions about what determines the telomere length equilibrium set point and how telomerase maintains telomeres within this telomere length distribution. The need for telomere length regulation is underscored by the consequences of shifting the telomere length equilibrium (Figure 1.2B). Telomere shortening leads to senescence, apoptosis, and short telomere diseases, while continuous telomere lengthening allows the growth of cancer cells.

1.3 Telomere length and human health

Telomere length regulation sets a balance between unregulated cell growth and age related degenerative diseases (Stanley & Armanios 2015). An increased understanding of the biology underlying inherited forms of telomere syndromes has advanced our understanding of telomerase and telomere length regulation. Both cancer and short telomere syndromes can be traced back to changes in the telomere length equilibrium.

One hallmark of cancer is the ability of cells to divide indefinitely, also known as replicative immortality. To achieve this, a cell must find a way to maintain its telomeres, and over 90% of human cancers do this by activating telomerase (N. W. Kim et al. 1994).

Also, certain genetic variants that lead to telomere elongation cause predisposition to familial melanoma and other cancers (Robles-Espinoza et al. 2014; Trigueros-Motos 2014; Shi et al. 2014).

Short telomere syndromes are a clinically heterogeneous collection of diseases that share the common etiology of short telomeres. The short telomeres in these patients cause defects in tissue renewal, leading to disease in a variety of different tissues. These diseases include both common diseases of pulmonary fibrosis and liver fibrosis and rare diseases such as Dyskeratosis Congenita and Hoyeraal-Hreidarsson syndrome. While these diseases are often fatal due to bone marrow failure or pulmonary fibrosis, patients may also have abnormal skin pigmentation, premature hair graying, liver cirrhosis, gastrointestinal issues, and problems in other tissues.

1.4 Mutations in many different genes cause short telomere syndromes

Mutations in thirteen different genes have been identified to cause short telomere disease. The TERT and TR components of telomerase can be independently mutated in short telomere patients. Mutations in other factors involved in the processing and stability of telomerase RNA have also been found, including Dyskerin, NHP2, NOP10, Gar1, and Naf1 (Mary Armanios & Blackburn 2012). TCAB mutations also affect telomere length through disrupting telomerase trafficking from Cajal bodies. Mutations in two shelterin proteins, TIN2 and TPP1, as well as telomere replication factors RTEL1 and CST subunits, have also been identified in short telomere patients. These mutations are generally autosomal dominant and exhibit Mendelian inheritance (Nelson & Bertuch 2012). Because both the mutation and the parental telomere lengths are inherited, the disease often shows genetic anticipation, where progressive telomere shortening increases

the severity of the disease over multiple generations (Hao et al. 2005; Armanios et al. 2005; Savage & Bertuch 2010).

TIN2 was the first shelterin protein found to cause Dyskeratosis Congenita (DC) (Savage et al. 2008). Single base substitutions or deletions causing missense or nonsense mutations in the protein cause rapid telomere shortening in a single generation (Walne et al. 2008; Sasa et al. 2012). TIN2 mutations have also been identified in other telomere disease such as pulmonary fibrosis (Alder et al. 2014) (Figure 1.3). Patient mutations also cluster to a domain of unknown function, and understanding how these mutations cause short telomere disease has been challenging.

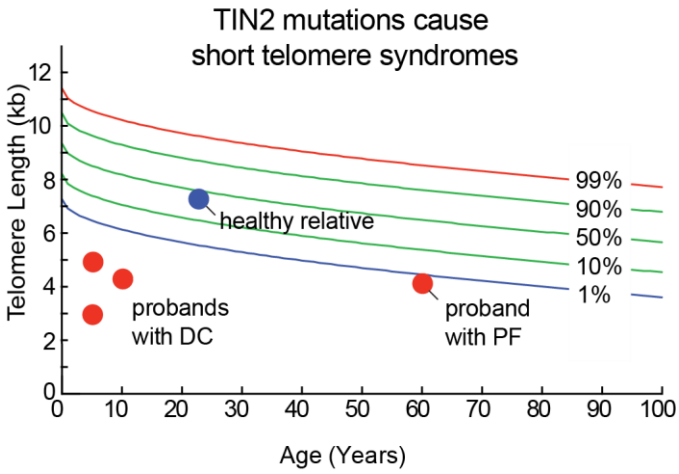

Figure 1.3. TIN2 mutations cause short telomere syndromes.
A telogram shows the percentiles for normal telomere lengths in the human population. Most TIN2 patients (red circles) present as children with severe telomere shortening (<<1%ile) with healthy, unaffected relatives. Other TIN2 mutations have been identified in older patients with pulmonary fibrosis.

After identification of TIN2 mutations in Dyskeratosis Congenita patients, other shelterin components have been identified in related diseases. Mutations in TPP1 were identified in Hoyeraal-Hreidarsson (Kocak et al. 2014; Guo et al. 2014), and several cases of Coats Plus have been linked to POT1 mutations (Takai et al. 2016). Interestingly,

different mutations in TPP1 or POT1 are linked to long telomeres in certain familial cancer syndromes (Shi et al. 2014; Robles-Espinoza et al. 2014; Trigueros-Motos 2014; Aoude et al. 2015). The complexity of the genetics underscores TPP1 and POT1 as important regulators of telomere length in humans.

1.5 Shelterin Regulation of Telomere Length

The shelterin proteins serve several roles, including preventing telomeric DNA damage response, helping with telomere replication, and regulating telomerase access to the telomere. The roles of these proteins in telomere length regulation is accepted, but not much is known about the mechanism through which they regulate telomere length.

1.5.1 TRF1, TRF2, and Rap1

Double-stranded telomere binding proteins have roles in regulating telomere length maintenance. In humans, TRF1 and TRF2 specifically bind telomeric double-stranded DNA (Zhong et al. 1992; Broccoli et al. 1997; Bianchi et al. 1999). TRF1 and TRF2 each have a single Myb-like DNA binding domain, and they each form a homodimer that contacts DNA with the two adjacent subunits. Each TRF protein also has a homodimerization domain, TRFH, which serves as a docking site for TIN2 and other proteins that interact with TRF1 and TRF2 (Fairall et al. 2001; Chen et al. 2008). Interestingly, in *Saccharomyces cerevisiae*, *Sc*Rap1 is not a homolog of TRF1 or TRF2 but contains two Myb domains and binds double-stranded telomeric DNA as a monomer. Rap1 is conserved in humans but has lost its DNA binding domains, instead interacting with telomeres through TRF2.

TRF1 overexpression results in progressive telomere shortening, while overexpression of a dominant-negative TRF1 that cannot bind DNA causes telomere

elongation (van Steensel & de Lange 1997; Smogorzewska et al. 2000). Similarly, TRF2 overexpression causes telomere shortening over time, but neither TRF1 nor TRF2 appear to have a direct effect on telomerase activity (Smogorzewska et al. 2000).

TRF2 deletion triggers an ATM- and p53-mediated DNA damage response and chromosome end fusions (Karlseder et al. 1999; Denchi & de Lange 2007), while TRF1 deletion leads to an ATR-mediated DNA damage response (Sfeir et al. 2009). These observations have led TRF1 and TRF2 to be described as repressors of ATM and ATR, respectively, but it should be noted that these two DNA damage signaling pathways may not be actively suppressed, but rather activated upon removal of these proteins. Indeed, telomerase elongation in cells requires ATM kinase, so telomere elongation may depend on balancing signals from these different proteins (Lee et al. 2015; Tong et al. 2015).

Rap1 function in human cells is poorly understood compared to its homolog in yeast. While Rap1 overexpression causes telomere elongation (Li et al. 2000) and certain Rap1 deletion constructs alter telomere length heterogeneity in cells (Li & de Lange 2003), it does not appear to have an important role in mammalian telomeres. Deletion of Rap1 does not cause any telomere dysfunction or telomere length effects, and it is thought to serve largely non-telomeric functions as a transcription factor in human cells (Kabir et al. 2014).

1.5.2 TPP1 and POT1

TPP1/POT1 form a heterodimer that functions as a telomerase processivity factor and is also important for telomere end protection in cells. POT1 binds the telomeric single-stranded DNA (ssDNA) footprint TAGGGTTAG using its two N-terminal OB fold domains (Loayza et al. 2004) (Figure 1.4). Overexpression of POT1 does not lead to

major telomere length changes, while overexpressing the POT1ΔOB1 construct that cannot bind DNA causes telomere elongation (Loayza & de Lange 2003). Additionally, shRNA knock-down of POT1 leads to increased γ-HRAX foci in cells (Hockemeyer et al. 2005). Deletion of POT1a and POT1b in mice also leads to increased γ-H2AX foci in cells as well as an increased frequency of chromosome fusions and single-stranded telomeric DNA (Hockemeyer et al. 2006). TPP1 uses an internal POT1-binding domain (PBD) to interact with the POT1 C-terminal OB-fold, and this interaction is important for TPP1/POT1 function in cells (Figure 1.4).

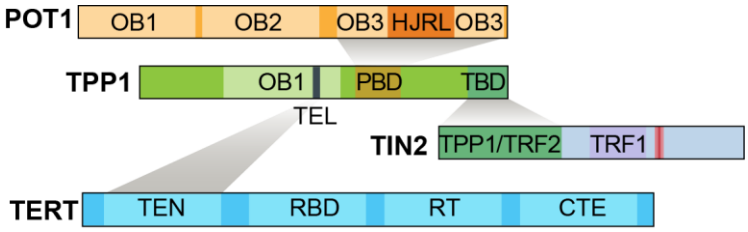

Figure 1.4 Schematic of POT1—TPP1—TIN2 and TERT.
Schematics of proteins outlining the structural and functional domains. Grey boxes mark the interacting domains between the depicted proteins. OB, OB-fold; HJRL, Holliday junction resolvase-like domain; PBD, POT1-binding domain; TBD, TIN2-binding domain. TEN, telomerase essential amino-terminal; RBD, RNA binding domain; RT, reverse transcriptase; CTE, C-terminal extension.

TPP1 also has a TPP1 glutamate (E) and leucine (L)-rich domain (TEL-patch) in its OB-fold domain that directly interacts with the telomerase essential amino-terminal (TEN) domain (Nandakumar et al. 2012; Sexton et al. 2012; Zhong et al. 2012) (Figure 1.4). The TEL-patch/TEN domain interaction is important for both telomerase recruitment and stimulation. TPP1/POT1 is thought to stimulate telomerase processivity by preventing telomerase dissociation from the single-stranded telomeric DNA, thereby promoting translocation and processive telomere elongation (Latrick & Cech 2010). TIN2 interacts with the TPP1 C-terminal domain and this interaction is essential for the

function of TPP1/POT1 in cells (David Frescas & de Lange 2014a; Takai et al. 2011; Abreu et al. 2010; Frescas & De Lange 2014) (Figure 1.4).

Short telomere patients have been identified with a TPP1 ΔK170 mutation that deletes one residue from the TEL-patch, deforming the TEN domain binding interface and disrupting the TPP1-telomerase interaction (Kocak et al. 2014; Bisht et al. 2016). This leads to decreased telomerase association with telomeres and decreased telomerase processivity. A POT1 S322L mutation in Coats Plus is thought to cause short telomeres through defective telomere replication, but the mechanism for this is unclear (Takai et al. 2016).

While the biochemical interactions of TPP1/POT1 with telomeric DNA and telomerase are fairly well understood *in vitro*, the *in vivo* regulation of telomerase has been challenging to study. Most of the information about telomere length regulation in human cells has been studied by knock-down/knock-out or overexpression studies of different shelterin proteins followed by measurement of telomere length changes. Telomere binding proteins are ubiquitously expressed, but typically at low levels. Disrupting the protein levels may change telomere length by disrupting stoichiometry and protein localization, rather than identifying a true mechanism of telomere length regulation. For example, both TPP1 and POT1 were initially identified as negative regulators of telomere length through knock-down and overexpression studies, but TPP1/POT1 acts as a processivity factor in vitro. For further discussion, see Chapter 2.

1.5.3 TIN2

TIN2 is encoded by the *TINF2* gene on chromosome 14. The TIN2 protein is required for TPP1/POT1 localization and telomere end-protection and has been described

as a molecular bridge between the dsDNA- and ssDNA- binding shelterin proteins. TIN2 is expressed as two isoforms, TIN2S and TIN2L, but most of the research on TIN2 has been performed in the shorter isoform TIN2S, which was described first. TIN2L contains all 354 amino acids of the TIN2S sequence, with an additional 97 C-terminal amino acids, and it has been described as being associated with the nuclear matrix (Kaminker et al. 2009) (Figure 1.5).

TIN2S was initially discovered as a TRF1 interacting factor through a yeast two-hybrid screen (Kim et al. 1999). An internal region of TIN2 contains the sequence FxLxP, a TRF1-interaction motif that binds directly with the TRF1 homodimerization (TRFH) domain (Chen et al. 2008). It was later observed that TIN2 also interacts with TRF2 (Kim et al. 2004; Ye, Donigian, et al. 2004) and TPP1 (Ye, Hockemeyer, et al. 2004; Houghtaling et al. 2004) (Figure 1.5). TIN2 is required for assembly of shelterin and its localization to the telomere (O'Connor et al. 2006; Kim et al. 2008; Ye, Donigian, et al. 2004; Liu, O'Connor, et al. 2004). Removal of TIN2 by shRNA or Cre-mediated TIN2 deletion coincides with a loss of telomeric TRF1, TRF2, TPP1, and POT1 staining by immunofluoresence (Kim et al. 2004; Ye, Donigian, et al. 2004; Takai et al. 2011; David Frescas & de Lange 2014a). Disrupting shelterin localization then leads to a telomeric DNA damage response and cell death. TIN2 knock-out mice have been created, and while the heterozygous mice are viable, the TIN2 homozygous deletion is embryonic lethal (Chiang et al. 2004). Interestingly, no other information has been reported about the telomere length effects in the heterozygous mice.

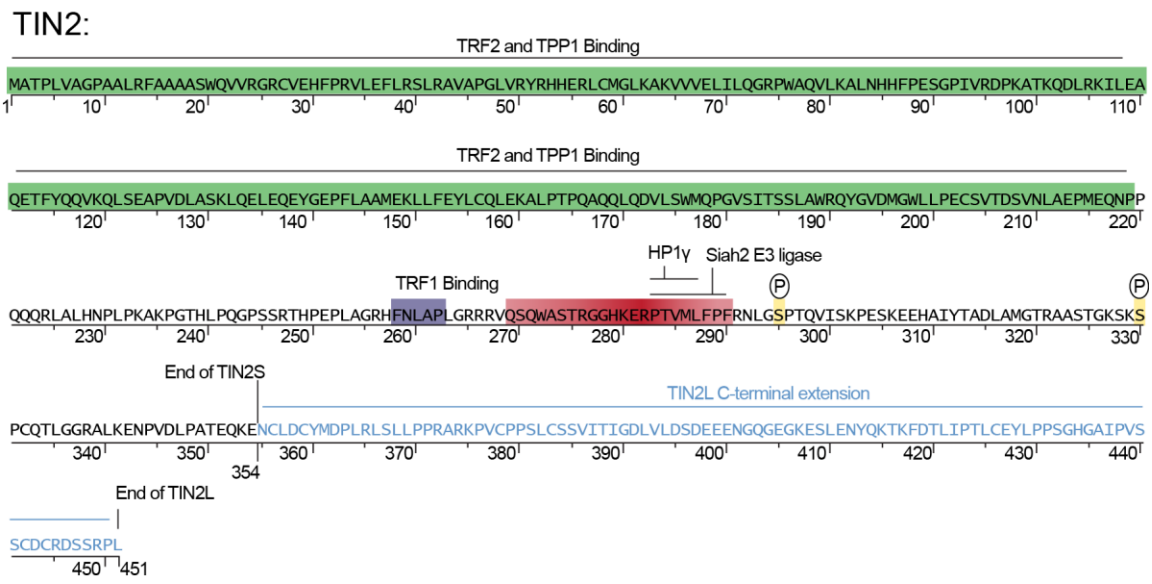

Figure 1.5 TIN2 amino acid sequence.
The patient mutation cluster is marked with red, and the gradient indicates the disease severiy associated with that position. Green = TRF2 and TPP1 binding domain; Purple = TRF1 binding motif; Yellow = phosphorylation sites. Other binding motifs are indiated with text. Blue = TIN2L C-terminal extension, the 97 residues found in TIN2L but not TIN2S.

TIN2 has also been shown to interact with several other factors that may be important for its function at the telomere. TIN2 protects TRF1 from poly(ADP-ribosyl)ation by tankyrase1, a modification that destabilizes the TRF1-DNA interaction (Ye & de Lange 2004). Additionally, TIN2S has also been shown to interact with heterochromatin protein 1-gamma (HP1γ) through the sequence 283-PTVML-287, which is a canonical PxVxL HP1-binding motif (Canudas et al. 2011). This interaction domain is within the patient mutation cluster and has been proposed to be important for sister telomere cohesion. An overlapping binding site, 283-PTVMLFP-289, interacts with the ubiquitin ligase Siah2, which ubiquitinylates TIN2 and targets it for degradation (Bhanot & Smith 2012). Interestingly, post-translational depletion of TIN2 by 65% did not destabilize TRF1 and TRF2 localization, but did lead to loss of telomeric TPP1 foci in over 90% of the cells scored by immunofluorescence. Mitotic phosphorylation of TIN2

at S295 and S333 by RSK2 has also been demonstrated, but the consequences of this modification are not clear (Yang & Counter 2013).

TIN2 has been referred to as a negative regulator of telomere length based on results from knockdown and overexpression experiments. Overexpression of TIN2S in telomerase positive cells led to a slight repression of telomere elongation (Kim et al. 1999; Yang et al. 2011). N-terminal truncation of the first 196 amino acids in the TIN2-13 construct caused rapid telomere elongation (Kim et al. 1999; Yang et al. 2011). This was interpreted as alleviation of TIN2 repression of telomere elongation. The TIN2 N-terminus was later found to contain the TRF2- and TPP1-interaction domain (Kim et al. 2004; Houghtaling et al. 2004). Similarly, deletion of the TPP1 TIN2-binding domain abolishes TPP1 telomeric localization and causes telomere elongation in telomerase positive cells (Houghtaling et al. 2004; O'Connor et al. 2006). These results also mimic the loss of POT1 telomeric localization (see previous section and Chapter 2.3). It is increasingly clear that TIN2 is required for TPP1/POT1 localization and function at telomeres (Takai et al. 2011; David Frescas & de Lange 2014a; Abreu et al. 2010).

Based on the classification of TIN2 as a negative regulator of telomere length, it was surprising to find *TINF2* mutations that cause short telomere disease. The patient mutations are mostly single base changes that result in missense or nonsense mutations in the protein, and they all cluster in a domain of unknown function in exon 6 (Savage et al. 2008; Walne et al. 2008; Sasa et al. 2012). Mutations in this cluster often cause rapid telomere shortening in one generation, which is striking compared to other short telomere disease mutations that cause gradual telomere shortening over multiple generations (Walne et al. 2008; M Armanios & Blackburn 2012) (Figure 1.3 &1.5).

Interestingly, the TIN2 patient mutations do not seem to disrupt interactions with its binding partners TRF1, TRF2, or TPP1 when tested by co-immunoprecipitation of overexpressed TIN2S and the respective binding partners (Yang et al. 2011; Xin & Ly 2012). Mutant TIN2S proteins also localize to the telomere (Yang et al. 2011). Because the patients are heterozygous for the disease causing mutations, the mutations are thought to function in a dominant negative manner.

Several mechanisms have been proposed for telomere shortening with TIN2 mutations, but the true mechanism is not clear. Co-immunoprecipitation of telomerase with the patient mutations in TIN2S brought down less telomerase activity measured by the telomeric repeat amplification protocol (TRAP) assay and less telomerase RNA measured quantitative real-time PCR (qRT-PCR), leading to the proposal that the TIN2 mutants are defective at recruiting telomerase through TPP1 (Yang et al. 2011). Knock-in of the R282H mutation in human cell lines also decreased telomerase association with the telomere (Frank et al. 2015). Others, however, have argued that there are also telomerase-independent mechanisms of telomere shortening. The HP1γ binding site is within the patient mutation cluster, and disrupting the TIN2S-HP1γ interaction leads to decreased sister telomere cohesion as measured by the distance between sister telomeres before mitosis (Canudas et al. 2011). While it is not clear how sister telomere cohesion can cause a defect in telomere length maintenance, we conjecture that it may reflect an uncoupling of the leading and lagging strand replication machinery (see Chapter 4). Another experiment suggesting a role of fork collapse in telomere shortening is that knock-in of the corresponding K280E mutation in a telomerase RNA (TR) knock-out

mouse (K267E) is argued to cause more rapid telomere shortening than TR knock-out alone (D Frescas & de Lange 2014).

While two studies of TIN2 mutations have been performed at the endogenous locus, most of the telomere length effects of normal and mutant TIN2 have only been studied in the TIN2S isoform using either overexpression or knockdown methods. Additionally, while there are many proposals about how TIN2 mutations may affect telomere length, the mechanism of telomere shortening in patients with TIN2 mutations remains unclear. Here we set out to learn more about the two TIN2 isoforms and test whether they affect telomerase activity through the TIN2-TPP1 interaction. We found that TIN2 is actually expressed as three isoforms that have different effects on telomere length in cells. We also found that TIN2 stimulates telomerase processivity, implicating it as a player in the telomerase processivity complex. In light of these results and other recent findings in the field, we discuss the implications of TIN2 as part of a single-stranded binding complex that stimulates telomerase processivity and propose that TIN2 may be involved in coupling of lagging strand DNA replication with telomerase activity.

Chapter 2. TIN2 has multiple expressed isoforms in human cells

2.1 INTRODUCTION

TIN2 was discovered in a yeast two-hybrid screen for TRF1-interacting factors. The 39kDa interacting protein had 354 amino acids encoded by a cDNA containing exons 1 through 6 of the *TINF2* gene (Kim et al. 1999). Later analysis of the gene structure and comparison to the mouse TIN2 gene revealed conserved exons 7, 8, and 9 in the TIN2S 3'UTR (Kim et al. 2003). A second isoform was identified that splices together all 9 exons, encoding a 50 kDa protein with 451 amino acids (Figure 2.1A) (Kaminker et al. 2009). These two isoforms were renamed TIN2S and TIN2L. TIN2L contains the entire TIN2S sequence, with an additional 97 amino acids at the C-terminus. Both TIN2 isoforms are expressed in multiple different tissues and cell lines and contain the known interaction domains and the patient mutation cluster (Kim et al. 1999; Kaminker et al. 2009) (Figure 2.1). Mouse cells only express one TIN2 isoform that is 414 amino acids long and more closely resembles TIN2L (Kaminker et al. 2009).

TIN2 is only found in vertebrates, and multiple sequence alignment of known or predicted TIN2 proteins shows several regions of strong sequence conservation (Figure 2.1 B, Appendix B). The N-terminus, which binds TRF2 and TPP1, is highly conserved. This region is predicted to be coiled-coil, and the pattern of conserved residues suggests a conserved helical interaction interface. The TRF1 binding motif, FxLxP, and the patient mutation cluster are also both highly conserved (Figure 2.1) (Chen et al. 2008). Interestingly, the C-terminal region that is unique to TIN2L also contains a region of highly conserved residues that are present in mouse TIN2, but not TIN2S. Within this

conserved region is a patch of amino acids whose sequence identity is conserved across mammals. Because there is a conserved region in the long isoform that is missing from short isoform, we think there may be functional differences between the two isoforms.

Previous work on TIN2 has mostly studied TIN2S, and therefore any unique functional contribution of TIN2L has not been observed in these experiments. Initial TIN2S overexpression experiments in HT1080 cells, which maintain very short telomeres, showed TIN2S overexpression had no effect or slight shortening effects on telomere lengths. However mutants lacking the N-terminus, which includes the TRF2 and TPP1 interaction regions, exhibit telomere elongation in a telomerase-dependent manner (Kim et al. 1999). Later shRNA knockdown experiments showed a modest increase in telomere length with reduced levels of TIN2 (Ye & de Lange 2004). These results have led TIN2 to be described as a negative regulator of telomere length. While TIN2L has been described as nuclear matrix associated, its effects on telomere length have not been reported.

Because both TIN2 isoforms contain the patient mutation cluster, we sought to determine which is the predominant TIN2 isoform in human cells and to ask whether they contribute differently to telomere length regulation. To address the questions about the TIN2 isoforms in human cells, we tagged the endogenous locus using CRISPR/Cas9 (Jinek et al. 2012; Jinek et al. 2013). In edited clones, we found evidence for three expressed isoforms, not the expected two. Here we describe the identification of a new isoform, TIN2M.

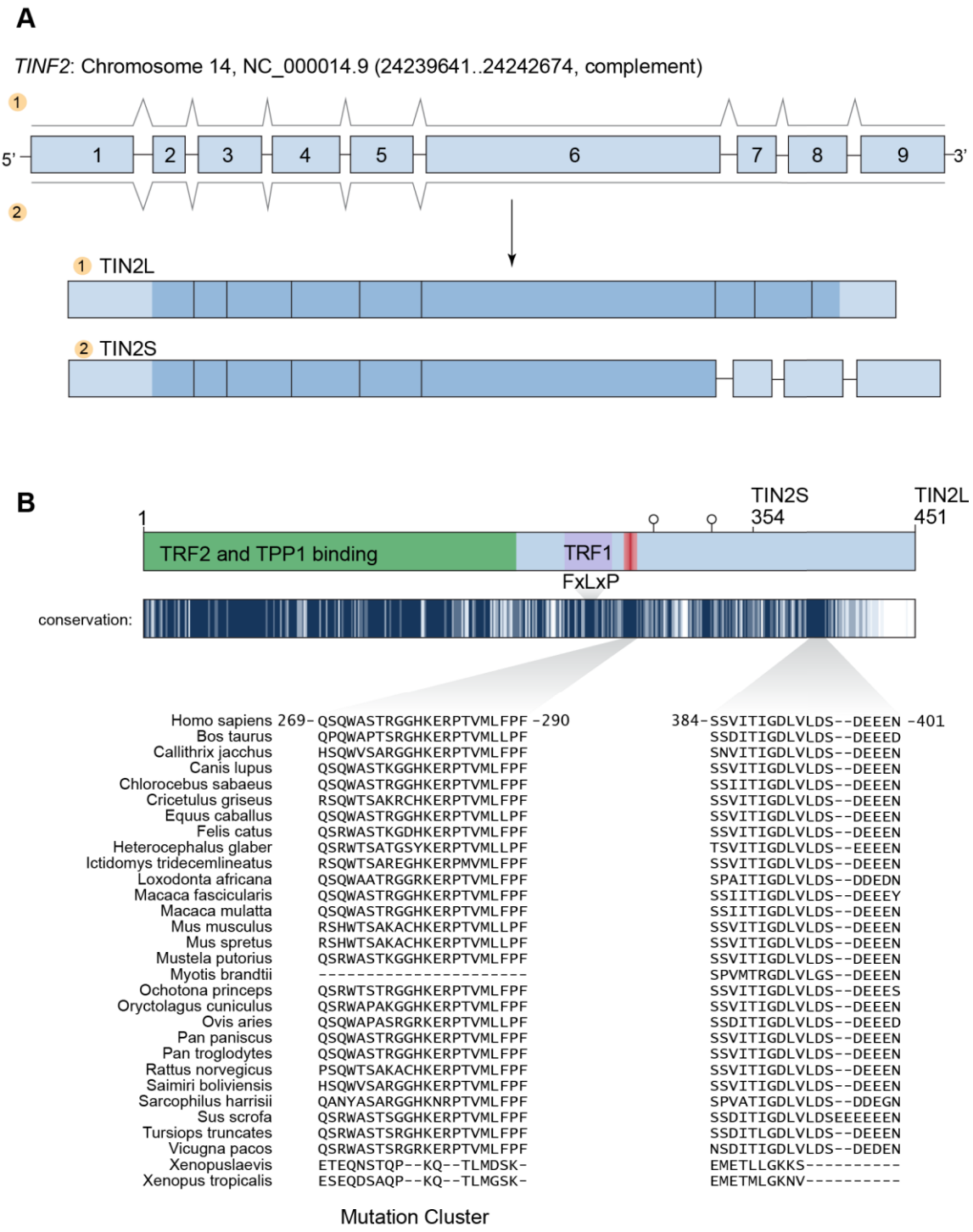

Figure 2.1 *TINF2* splicing and TIN2 protein domains.
(**A**) Architecture of the *TINF2* gene and alternative splicing of the TIN2S and TIN2L transcripts. (**B**) TIN2 protein schematic and binding domains. Below the protein schematic is a conservation track generated from the values generated from Praline alignment (see Materials and Methods). Conservation is colored from white=not conserved to navy=highly conserved. Highlighted are two conserved regions, the patient mutation cluster (269 to 290) and a highly conserved C-terminal region with unknown significance.

2.2 RESULTS

We wanted to address unanswered questions about the endogenous expression and functions of TIN2 isoforms in human cells. We were unable to identify a TIN2 antibody that specifically recognized TIN2 protein at endogenous levels. Therefore, to study the expression differences in expression between TIN2S and TIN2L, we decided to tag the endogenous gene in cultured cells.

2.2.1 CRISPR editing of the *TINF2* gene

We chose to perform CRISPR/Cas9 editing in 293FT cells because of their robust transfection efficiency (>90%) and growth. Using a guide RNA that targets Cas9 to make a cut just 3' of the start codon (Figure 2.2A), we transfected a plasmid containing Cas9-2A-Puro and the guide RNA, as well as a homology-directed repair template (Ran et al. 2013). Cells receiving Cas9 were enriched with a short puromycin selection and cloned by limiting dilution into 96-well plates. We screened the cells by PCR amplification of the locus and BglII digestion. Positive clones had a 30 base-pair insertion and a BglII cut site, so digested fragments can be identified on a 2% agarose gel (Figure 2.2A and B).

Of the 73 clones that grew and had interpretable PCR products, we found 77% had at least one edited allele, and 36% appeared to be homozygous for the insertion. The 293FT cell line, however, is hypotriploid with an unstable karyotype, making it challenging to assess true homozygosity. Also, we observed high endogenous Myc expression that interferes with western blotting for myc-tagged TIN2 (Figure 2.2 C, lane 2). These caveats make it difficult to study TIN2 in our knock-in cell lines, so future studies of endogenously edited TIN2 should repeat the targeting in a diploid cell line.

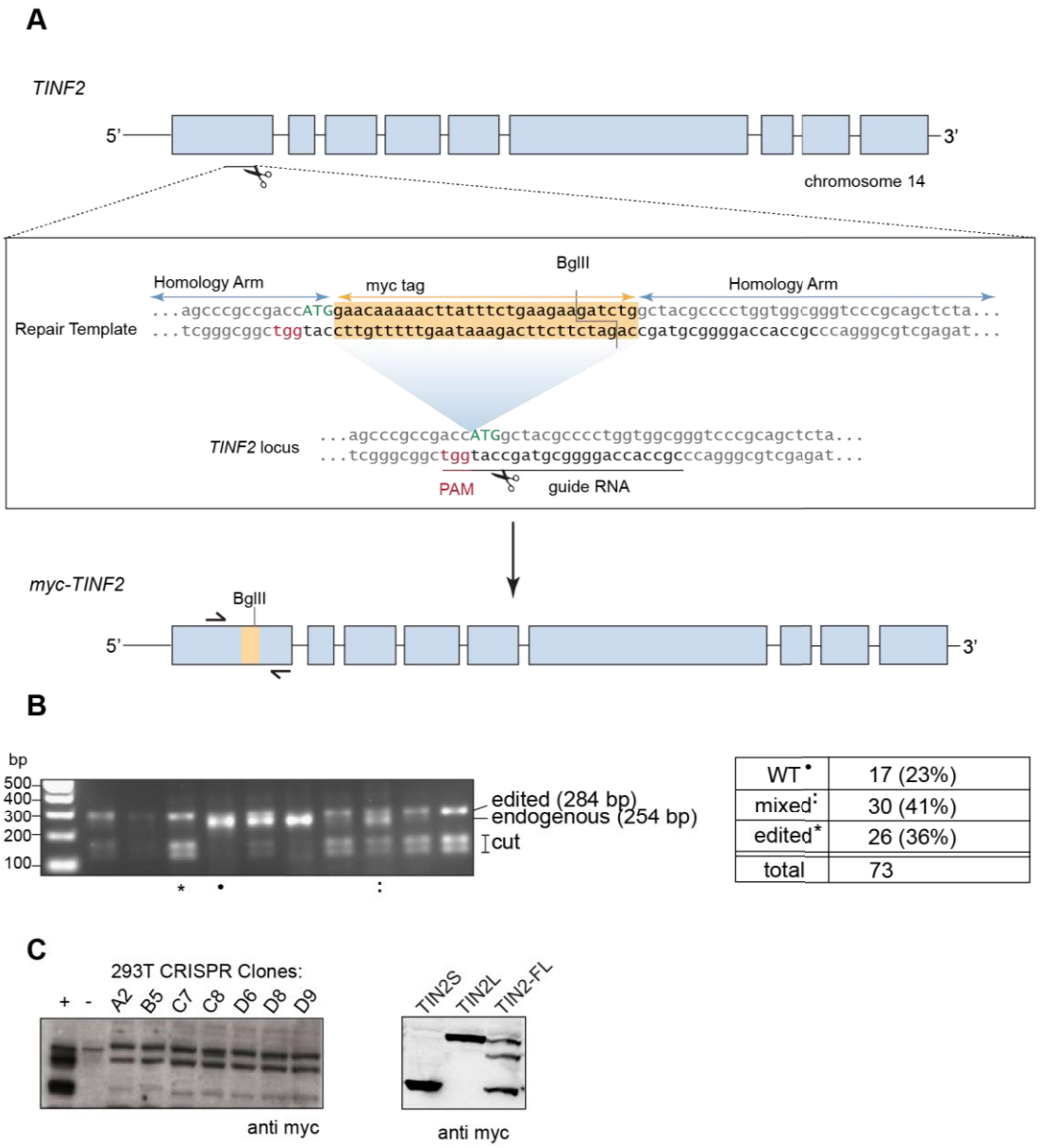

Figure 2.2 CRISPR/Cas9 editing of *TINF2*

(**A**) *TINF2* genomic editing schematic. CRISPR guide RNA was selected to cut just 3' of the start codon in exon 1 (green). The PAM sequence is in the *TINF2* 5' UTR. A repair template with ~250 base pair homology arms, a myc tag, and a BglII cut site was transfected with Cas9 to incorporate an N-terminal myc tag at the TIN2 locus. The myc tag creates an insertion that disrupts the guide RNA and PAM. (**B**) PCR and BglII partial digest of edited clones. PCR primers indicated in *A* amplify a 254 bp region in the endogenous locus and 284 bp in the edited region. Only edited clones have a cut site. Percentages from whole experiment are indicated in the table. •WT; *edited; :mixed. (**C**) Myc western blot of edited myc-TIN2 CRISPR clones (left) and western blot of the tagged TIN2 gene with myc-TIN2S and myc-TIN2L cDNA and the cloned myc-tagged full-length gene (TIN2-FL).

Western blots on several of the positive clones unexpectedly showed three distinct bands when probed with the myc antibody instead of the expected two bands (Figure 2.2C). To independently test this finding, we cloned and myc tagged the full-length TIN2 gene into an expression vector under the CMV promoter. In transfected cells overexpressing this construct, we again observed the three bands. Using cDNA for TIN2S and TIN2L, we compared the size of the bands and determined that the unidentified band was an intermediate band that ran at approximately 47 kDa (Figure 2.2 C, right). Because the middle band is discrete and not a smear, we suspected was a new isoform rather than a post-translational modification.

2.2.2 Identification of a new isoform, TIN2M

Although TIN2 is known to be alternatively spliced, we could not predict the sequence of the new isoform. To identify all spliced isoforms, we set out to sequence full-length TIN2 transcripts. To do this, we adapted 3'RACE (Frohman et al. 1988; Frohman 1993; Scotto–Lavino et al. 2007) combined with Pacific Biosciences (PacBio) Single-Molecule, Real-Time (SMRT) sequencing to sequence the transcript from the 5'UTR through the polyA tail. Sequencing full-length transcripts is feasible because the entire TIN2 gene is less than 4 kb, and PacBio sequencing is capable of generating long sequence reads (Pan et al. 2008; Carneiro et al. 2012; Steijger et al. 2013).

First, we reverse transcribed mRNA from several different cell lines with an oligo-dT_{20} primer with an adapter sequence, then PCR amplified the cDNA using primers targeting the adapter sequence and the 5'-UTR (Figure 2.3A). This PCR amplification did not produce discrete bands on agarose gels, but TOPO cloning and sequencing indicated that most inserts were specific TIN2 amplicons.

To sequence full-length PCR products with PacBio SMRT-sequencing, we prepared libraries from the 1-3kb fraction of the PCR products after size selection. Sequencing reads were processed in the SMRT Analysis v4.0 software, which generates circular consensus sequence (CCS) reads. Full-length reads were identified based on the presence of the polyA and primer sequences. The program then clusters the reads to generate high-quality sequences (Gordon et al. 2015). These reads were aligned to the genome using HISAT2 and assembled into potential transcripts using StringTie (Figure 2.3A) (Pertea et al. 2015; Kim et al. 2015; Pertea et al. 2016).

When we amplified and sequenced endogenous TIN2 transcripts from 293T cells, we found that TIN2S and TIN2L are expressed along with a third major isoform, "TIN2M". TIN2M results from retention of the last intron, between exons 8 and 9, resulting in some unique sequence coded from the intron before reaching a stop codon (Figure 2.3B). FPKM values output by StringTie indicate that TIN2M and TIN2L transcripts are expressed at the same levels, and TIN2S is about 10-fold higher. The relative abundance can also be visualized by looking at the coverage across *TINF2* (Figure 2.3C). About one-third of the reads contain the retained intron between exons 6 and 7, which is present in TIN2S only. Roughly two-thirds of the reads contain the retained intron between exons 8 and 9, which is present in both TIN2S and TIN2M, but not TIN2L. This suggests that the isoforms are expressed at similar levels. However, because of the PCR amplification step, these results are not quantitative and represent a rough estimate of the relative abundance of the transcripts.

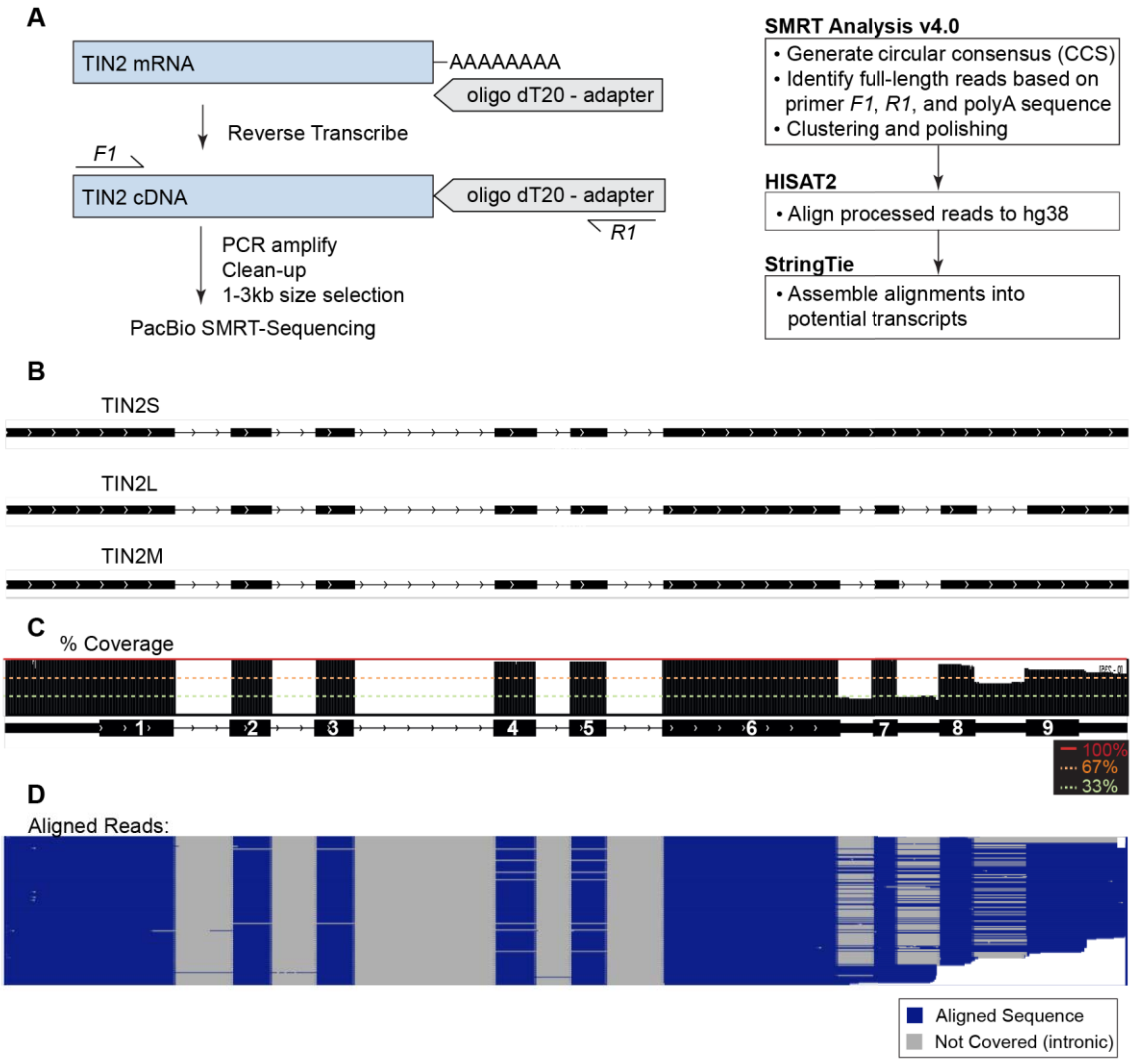

Figure 2.3 Identification of a new isoform, TIN2M
(**A**) 3'RACE strategy to amplify and sequence full-length TIN2 transcripts (*left*) and data analysis pipeline (*right*). (**B**) StringTie-generated potential TIN2 transcripts from combined data from 293T, HeLa, RPE-1, K562, and LCL cell lines shows TIN2S, TIN2L, and the new isoform, TIN2M. (**C**) Coverage track from all 293T aligned full-length reads. Most transcripts contained exons 1-6 (red line = 100% coverage). One-third of transcripts retained the intron between exons 6 and 7, indicative of TIN2S (green dashed line=33%) and nearly two-thirds of transcripts contained the retained intron between exons 8 and 9 (orange dashed line=67%), indicative of TIN2S+TIN2M. The remaining transcripts, about one-third, spliced out all of the three downstream exons, indicative of TIN2L. (**D**) "Squished" view of all aligned reads. Each row is one read. Aligned sequence in blue, and absent sequence is gray, indicating it is spliced out. This view provides an alternative illustration of the coverage at each exon and intron. Alternative polyadenylation events are also apparent as steps from the 3' end, which were confirmed as polyadenylated sites by referencing the FASTA sequence of the original ccs read. *See also Appendix C*.

To determine whether TIN2M is expressed in other cell types, we sequenced RNA from four other human cell lines (HeLa, K562, RPE-1, and an LCL) and two cell lines from different mouse strains, C57BL/6 and CAST/EiJ. TIN2M was present as a major isoform in all of the human cell lines in similar ratios to what we had seen in the 293T cells. Mouse TIN2 was only expressed as one isoform in both strains, as previously described (Kim et al. 2003; Kaminker et al. 2009) (Appendix C).

When we looked at the processed, aligned reads, we noticed many recurrent and unique minor TIN2 splice variants in the human cell lines in addition to the three major isoforms. These variants include skipping of exon 2 (Ishdorj et al. 2017), skipping exons 4 and 5, skipping exons 2-5, or retention of the first intron (Figure2.3D). In addition, alternative polyadenylation was also observed on all three isoforms. These abnormal splicing events were observed specifically in human and not the mouse cell lines.

Publicly available data from PacBio IsoSeq, which is a whole genome RNA-seq method using PacBio sequencing technology with no PCR amplification step, show expression of TIN2M and other variants in mcf-7 breast cancer cells (Pacific Biosciences 2015). Genome-wide ribosome profiling data from GWIPS-viz also suggest that TIN2M may be translated in human cells, as ribosome peaks are present in the unique coding region of the retained intron between exons 7 and 8 (Michel et al. 2014).

Having discovered a new TIN2 isoform, we wanted to determine its effects at the telomere. All three isoforms share exons 1-6, which contain the known interaction domains, binding motifs, and the patient mutation cluster, but differ in their C-terminal domains. To determine whether they have different effects in human cells, we overexpressed cDNA encoding TIN2S, TIN2M, or TIN2L with or without the K280E

patient mutation in HeLa cells and looked at the localization and telomere length effects in these cells.

2.2.3 TIN2 isoforms localize to the telomere

To test whether the three isoforms of TIN2 localize to the telomere, we performed immunofluorescence on fixed cells. We generated cell lines stably overexpressing N-terminally myc-tagged TIN2S, TIN2M, or TIN2L under the CMV promoter in HeLa cells using the Invitrogen FLP-in system. Briefly, FLP-in cell lines have an FRT site at a single genomic locus along with a promoter and start codon for the selectable marker. The pcDNA5/FRT expression vector contains a selectable Hygromycin marker lacking a promoter and ATG start codon, so cells only express Hygromycin resistance if the plasmid integrated at the FRT locus. By using this system, we can ensure that each cell has one copy of the TIN2 expression construct.

Since shelterin is constitutively localized to telomeres, telomeres can be visualized by TRF2 immunofluorescence. We used myc antibodies to determine the localization of the TIN2 isoforms in these cell lines. Immunofluoresence showed punctate TRF2 staining, marking the telomeres. Myc antibodies marking TIN2 showed a similar staining pattern with foci that co-localize with TRF2. This pattern was seen for in all three isoforms, indicating that the TIN2 isoforms all localize to the telomere (Figure 2.4). When we tested localization of TIN2S-K280E, TIN2M-K280E, or TIN2L-K280E, we found that they were also localized to telomeres. This is consistent with previously reported data on TIN2S mutants (Yang et al. 2011). Previous work to understand the defects in TIN2 mutants showed that the localization and protein-protein interactions of TIN2S were not disrupted by the patient mutations. We have expanded this to show that

the K280E patient mutation in any of the three TIN2 isoforms does not disrupt telomeric localization. This supports the hypothesis that any differences in TIN2 isoforms and mutants are not in their telomeric localization but rather in some unknown TIN2 function.

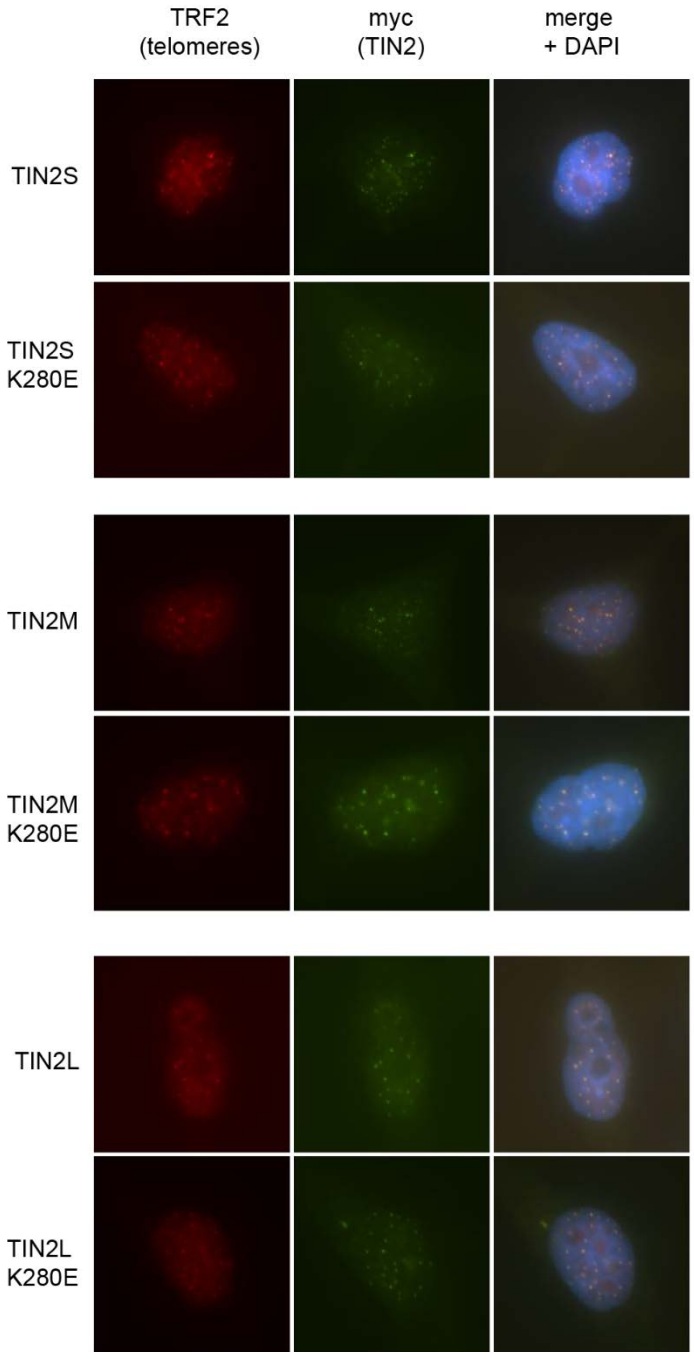

Figure 2.4 TIN2 isoforms localize to the telomere
Immunofluoresence of TIN2 expressing cell lines. TRF2 marks telomeres (red) and myc antibodies mark TIN2 (green). Slides were counterstained with DAPI. Merge image shows telomeric foci with colocalized TRF2 and TIN2 staining. Isoform and mutation status are indicated on the left.

2.2.4 TIN2 isoforms have different effects on telomere length

The HeLa-TIN2 cell lines were passaged to monitor telomere length changes over time. TIN2S overexpression has been suggested to shorten telomeres (Kim et al. 1999; Yang et al. 2011), but the effect of TIN2L has not been reported. We passaged HeLa-TIN2 and HeLa-GFP control cells for eight weeks. We found that GFP and TIN2S overexpressing cell lines did not have significant changes in telomere length. In contrast, TIN2M and TIN2L overexpressing lines had increased telomere length (Figure 2.5).

We also examined the effects of the K280E patient mutation on telomere length in all three isoforms. Previous work in TIN2S showed that overexpression of TIN2S-K280E, TIN2S-R282S, or TIN2S-R282H (Yang et al. 2011) decreases telomere length more than overexpressing wild-type TIN2S. Endogenous knock-in of the TIN2-R282H mutation in human cells showed a decrease in telomere length, although the degree of shortening varied between clonal cell lines (Frank et al. 2015).

In our hands, TIN2S-K280E and GFP cell lines did not have significant telomere length changes. These cells have very short telomeres, so it may be that they are already on the shorter end of tolerated telomere lengths. TIN2M-K280E and TIN2L-K280E, however, had a surprising increase in telomere length over time. This telomere elongation with TIN2 has only before been observed with overexpression of TIN2-13 construct (Kim et al. 1999), which lacks the amino acids 1-196 in TIN2S, consisting of the TPP1/TRF2 binding domains.

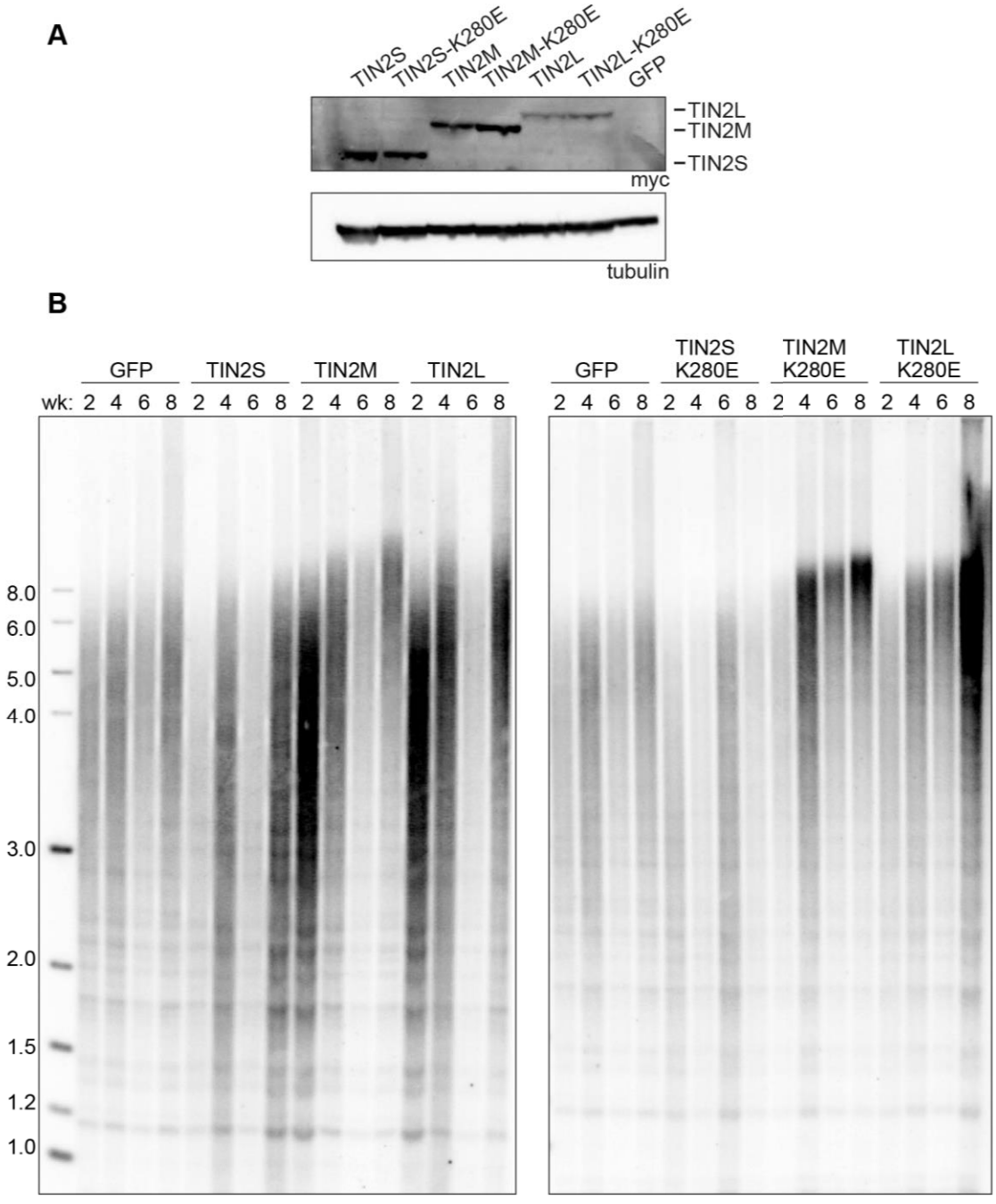

Figure 2.5 TIN2 isoforms have different effects on telomere length.
(**A**) Western blot of myc-TIN2 overexpressing cell lines (**B**) Southern blot of genomic DNA from TIN2 cell lines at over 8 weeks in culture. Timepoint is indicated as weeks in culture (wk). Left, 2-log ladder values in kb.

In these experiments, we used genomic editing to identify a new TIN2 isoform, TIN2M, in addition to the known TIN2S and TIN2L isoforms. We were able to sequence full-length TIN2 transcripts to identify that TIN2M results from a retained intron and contains all of the coding sequence of TIN2S, some of the TIN2L C-terminal sequence, and a short stretch of unique amino acids coded from the retained intron. All three isoforms localize to the telomere, and the K280E patient mutation does not disrupt telomeric localization. We found that, in contrast to TIN2S overexpression, TIN2M and TIN2L overexpression caused telomere elongation regardless of whether the patient mutation is present. We think this is evidence that the TIN2 isoforms have different functions in the cell that are not yet known.

2.3 DISCUSSION

In our analysis of TIN2, we found that human cell lines express three major TIN2 isoforms that localize to the telomere but have different effects on telomere length. Our surprising results showing three isoforms suggest that, while we have many robust tools to study gene expression and function, unbiased approaches may reveal unexpected information about a gene of interest. The N-terminal tagging of the full-length *TINF2* gene revealed an unknown expressed isoform that would not have been observed by studying the isoforms described and annotated in the literature.

2.3.1 Genomic editing and long-read sequencing identify unpredicted splicing events

The ability to analyze full-length reads of TIN2 cDNAs using PacBio SMRT-sequencing identified transcript variants that would be missed in short-read sequencing

platforms. The long-read sequencing allowed us to identify a new isoform that does not have a novel splice junction, but rather a unique combination of splicing and intron retention. PacBio read lengths allow sequencing of the entire TIN2 transcript, and can be used to sequence much longer transcripts as well. In addition to identifying events of exon skipping, intron retention, and alternative polyadenylation, we can resolve which splicing events are happening in the same transcript. A recent study discovered an unusual TIN2 splice variant in chronic lymphocytic leukemia (CLL) cells (Ishdorj et al. 2017). This variant skips exon 2 in the context of TIN2S, however their methodology does not definitively show this event is exclusively in TIN2S transcripts, and it may be present in other isoforms. We observed rare occurrences of this variation. While some were in TIN2S transcripts, others were in transcripts truncated by early alternative polyadenylation or with varying downstream splicing events not seen in TIN2S.

PacBio SMRT sequencing is not often used due to its high frequency of insertions and deletions, but it is a valuable method for identifying isoforms with specific sequence structure, where the arrangement of exons is more relevant than nucleotide variation. As long-read sequencing technologies improve, they should become the default choice for examining expressed mRNA sequences.

Having identified three TIN2 isoforms, we still need to investigate what TIN2 is doing at the telomere to regulate telomere length. *In vivo* or cell culture studies are also needed to determine the roles of each isoform in the cell. Previous work on TIN2 has used methods such as shRNA knock-down that perturb protein levels or cDNA overexpression that biases isoform expression as well as perturbing protein levels. Because the stoichiometry of telomere proteins is tightly regulated, new approaches

should take advantage of advances in genome editing technologies. The field has been moving in this direction by generating a TIN2 mutant knock-in mouse and by using editing technologies to knock-in patient mutations in human cell lines (D Frescas & de Lange 2014; Frank et al. 2015), but more mechanistic studies are required to fully understand TIN2 function.

2.3.2 Challenges in inferring telomere protein function

One major drawback to the way telomere binding proteins have been studied is that the use of knock-down, knock-out, or overexpression experiments disrupt the delicate stoichiometry of telomere binding proteins, which is crucial to their functions. Most proteins have been defined as either positive or negative regulators of telomere length based on telomere length changes observed using these methods. These changes, however, are more likely to be results of disruption of stoichiometry, which can titrate important factors away from the telomere, rather than of direct functions of the protein.

TPP1 and POT1, for example, were initially thought to be negative regulators of telomere length. POT1 overexpression does not lead to major telomere length changes, but expression of POT1ΔOB1 elongates telomeres due to failure to bind telomeric ssDNA (Loayza & de Lange 2003). Overexpression of TPP1 leads to telomere shortening in HTC75 cells, but overexpressing TPP1 that cannot interact with TIN2 elongates telomeres (Houghtaling et al. 2004). Additionally, shRNA knock-down of TPP1 or POT1 leads to significant telomere elongation (Ye, Hockemeyer, et al. 2004; Veldman et al. 2004), and disrupting the POT1/TPP1 interaction mimics the telomere elongation of a POT1 knockout (Liu, Safari, et al. 2004).

These *in vivo* observations, however, are challenging to reconcile because the biochemical function of TPP1/POT1 suggest it is a positive regulator of telomere length. The TPP1/POT1 heterodimer serves as a telomerase processivity factor that binds telomerase and is required for telomerase localization to telomeres (Xin et al. 2007; Wang et al. 2007; Zhang et al. 2013; Zhong et al. 2012; Nandakumar et al. 2012). Disrupting the stoichiometry or localization of these complexes in cells could cause telomere length changes that are independent of the proteins' normal functions.

Overexpression TIN2, TPP1, or POT1 could sequester necessary components in non-telomeric locations, while knockdown of one component could cause a nonfunctional or partially functional complex. Similarly, TIN2M or TIN2L overexpression could sequester functional TPP1/POT1 complexes away from their telomeric location, causing a telomere elongation phenotype similar to what is observed in POT1 knockouts. Indeed, many telomere proteins, including TPP1 (Bisht et al. 2016) and telomerase (Armanios et al. 2005), exhibit haploinsufficiency, suggesting the stoichiometry is important for telomere length maintenance.

Future experiments to study the TIN2 isoforms should employ endogenous genome editing with CRISPR/Cas9 to preserve the stoichiometry. One question is whether each isoform of TIN2 is sufficient for cell survival, which can be addressed by forcing expression of one isoform and monitoring cell growth and telomere length. It would be easy to force expression of TIN2S or TIN2M by mutating downstream splice sites, but forcing TIN2L expression may be more challenging. Recombination-mediated cassette exchange (RMCE) (Toledo et al. 2006) may be a way to flank the endogenous gene with LoxP sites and concurrently remove endogenous TIN2 to force expression of a

downstream TIN2 isoform cDNA using the endogenous TIN2 promoter. We have designed an approach for this (Appendix F).

While there are still many questions about the different TIN2 isoforms expressed in human cells, our experiments underscore the functional importance of the TIN2 patient mutation cluster and the C-terminus of TIN2. Telomeric localization of the three isoforms containing a patient mutation further supports the dominant roles of the TIN2 mutants. The telomere length difference between the isoforms also suggests that the different TIN2 isoforms may have distinct roles in telomere length regulation, but the mechanism remains unclear

2.4 MATERIALS AND METHODS

2.4.1 Multiple Sequence Alignments

TIN2 sequences from vertebrates with known or predicted TIN2 proteins were obtained from NCBI. The longer isoform was chosen for organisms with multiple reported isoforms. A list of organisms and accession numbers is reported in Appendix B. Sequences were uploaded to PRALINE multiple sequence alignment using the default parameters (Simossis & Heringa 2003; Simossis & Heringa 2005). To make the sequence conservation heat map, PRALINE output was imported into Microsoft Excel, and the alignment scores (0-10) of human TIN2 were colored from white=0, not conserved to navy=8-10, highly conserved.

2.4.2 Generation of TIN2 constructs

TIN2 Expression Constructs

TIN2S cDNA was purchased as an Invitrogen Ultimate ORF clone (IOH80607), in the pENTR221 Gateway Entry vector. The stop codon was mutated to serine using site-directed mutagenesis for downstream expression of a C-terminal epitope tag. TIN2L was generated from the TIN2S entry clone by Gibson assembly with a synthetic gBlock Gene Fragments from Integrated DNA Technologies (IDT). The TIN2L gBlock contained the downstream TIN2 sequence with silent mutations for shRNA resistance (lowercase) and 9bp overlaps for overlap:

CAAAAGGAGAATTGtctcGATTGtTACATGGACCCCCTGAGACTATCAT
TATTACCTCCTAGGGCCAGGAAGCCAGTGTGTCCTCCGTCTCTGTGCAGCTCC
GTCATTACCATAGGGGACTTGGTTTTAGACTCTGATGAGGAAGAAAATGGCC
AGGGGGAAGGAAAGGAATCTCTGGAAAACTATCAGAAGACAAAGTTTGACA
CCTTGATACCCACTCTCTGTGAATACCTACCCCCTTCTGGCCACGGTGCCATA
CCTGTTTCTTCCTGcGAtTGcAGAGACtctagtAGACCTTTGAACCCAGCT

TIN2M was amplified from RT-PCR products that were cloned into PCR-II by TOPO cloning. Linearized TIN2 entry vectors were cloned into Gateway Destination vectors pLenti6/UbC/V5-DEST (ThermoFisher V49910) or pcDNA-DEST40 (ThermoFisher 11274015) using Gateway LR Clonase II (Invitrogen, 11791-020).

TINF2, the TIN2 full-length gene inclusive of introns, was cloned into pcDNA5/FRT (ThermoFisher V601020) by amplifying the locus from a BAC (RPCI.11c clone number 368G9) and an N-terminal myc tag was incorporated just after the ATG start codon (Alder et al. 2015). TIN2 isoform cDNAs were also cloned into pcDNA5/FRT by PCR amplification with primers containing HindIII and NotI restriction sites, an N-terminal myc tag, and a stop codon, followed by restriction cloning into the pcDNA5/FRT backbone.

All constructs and mutants were sequence verified by Sanger sequencing (Sanger & Coulson 1975) at the JHU Synthesis & Sequencing Facility.

Site Directed Mutagenesis

Site-Directed Mutagenesis (SDM) (Kirsch & Joly 1998; Sarkar & Sommer 1990) was used to generate patient mutations in the TIN2 vectors, and to mutate the TAG stop codon to TCG serine for C-terminal tag expression. Primers were designed with 10-15 bases on either side of the mismatch, a Tm ≥ 78°C, about 40% GC content, and beginning and ending in G or C where possible. The primers used were A4/A5 (mutating stop codon, see TIN2 Constructs), A6/A7 (K280E), A8/A9 (R282S), and A10/A11 (R282H) (Appendix A).

SDM PCR was performed with Pfu Turbo Polymerase (Agilent, 600252) using 14 cycles of PCR with 55°C annealing temperature and 72°C extension. PCR products were digested with DpnI (NEB, R0176L) for one hour at 37°C and transformed into subcloning efficiency DH5α (LifeTech, 18265017) and plated on 30μg/ml kanamycin for pENTR221 or 100 μg/ml carbenicillin (US Biological, C1100) for pcDNA5 backbones. Mutations were confirmed and the TIN2 coding sequence was checked for suprious mutations by Sanger sequencing.

Overlap Extension PCR

TIN2 truncation mutation K280X was generated by amplifying the pENTR221-TIN2S plasmid with primers A14 and A19, and A17 and A20 (Appendix A). A19 and A20 each contain a 9nt complimentary overhang. Products were gel purified and 10ng

each were used as template in a secondary PCR reaction with primers A14 and A17. The full-length amplicon was then used directly in the Gateway LR reaction to clone into the expression vector.

2.4.3 Cell culture methods

Cell lines were cultured in the indicated media supplemented with 10% heat-inactivated FBS (Invitrogen, 10082147) and 1% penicillin/streptomycin/glutamine (PSG, Invitrogen 10378-016) unless otherwise stated. HeLa, 293T, 293FT, and 293TREx FLP-in cells were cultured in DMEM (Gibco), hTERT-RPE1 cells were cultured in DMEM/F12 (Corning), patient-derived lymphoblastoid cell lines (LCLs) were cultured in RPMI (Gibco), and K562 cell lines were cultured in IMDM (Gibco).

Generating Stable Cell Lines with the FLP-in system

293 TREx FLP-in (Invitrogen, R78007) or HeLa TREx FLP-in cell lines (Invitrogen, R71407) were kind gifts from the Holland and Armanios labs. To constitutively overexpress TIN2 isoforms, the respective TIN2 cDNA in the pcDNA5/FRT vector for expression under the CMV promoter was flipped into HeLa TREx cells. A control cell line was generated with pcDNA5/FRT-EGFP. To generate these cell lines, on Day 0, $2x10^5$ cells were plated into 3 wells per construct in 6-well dishes. On Day 1, 900 ng pOG44 Flp-Recombinase (Invitrogen V600520) and 100 ng of the pcDNA5/FRT construct were transfected into each well using Lipofectamine 2000 (Invitrogen, 11668019). A set of negative control wells was included with pOG44 only, but no pcDNA5/FRT plasmid. Once the wells were confluent (Day 2 or Day 3), the wells

containing the same construct were pooled and transferred to a 15cm dish and allowed to adhere to the plate. The next day, hygromycin B (Roche, 10843555001) was added to a final concentration of 200µg/ml in DMEM. Cells were maintained under selection for two weeks, changing the media with fresh antibiotic every 3 days, until all pOG44 only cells have died and colonies of hygromycin resistant cells were apparent on the FLP-in plates.

2.4.4 CRISPR targeting of the endogenous *TINF2* gene

Constructs and Cloning

Guide RNAs were selected using the Zhang Lab CRISPR design tool (http://crispr.mit.edu/). For endogenous tagging of TIN2, the guide selected was cgccaccaggggcgtagccaTGG, which cuts just 3' of the ATG start codon. The guide oligos were ordered with BbsI overhangs for subsequent cloning. Oligos were phosphorylated and annealed by combining 1µl of each oligo with 10X T4 ligation buffer, T4 ligase (NEB M0202L), and water in a 10 µl reaction, and incubated at 37°C x 30 min, 95°C x 5min, ramp down 5°C/minute to 25°C. 3µg of the backbone, pX459-U6- Chimeric_BB-CBh-hSpCas9-2A-Puro (Ran et al. 2013) was digested with BbsI (NEB, R0539S) at 37°C for an hour, then run on a 1% agarose gel and extracted. A 1:200 dilution of the annealed primers was ligated to the digested backbone.

The donor template for the N-terminal myc tag was generated by PCR from the cloned *TINF2* genomic locus with an incorporated myc tag. To generate the linear donor DNA, the mycTINF2 construct was amplified with Phusion DNA polymerase (NEB, M0530L)

using two primers (A111, A112) that generate 250bp homology arms on either side of the myc tag. Products were column purified and concentration was determined with the Nanodrop.

CRISPR/Cas9 Editing in 293T cells

To edit 293T cells, $4x10^5$ cells were played on D0. On D1, 1µg of Cas9-2A-Puro+TIN2 guide was transfected with 10 molar equivalents of the repair template using XtremeGENE9 (Roche, 6365787001) according to the manufacturer's protocol. As a transfection control, FUGW was transfected and checked for GFP fluorescence on the inverted fluorescent microscope, which allowed estimation of 80% transfection efficiency. On D2, cells were split 1:3 and 3µg/ml puromycin was added. After 48-72 hours, most control cells and many of the Cas9 transfected cells died. The surviving edited cells were trypsinized and plated for limiting dilution cloning.

Screening Clones for editing events

To screen the edited cells, one 96-well plate was expanded to two 48-well plates. When confluent, the cells were disrupted and half were passaged into a fresh 96-well plate and half were harvested for a genomic DNA prep. For gDNA isolation, cells were tripsinized and transferred to a 96-well round bottom plate, washed with PBS, and resuspended in 50µl Bradley lysis buffer (10mM Tris-HCl pH7.5, 10 mM EDTA, 0.5% SDS, 5M NaCl, 1mg/ml Proteinase K) and incubated overnight in a humidified 55°C chamber. DNA was precipitated with 100µl ice-cold ethanol/NaCl (100%/5M) for 30 minutes at room temperature, and then spun at 3000rpm for 20 minutes. DNA pellets were washed with

ice-cold 70% ethanol, dried, and resuspended in 30µl warm TE pH 8.0. TE volume was later brought up to 50 µl because of the high viscosity.

PCR screening was done on 1µl of genomic DNA in 96-well plate format with primers A109 and A110 (Appendix A) and TaKaRa Ex Taq polymerase (Clontech, RR001A) according to manufacturer instructions, with 35 cycles and annealing temperature of 65.2°C. Clones yielded a 284 bp band with BglII cut site. To identify proper editing, BglII was diluted in NEB3 buffer and added to 10µl PCR products and incubated at 37°C for 1 hr. Only partial BglII digestion was achieved in PCR buffer, and positive and negative clones could be discerned by the shift in PCR band and presence of BglII digestion products. Presence of myc-TIN2 was subsequently tested by western blotting on select clones.

2.4.5 Western Blotting

Expression of myc-TIN2 CRISPR clones was assayed by western blotting. Lysates were generated by harvesting one well of a 6-well plate in 100µl RIPA buffer (Sigma, R0278-50ML), lysing on ice for 30 minutes with vortexing, and clearing the lysates by centrifugation at 4°C for 10 minutes at 8000rpm. Samples were denatured with 30 µl 4X LDS (Invitrogen, NP0008) with 50 mM DTT and heated at 65°C for 10 minutes. Proteins were separated by reducing SDS-PAGE electrophoresis on a 4-12% Bis-Tris gel (NuPAGE, NP0323) in 1X MOPS buffer (Invitrogen, NP0001) and transferred to PVDF (Immobilon FL, IPFL00010) in 1X NuPAGE Transfer Buffer (Invitrogen, 00061) with 10% Methanol. 3 µl of the SeeBlue Plus2 (Thermo, LC5925) prestained ladder are included to estimate molecular weight. Membranes are then blocked in 1X TBS + 0.1%

Tween20 (TBST), 5% milk (Bio-Rad 170-6404) for 30 minutes at RT or overnight at 4°C. Primary antibody was diluted in blocking buffer and incubated with agitation at room temperature for 30 minutes to 2 hours. Primary antibodies and concentrations are as follows: mouse anti-myc 4A6 (Millipore 05-24), 1:2000; rabbit anti tubulin (Abcam, ab6046), 1:5000; mouse anti-V5 (Invitrogen R96025), 1:5000. Blots were washed 3 times with TBST and incubated with the appropriate secondary, anti-rabbit HRP or anti-mouse HRP (Cell Signaling), diluted 1:10,000 in TBST. After 3 washes with TBST, blots are developed with SuperSignal West chemiluminescence substrate (Thermo, PI34095) and imaged on an ImageQuant LAS4000 imager.

2.4.6 Determination of TIN2M isoform

To determine whether the unidentified myc-TIN2 band is a previously unknown spliced variant, we performed a modified 3'RACE protocol where we amplified *TINF2* transcripts from the 5'UTR through the polyA sequence. PacBio sequencing allowed generation of full-length reads across the transcripts. The 3'RACE and sequencing was performed using samples from five human cell lines (293T, HeLa, RPE-1, K562, LCL) and two mouse samples (CAST/EiJ MEFs, C57BL/6 liver).

Isolation of RNA

RNA was isolated from $\geq 10^6$ cells using the RNeasy Kit (Qiagen, 74104). Cells were washed with PBS and disrupted in RLT using QIAshredder spin columns (Qiagen, 79654). The RNA isolation follows the manufacturer protocol with an on-column DNase

digestion using the RNase-free DNase kit (Qiagen, 79254) to remove any genomic DNA, followed by RNA clean-up. Concentration was estimated by NanoDrop.

Modified 3'RACE

3'RACE was performed as described in Molecular Cloning: A Laboratory Manual (Fourth Edition, CSHL Press, 2012) with modifications. To sequence full-length TIN2 transcripts, 1.5ug RNA was reverse transcribed with the primer A124, an oligo-dT_{20}-Adapter primer, using the SuperScript III First Strand Synthesis Kit (Qiagen, 18080-051). 5 μl of the resulting cDNA was amplified with Hot Start Phusion Polymerase (Thermo, F-549L) primers to the 5'UTR (Human-A111, Mouse: A142, Appendix A) and to the adapter (A123), using the annealing temperature of 46°C and a hot-start protocol to promote specific primer binding. 3-5 replicate PCR reactions were combined and purified with the QIAquick PCR Purification Kit (QIAGEN, 28104) and submitted to the Johns Hopkins Deep Sequencing & Microarray Core Facility for sequencing.

PacBio Sequencing and Analysis

2-3 μg of purified PCR product was submitted to the Deep Sequencing & Microarray Core Facility. Quality Control was performed on a 1:200 dilution of samples using a Bioanalyzer (Agilent, G2939A) High Sensitivity DNA Assay. Products were size selected for the expected size range of 1-3kb because of populations of both very low and high MW products. 1 SMRT cell was sequenced per sample. 8000 to 40,000 ccs reads were acquired from each SMRT cell.

Sequencing reads were filtered and trimmed in the SMRT Analysis v4.0 software (Gordon et al. 2015). This program generates the circular consensus sequence (ccs), then selects full-length reads that pass a quality threshold. These reads were aligned to chromosome 14 (hg38 assembly) using HISAT2 (Pertea et al. 2016). Gene models were then assembled with StringTie (Pertea et al. 2015; Pertea et al. 2016; Kim et al. 2015). StringTie was first run for individual samples using the default settings except the minimum isoform fraction was set to 0.01 instead of 0.1. To build a gene model for all human reads, StringTie --merge was run with the minimum isoform fraction set to 0.05. HISAT2 and StringTie results were viewed in IGV (Thorvaldsdottir et al. 2013; Robinson et al. 2011).

2.4.7 Immunofluoresence

HeLa FLP-in cells were plated in chamber slides. The following day, media was removed and the cells were washed with PBS and incubated with 4% paraformaldehyde (PFA) for 20 minutes. Slides were washed twice for 5 minutes with PBS, once with 0.5% Triton in PBS for 15 minutes, washed two more times with PBS. Slides were blocked in 10% goat serum in PBS for 30 minutes (Sigma G0923) and incubated with primary antibody for 1 hour at room temperature. Then they were washed with PBS three times for five minutes and incubated in secondary antibody for one hour at room temperature. They were washed again three times with PBS and then a coverslip with Dapi/Vectashield was added to the slide. Primary antibodies and dilutions were mouse anti-myc clone 4A6 (Sigma 05-724), 1:200 and rabbit anti-TRF2 (Novus Biologicals NB110-57130), 1:800. Secondary antibodies goat anti-mouse IgG1 cross-adsorbed to AlexaFluor 488 (Invitrogen #21121) or goat anti-rabbit IgG highly cross adsorbed to AlexaFluor555

(Invitrogen# 21429) were diluted 1:400. Slides were imaged on a Nikon Eclipse Ni microscope with a 60x objective using the NIS Elements software.

2.4.8 Southern Blotting

Genomic DNA Isolation

Cell pellets were washed in PBS then stored at -80°C until use. Pellets were resuspended in 300 µl SNET (20mM Tric-Cl, pH 8.0, 5 mM EDTA, 500mM NaCl, 1% SDS) supplemented with 400 µg/ml proteinase K and lysed on a shaking platform at 55°C overnight. Proteins were removed with an equal volume of phenol:chloroform, 1:1, with gentle rocking for 30 minutes. After a 5-minute spin at 13,000xg, the aqueous layer was transferred to a new tube and DNA was precipitated with an equal volume of isopropanol. DNA was pelleted by spinning for 15 minutes in a microfuge at 13,000xg, washed with 70% ethanol and dried to remove residual ethanol. Pellets were resuspended in 50-100µl TE supplemented with RNaseA with shaking at room temperature overnight.

Sample Preparation, Electrophoresis, and Transfer

Genomic DNA was digested in 50µl reactions in 1X CutSmart Buffer (NEB) and 2 µl MseI (NEB R0525M) overnight at 37°C. Double-stranded DNA was measured using the Qubit dsDNA BR Assay kit per the manufacturer instructions. Samples were prepared in 1X Blue Juice loading dye (1% SDS, 0.3% Bromophenol Blue, 250mM EDTA, 40% sucrose) and normalized to the concentrations calculated from the Qubit measurements. 10ng of 2-log DNA ladder (NEB) is loaded in the first lane.

Samples were run on a 0.7% TTE (20X TTE=1.78 M Tris base, 0.57 M taurine, 0.01 M EDTA) gel containing 0.5µg/ml ethidium bromide at 45 V overnight for about 20

hours. The gel was denatured for 30 min in 0.2 M sodium hydroxide (NaOH), 0.34M NaCl and neutralized for 30 min in 1.5 M NaCl, 0.5 M Tris, pH 7.0. Gels were transferred by vacuum blotting (Boekel Appligene) at ≤60 mbar onto Amersham Hybond-N+ membrane (GE Healthcare) in 10X SSC (1.5 M NaCl, 0.17 M sodium citrate) for 1 hr. The membrane was UV-crosslinked twice using the auto-crosslink function (UV Stratalinker 2400, Stratagene) and prehybridized for 1–2 hr in Church buffer (0.5 M Tris, pH 7.2, 7% SDS, 1% bovine serum albumin, 1 mM EDTA).

Probe labeling and hybridization

25ng of JHU821 plasmid and 2-log ladder are labeled by random priming according to the manufacturer protocol using α^{32}P-dGTP and cleaned up using a G50 mini spin column. Membranes were hybridized overnight with JHU821 and 2-log ladder probe, washed, and exposed to GE Storage Phosphor screens and scanned with a STORM 825 imager.

Chapter 3. TIN2 cooperates with TPP1/POT1 to stimulate telomerase processivity

3.1 INTRODUCTION

The mechanism by which TIN2 affects telomere length is not known. Most short telomere disease mutations affect telomerase activity, biogenesis, or stability, so we explored potential mechanisms through which TIN2 could be affecting telomere elongation by telomerase. We noted that TIN2 interacts directly with TPP1, a telomerase processivity factor that binds directly to telomerase (Houghtaling et al. 2004; Wang et al. 2007; Xin et al. 2007). Therefore, we investigated the TIN2-TPP1 interaction as a potential mechanism of TIN2 regulation of telomere length.

TPP1 interacts directly with the TEN domain of telomerase reverse transcriptase (TERT) through its TEL-patch region in its OB-fold (Figure 3.1) (Nandakumar et al. 2012; Sexton et al. 2012; Zhong et al. 2012). TPP1 forms a heterodimer with POT1, which is the single-stranded binding component of the shelterin complex (Ye, Hockemeyer, et al. 2004; Liu, Safari, et al. 2004; Chen et al. 2017; Rice et al. 2017). POT1 binds single-stranded telomere repeats specifically with its two N-terminal OB folds (Lei et al. 2004; Loayza et al. 2004). Together, TPP1/POT1 recruits telomerase to the single-stranded telomeric DNA and stimulates its processivity (Xin et al. 2007; Zhang et al. 2013; Sexton et al. 2014). Deletion of TIN2 in mouse cells causes loss of TPP1 and POT1 telomeric localization to telomeres as detected by immunofluroesence and ChIP (Takai et al. 2011). Expressing a TIN2 allele that does not bind TPP1 cannot rescue the TPP1/POT1 localization defects observed in TIN2 knockout cells (Frescas & De Lange 2014). Additionally, TPP1ΔC22 which lacks the TIN2 binding domain cannot localize to

the telomere when expressed in human cells (O'Connor et al. 2006). We asked whether the TIN2-TPP1 interaction also affects telomerase activity.

Telomerase has two core components: a reverse transcriptase (TERT) and an RNA component (TR). Telomerase binds the 3' telomere end and uses its internal RNA template to align to the single stranded DNA and add nucleotides (Greider & Blackburn 1989; Autexier & Greider 1995). Once it fills in a telomere repeat from its template, it translocates to add more repeats or stops and dissociates (Greider 1991). The term *processivity* refers to the average number of telomere repeats added in a single telomerase binding event.

While it is not precisely known how many telomeres get elongated each cell cycle, or how many repeats are added with each telomere addition event, we know that the processivity is important for maintaining telomere length. Changes to either telomerase catalytic activity or to its processivity are each sufficient to cause short telomere disease in humans (Nelson & Bertuch 2012). Several mutations in TERT that specifically reduce processivity have been identified in short telomere diseases (Alder et al. 2011; Gramatges et al. 2013). Mutations affecting the TPP1 TEL-patch also cause disease through reduced TPP1-telomerase association resulting in decreased processivity (Kocak et al. 2014; Bisht et al. 2016).

Processivity can be measured using an in vitro telomerase assay, called the direct telomerase activity assay (Greider 1991; Sun et al. 1999; Chen & Greider 2003). This assay is performed by providing telomerase a short telomere primer in excess and allowing it to add telomere repeats for a defined amount of time. A more processive enzyme will have longer extension products, while a less processive enzyme will have

shorter extension products. The intensity of the bands on a gel corresponds to the amount of product synthesized at that length. Relative processivity can be determined by calculating the proportion of high molecular weight products to lower molecular weight products. While processivity is traditionally measured by pulse-chase assays, using a vast primer excess assures that the long products come from processivity and not from dissociation and re-binding events (Chen & Greider 2003; Wang et al. 2007).

Telomerase assays have often been performed using enzyme reconstituted in rabbit reticulocyte lysates, because telomerase is not soluble (Gillis et al. 2008). An alternative method is to overexpress components in cells and assay telomerase in cell lysates (Cristofari & Lingner 2006; Latrick & Cech 2010). While using purified proteins allows more control over concentration and stoichiometry, co-expression of telomerase assay components in cell lines ensures proper folding and interactions of the target proteins. A cell-based system overexpressing TERT/TR, POT1, and TPP1 was developed by Nandakumar et. al., and it showed robust telomerase processivity which was used to identify the effects of the TEL-patch residues (Nandakumar et al. 2012). We built on this idea, generating a system overexpressing TERT/TR, TPP1, and POT1, where we were able to introduce different TIN2 constructs with or without the patient mutations to define their effects on telomerase processivity.

We found that wild-type TIN2 stimulates telomerase processivity over that of TPP1/POT1 alone. This stimulation was not seen with the K280E patient mutation. TIN2 stimulation of telomerase required functional TPP1/POT1, as it was not detected in cell lines with TPP1 TEL-patch mutations or cell lines only overexpressing TERT/TR. We conclude that TIN2 cooperates with TPP1/POT1 to stimulate telomerase processivity.

These data suggest that TIN2/TPP1/POT1 function as a heterotrimeric processivity complex that binds ssDNA and stimulates telomerase.

3.2 RESULTS

3.2.1 Generation of Telomerase Assay Cell Lines

To generate telomerase assay cell lines, we wanted to create uniform expression of each of the different components: TERT, telomerase RNA (TR), TPP1, and POT1. Early experiments used transfection of multiple plasmids expressing individual components, but this resulted in high variability in expression and experimental results. To remove sources of variability, we decided to generate cell lines uniformly overexpressing these components where TIN2 could be introduced.

First, we generated a construct with self-cleaving 2A peptides to clone TPP1-POT1-TERT into a single polycistronic expression cassette. This polycistron ensures even expression of the protein components. 2A peptides allow co-expression of proteins from a single transcript by causing ribosome skipping over a specific sequence (Ryan et al. 1991; Ryan & Drew 1994; Doronina et al. 2008; Szymczak et al. 2004). This method has been used to improve expression cassettes for making induced pluripotent stem (iPS) cells, among other applications (Carey et al. 2009). The 2A peptides leave a small tag on the downstream proteins, so TERT was added in the last position of the expression cassette because it is not functional with C-terminal tags (Counter et al. 1998; Armbruster et al. 2001; Chiba et al. 2017). 3X-FLAG tagged TERT, TPP1, and POT1 constructs were a kind gift from the JK Nandakumar and the Cech lab. The FLAG tag allows all three proteins to be detected together in a western blot. We also created a construct with

a TPP1 TEL-patch mutation, E169A/E171A (Nandakumar et al. 2012), that will be referred to as TPP1^{TEL} and a construct expressing TERT only to test the dependence of TIN2 on TPP1/POT1 (Figure 3.1A).

We cloned the polycistronic expression cassettes into the pcDNA5-FRT vector for use in the TREx FLP-in system, and flanked the cassette with restriction sites for cloning into other expression vectors (see Materials and Methods). These FLP-in cell lines have an FRT site located at a single genomic locus along with a promoter and start codon for the selectable marker. The FRT expression vectors contain a selectable Hygromycin marker lacking a promoter and ATG start codon, so they will only survive selection if the plasmid is integrated at the correct genomic locus. By using this system, we can ensure that each cell has one copy of the expression construct.

Before incorporating the protein expression cassettes, we transduced 293TREx FLP-in cell lines with a telomerase RNA expressing lentivirus and selected high TR expressing clones for uniform background overexpression of TR. Then, we used the FLP-in system to integrate each expression construct into a single genomic locus. The three resulting cell lines will be referred to as TPP1/POT1/TERT, TPP1^{TEL}/POT1/TERT, or TERT only (Figure 3.1B).

We validated protein expression by a FLAG western blot in parallel with transfection of the individual components and saw that all three proteins were expressed (Figure 3.1C). We did not observe high molecular weight species that would indicate failure of 2A peptide cleavage. Interestingly, we noticed that TERT expression is much

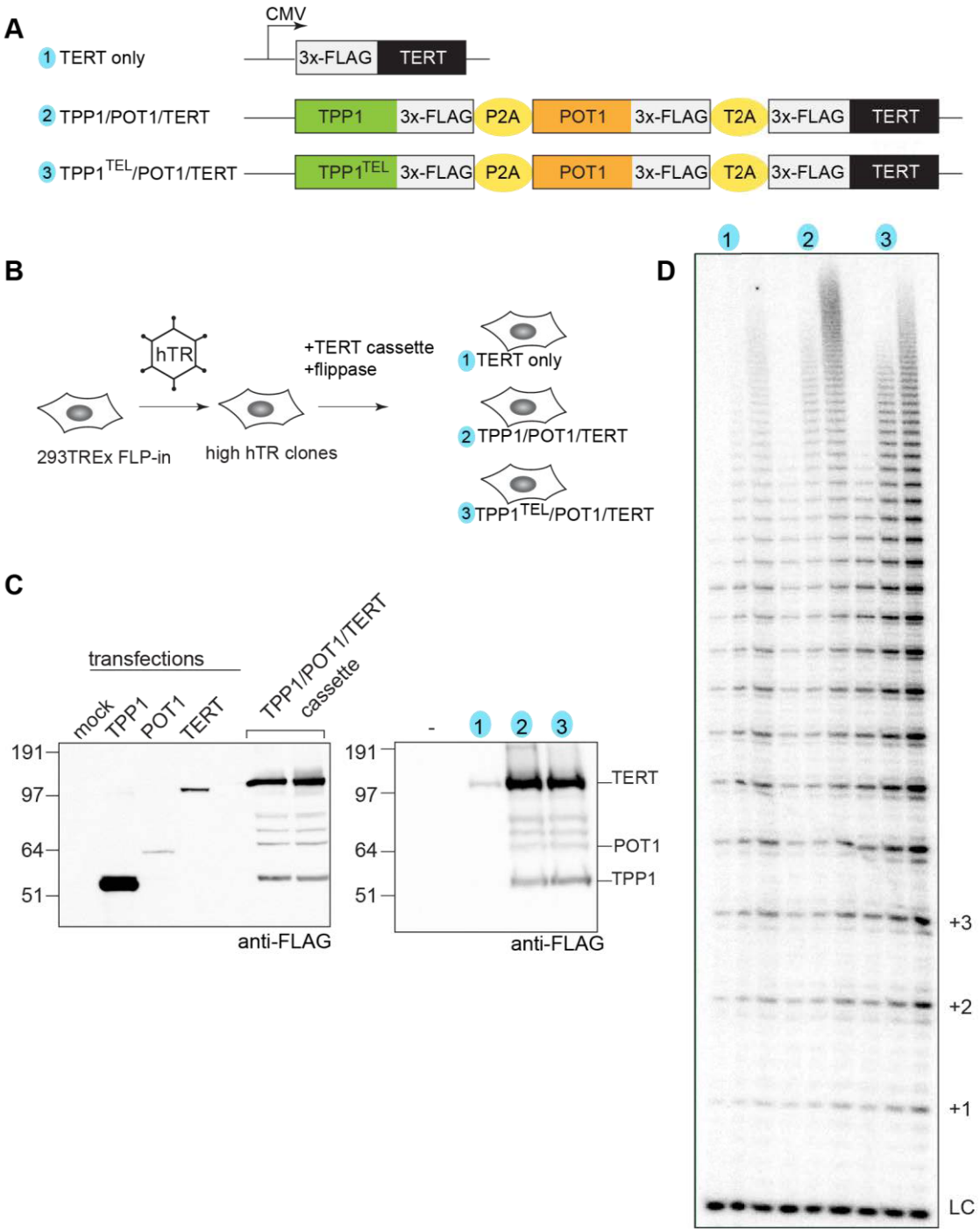

Figure 3.1 Generation of Telomerase Assay Cell Lines
(**A**) Schematic of the expression constructs used in this study. (**B**) Flowchart of cell line generation (**C**) FLAG western blot of telomerase assay cell lines. Transfections of TPP1, POT1, and TERT serve as size references from the bands generated from the expression cassettes (left). Slight size shifts result from the amino acids from the 2A peptide. Bands above POT1 are unidentified but may be TERT degradation products. (**D**) Telomerase assays stopped at 10, 20, and 40 minutes for each cell line. Telomere repeats are indicated by +1, +2, etc. LC=loading and purification control

higher in the polycistronic context than alone. We tested a GFP-2A-TERT construct to see if the polycistronic context would give higher TERT expression, but that cell line also had low TERT expression. We have not been able to determine if this difference is an artifact of the expression system or due to stabilization of the telomerase by TPP1/POT1 (Appendix G). We also observed two unidentified bands in the polycistron cell lines that may be TERT degradation products based on their size.

Telomerase assays were performed by incubating 3-5µl of clarified cell lysates with a telomere seed primer a5 (TTAGGGTTAG**C**GTTAGGG) (Lei et al. 2005; Wang et al. 2007) at 30°C for the indicated time. Products were purified and separated on a sequencing gel (see Materials and Methods). In telomerase assays of the parent cell lines, stopped after 10, 20, or 40 minutes, the TPP1/POT1/TERT cell line has higher processivity, indicated by the intensity of the higher molecular weight bands, than the $TPP1^{TEL}$/POT1/TERT or TERT only cell lines (Figure 3.1 D).

3.2.2 Method of Processivity Calculation

Telomerase processivity can be quantified in several ways. Telomerase catalytic activity of the enzyme is assessed by measuring the intensity of the first repeat, and specific activity refers to the total activity relative to the amount of telomerase in the reaction. Processivity is independent of the amount of enzyme in the reaction and only depends on the ratio of different size bands within a lane.

When the major pause bands can be discriminated on a gel, each band is quantified and normalized to the number of radioactive dGTPs incorporated and to the total intensity of repeats below it. Plotting this relative intensity against repeat number generates a line with negative slope, as telomerase has a higher probability of dissociating

over time. In this method of processivity calculation, the telomerase processivity is defined by the repeat number where the intensity is half maximal. For more details, see Materials and Methods.

A simpler way to measure processivity is also necessitated by the inability to separate and quantitate high molecular weight bands generated by processive telomerase. This relative processivity measure called the "+15 method" measures the relative intensity of the high molecular weight bands from repeat 15 and above, and expresses it as a ratio to the total intensity of a lane. This method does not account for the number of radioactive dGTP incorporated into the high molecular weight bands, which should be considered a caveat for this measurement. However, it has successfully been used to identify changes in processivity (Nandakumar et al. 2012).

3.2.3 TIN2 forms a complex with TPP1/POT1/TERT

To determine whether TIN2 interacts with the TPP1/POT1/telomerase complex, we performed reciprocal co-immunoprecipitations of myc-tagged TIN2 and FLAG-TPP1/POT1/TERT. We transfected TIN2S, TIN2M, TIN2L, or the full-length gene with or without the K280E patient mutation, and GFP as a negative control.

Using a myc antibody to pull down TIN2, we saw that TPP1, POT1, and TERT all co-immunoprecipitated with TIN2 but not with the GFP control (Figure 3.2A). Using the reciprocal FLAG immunoprecipitation, we pulled down FLAG-TPP1, FLAG-POT1, FLAG-TERT complexes and saw a co-immunoprecipitation of all TIN2 isoforms (Appendix H). The patient mutations did not affect the association of TIN2 with these complexes. These assays, however, are not quantitative, so minor changes in the distribution of TIN2-containing complexes may not have been detected.

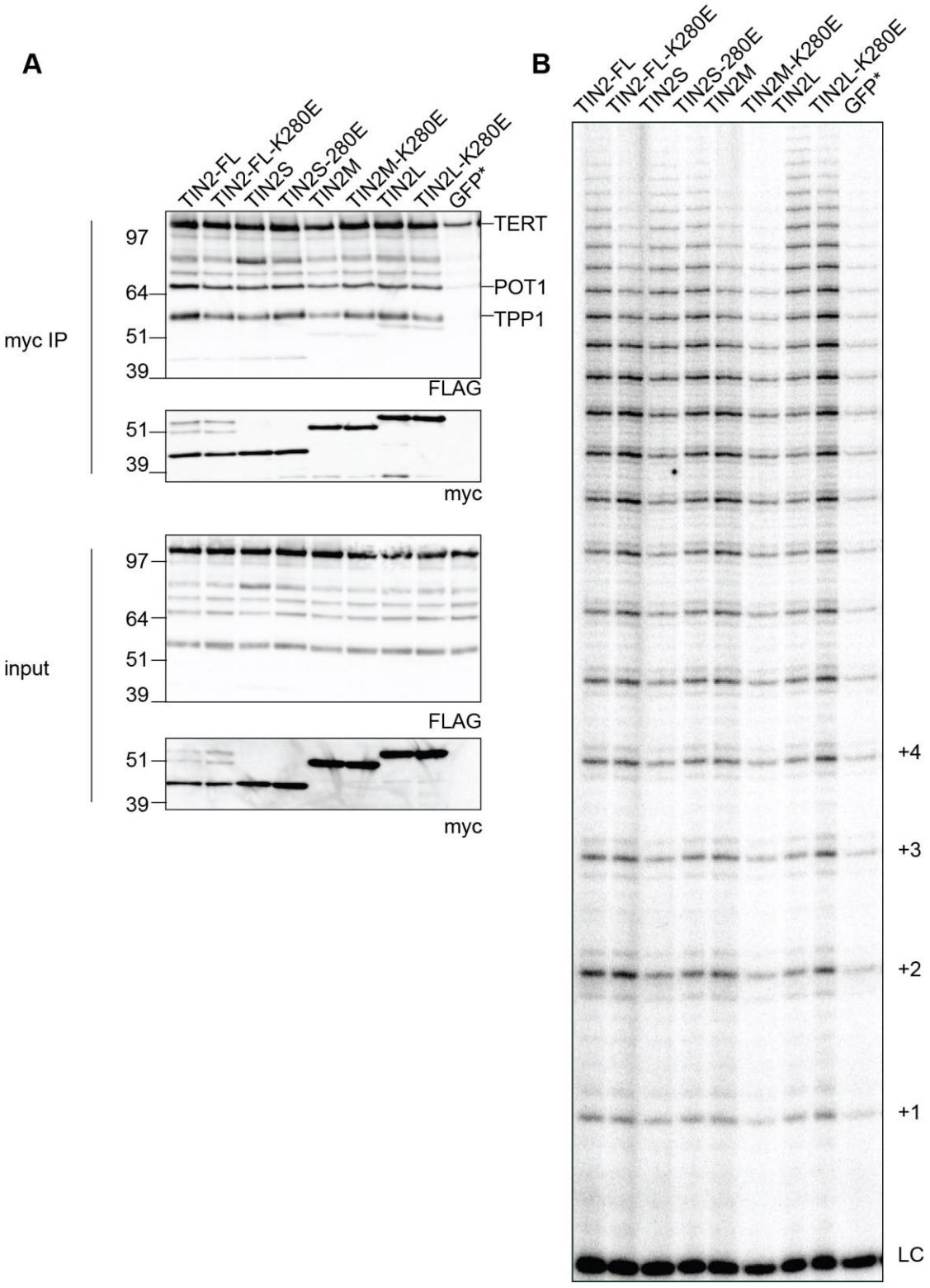

Figure 3.2 TIN2 forms a complex with TPP1/POT1/TERT.
(**A**) myc-TIN2 was transfected into TPP1/POT1/TERT cell lines. TIN2 complexes were immunoprecipitated with anti-myc. Top: western blot with myc and FLAG on myc-TIN2 immunocomplexes. Bottom: input. (**B**) Telomerase assays performed on myc-TIN2 immunocomplexes.

The telomerase enzyme that co-immunoprecipitates with TIN2 in these experiments is fully functional, active enzyme (Figure 3.2B). There is some background activity in the GFP negative controls (Figure 3.2A and B, asterisk). Still, all of the TIN2 IP samples had high amounts of telomerase activity, indicating that the TIN2-TPP1-POT1-telomerase complexes are active. Assays on TIN2 immunocomplexes were highly variable, however, so tests of telomerase function with TIN2 were performed on the whole cell lysates.

3.2.4 TIN2 stimulates telomerase processivity

To examine the effects of TIN2 on telomerase cell lines, we used several methods to introduce TIN2 into the telomerase assay cell lines. First, we transfected either the TIN2 full-length gene or individual TIN2 isoforms, and second we added increasing amounts of recombinantly expressed and purified TIN2L to prepared telomerase assay lysates. These assays are highly sensitive to stoichiometry of TIN2 with TPP1/POT1, but by using these approaches we have assayed telomerase in an excess of TIN2. By transfecting high amounts of TIN2 expression constructs, we hope to have all cells in the population transfected, thereby removing fluctuations in the experimental conditions.

Transient transfection of the full-length TIN2 gene (TIN2-FL) showed that all three isoforms were expressed with or without the patient mutations (Figure 3.3A). Direct telomerase assays on the TPP1/POT1/TERT cell line showed a surprising increase in telomerase processivity when cells were transfected with TIN2-FL compared to transfection of GFP (Figure 3.3B). The processivity stimulation was evident from the appearance of higher molecular weight bands at the 10-minute timepoint. TIN2-FL with

the K280E mutation, however, was unable to stimulate telomerase, and appeared to have slightly lower processivity than the GFP control. While we predicted that the TIN2 mutation might decrease processivity, we had not anticipated that TIN2 might actually stimulate telomerase beyond the processivity stimulation provided by TPP1/POT1.

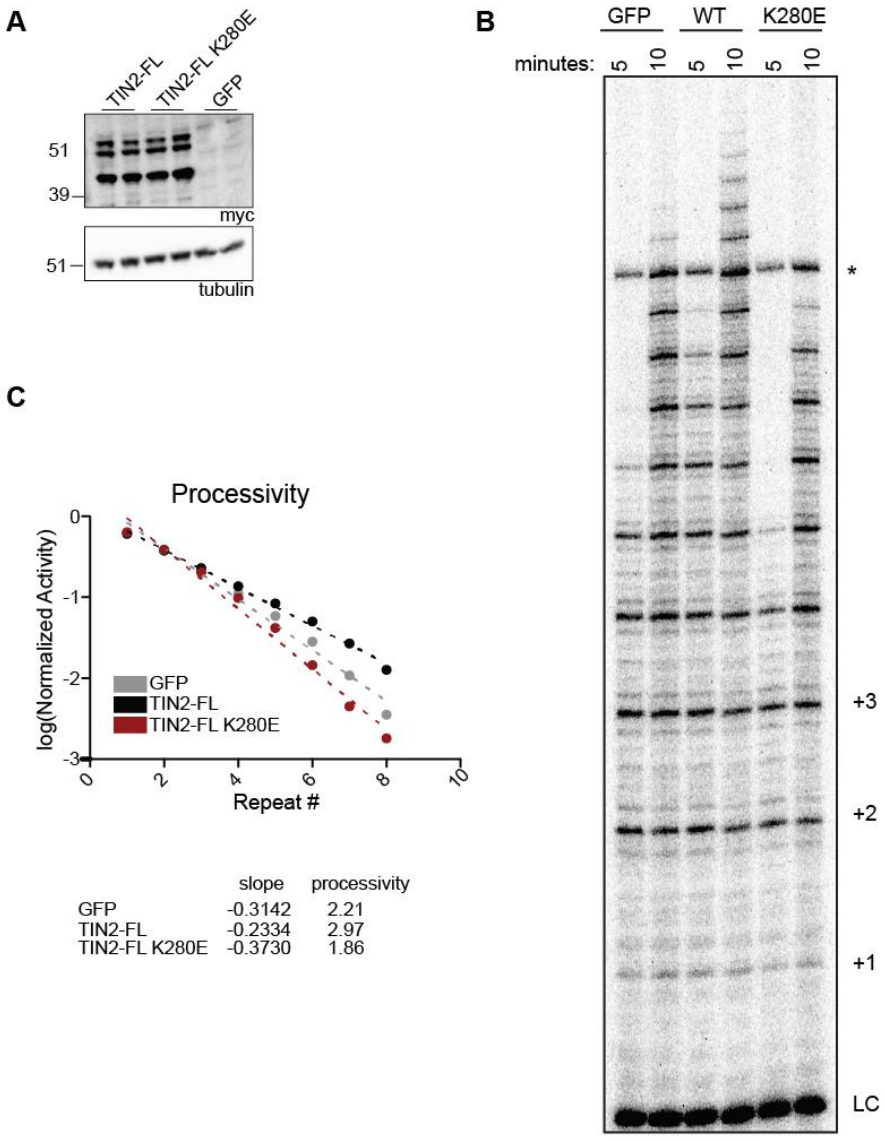

Figure 3.3 TIN2-FL stimulates telomerase processivity.
(**A**) Western blots of duplicate transfections of TIN2-FL, TIN2-FL K280E, or GFP into TPP1/POT1/TERT cell lines. (**B**) Telomerase assays of transfections from *A*, stopped after 5 or 10 minutes. LC, loading and purification control; +1, 2, etc, repeat number; *=nonspecific band. (**C**) Quanitification of assays in *B*. The log of normalized activity was plotted against repeat number according to the decay method of calculating telomerase processivity. Slopes and processivity values are displayed below the graph.

To determine if specific isoforms might be required for processivity stimulation by TIN2, we independently transfected the three different isoforms with an N-terminal myc tag into the TPP1/POT1/TERT cell line. We found a 10-20% stimulation of telomerase processivity with each of the isoforms. This result indicates that all three isoforms are able to stimulate telomerase processivity. It should be noted that there was no effect of C-terminally tagged TIN2S or TIN2L on telomerase in TPP1/POT1/TERT cell lines in previous assays, suggesting the C-terminal tag may interfere with TIN2 function (Appendix I).

3.2.5 TIN2 stimulation of processivity requires TPP1/POT1

To test whether processivity stimulation is dependent on TPP1/POT1/TERT, we repeated the transfections in the $TPP1^{TEL}$/POT1/TERT cell lines and in the TERT only cell lines. We found no stimulation of telomerase processivity in these cell lines (Figure 3.4, B and C). These results indicate that TIN2 stimulation of telomerase is dependent on TPP1/POT1.

As a third method to examine telomerase processivity, we added recombinant TIN2L, expressed and purified from *E. coli*, to telomerase assay lysates. First, we tested whether the N-terminally his-MBP-tagged TIN2L co-immunoprecipitates with TPP1/POT1/TERT by adding increasing amounts of his-MBP-TIN2L to the lysates and performing a FLAG immunoprecipitation (Figure 3.5A). We saw that his-MBP-TIN2L co-immunoprecipitated with the FLAG-complexes.

Using the range of TIN2 concentrations that bound to the FLAG complexes in the immunoprecipitations, we then added increasing amounts of his-MBP TIN2L to TERT/TPP1/POT1 lysates and tested telomerase processivity. Purified MBP alone served

as a negative control. We saw that 375nM TIN2 stimulated telomerase processivity (Figure 3.5 B and C). Adding more TIN2 beyond that amount did not further stimulate telomerase, indicating that the stoichiometry between TIN2, TPP1, and POT1 is more

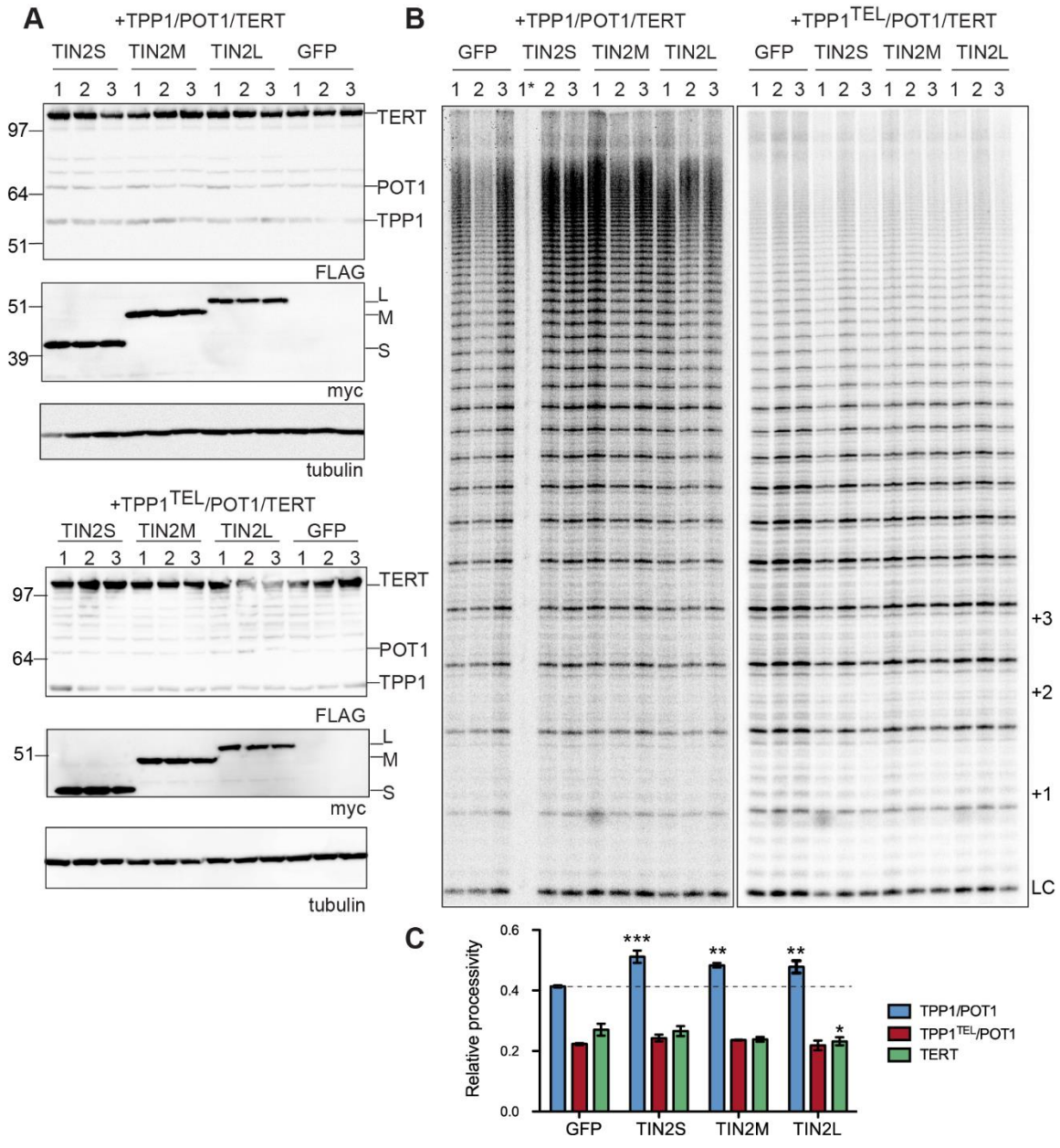

Figure 3.4 TIN2 isoforms stimulate telomerase through TPP1/POT1.
(**A**) Western blots of myc-TIN2 isoform triplicate transfections into TPP1/POT1/TERT or TPP1^{TEL}/POT1/TERT cell lines. TIN2 isoforms are indicated on the right of the myc blots. FLAG proteins are also labeled. (**B**) Telomerase assays stopped after 40 minutes of elongation. *=sample lost in preparation. (**C**) +15 quantification of samples in *B* and from results in the TERT only cell line. Data from each cell line was analyzed with a one-way ANOVA and Bonferroni's Multiple Comparisons test against the GFP control. ***, $p<0.001$; **, $p<0.01$; *, $p<0.05$.

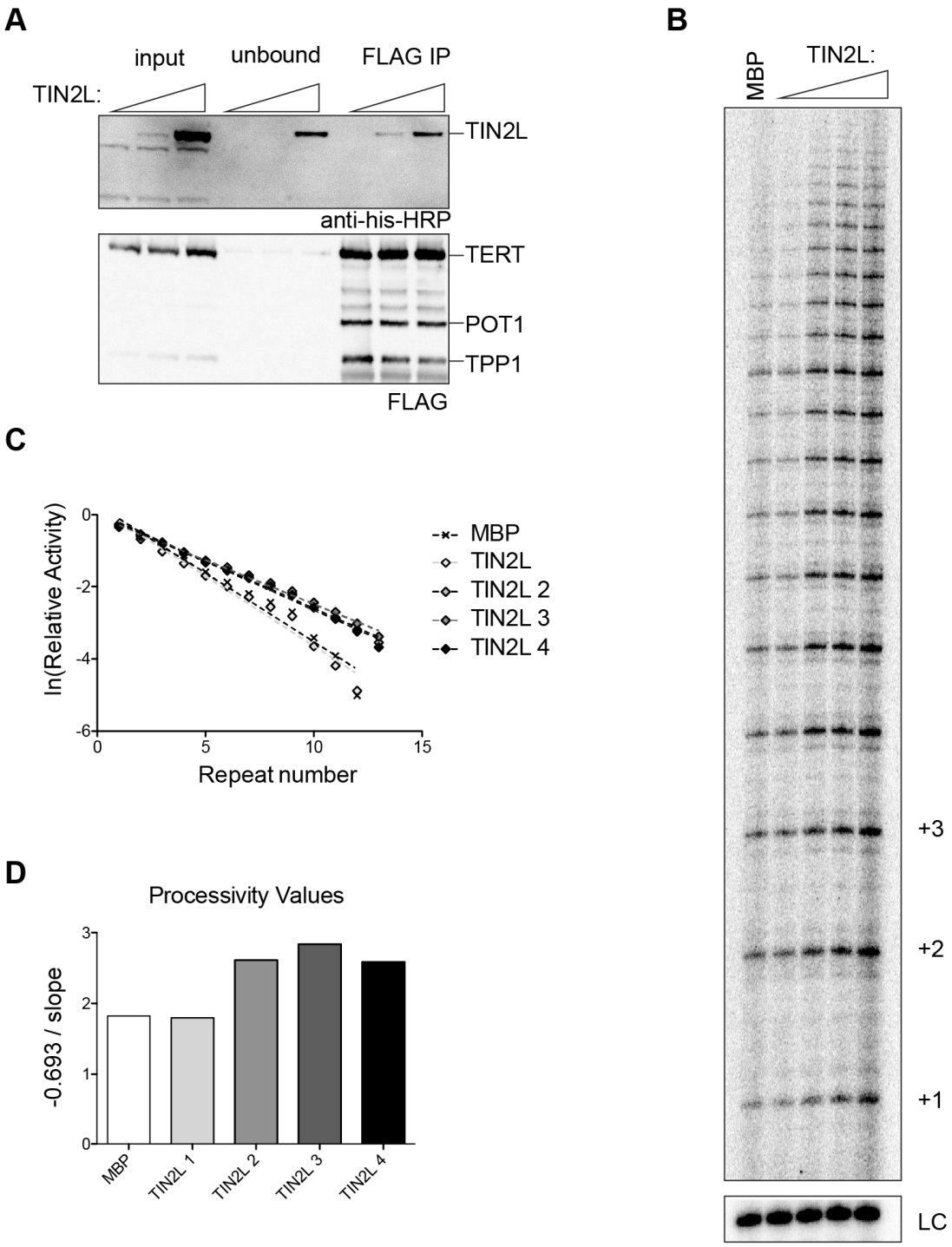

Figure 3.5 Recombinant TIN2L stimulates telomerase.

(**A**) FLAG immunoprecipitation of TPP1/POT1/TERT lysates with increasing amounts of recombinant his-MBP-TIN2L. TIN2L is probed with an anti-his-HRP antibody. Unbound = 10µl of the supernatant after incubation with antiFLAG-agarose beads. (**B**) Telomerase assays stopped at 10 minutes with (125nM-1.25µM) his-MBP-TIN2L or 1.25µM MBP as a negative control. (**C**) Quantification of the direct assay using the decay method of calculation (See Materials and Methods). Slope from a linear regression was used to calculate the processivity values shown in D.

important than the total amount of TIN2 in the reaction. MBP did not stimulate telomerase, indicating that the processivity stimulation is specific to the TIN2 protein and not due to the buffer content or increased protein in the samples. This data supports the conclusion from our other experiments that TIN2 completes the TPP1/POT1 telomerase processivity complex.

3.3 DISCUSSION

We have shown that all three TIN2 isoforms form a complex with TPP1/POT1 and telomerase and stimulates telomerase processivity through interaction with TPP1/POT1. The reproducible 10-20% increase in processivity suggests that TIN2 completes the TPP1/POT1 telomerase processivity complex. TIN2 could stabilize both the TPP1-telomerase interaction and the POT1-ssDNA interaction. This could result in a higher percentage of fully assembled, processive telomerase complexes or extend the lifetime of telomerase on the telomeric DNA.

While all three TIN2 isoforms stimulated telomerase in a TPP1-dependent manner, potential functional differences between the isoforms cannot be discounted. We saw stimulation of telomerase in N-terminally but not C-terminally tagged TIN2 constructs (Appendix I), and the differences in the three isoforms are at the C terminus. This supports our hypothesis that the TIN2 C-terminus is functionally important. Further studies on the isoform differences and the C-terminal extensions in TIN2M and TIN2L to identify interaction partners or tertiary structures are required to understand the mechanism of TIN2 function.

In addition to our finding of TIN2's participation in the processivity complex, it has previously been shown that TIN2 is required for several specific TPP1/POT1 functions in cells. TIN2 floxed mouse cell lines show less telomeric TPP1/POT1 localization by immunofluorescence (IF) and trigger ATM and ATR DNA damage responses (Takai et al. 2011). Knockdown of TIN2 by shRNA in HeLa cells similarly showed less TPP1/POT1 localization to the telomere by IF and was associated with less telomerase detected at the telomere by ChIP and FISH (Abreu 2010). Similarly, disruption of TIN2 telomeric localization by mutating the FxLxP TRF1 binding motif interaction prevents TPP1/POT1 accumulation at telomeric DNA in mouse cells, but localization can be rescued by tethering TIN2 to TRF2 (David Frescas & de Lange 2014a). Finally, deletion of the TPP1 binding region from mouse TIN2 also prevents localization of TPP1/POT1 to telomeres detected by IF (Frescas & De Lange 2014).

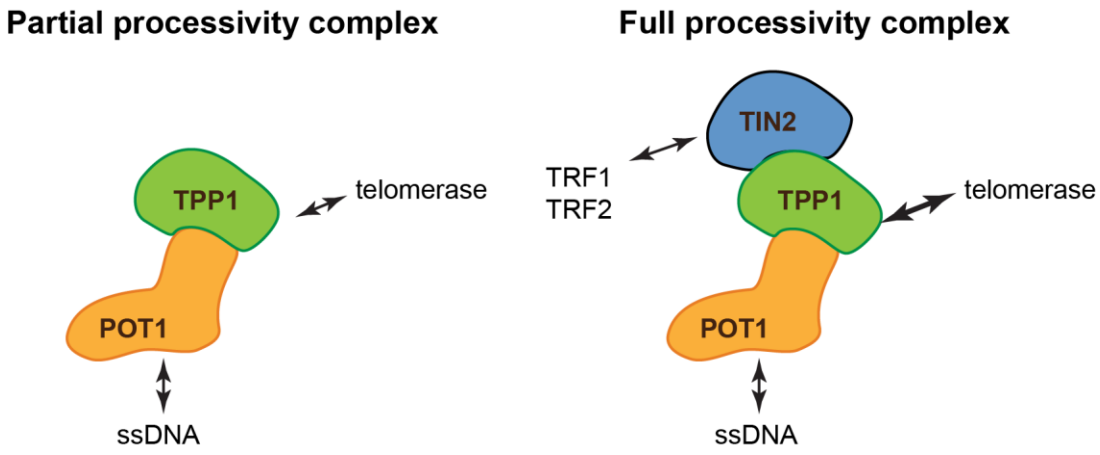

Figure 3.6 TIN2 completes the TPP1/POT1 processivity complex.
TIN2 may be stimulating processivity by completing the telomerase processivity complex. Forming a complex with TIN2 could enhance TPP1/POT1 stimulation of telomerase as well as enhance POT1-ssDNA interactions and aid in localization to the telomere through TIN2 interactions with TRF1 and TRF2.

Because TIN2 binds TRF1, TRF2, and TPP1/POT1, it is generally referred to simply as a "tether" or "bridging" molecule required to bring together the shelterin components, stabilizing them at the telomere. Our data suggest that TIN2 is part of the TPP1/POT1 complex. One main function of this heterotrimeric subcomplex is to bind single-stranded DNA and regulate telomerase, and TIN2 serves an important role of localizing the complex to the telomeres through its TRF1 and TRF2 interactions (Figure 3.6).

Further evidence for a TPP1/POT1/TIN2 heterotrimeric complex is the apparent stoichiometry of the proteins. We saw in the recombinant TIN2 assays that TIN2 only stimulated telomerase when it reached a certain concentration, which by co-immunoprecipitation appeared to be stoichiometric with TPP1/POT1. Excess TIN2 could not further stimulate telomerase, probably because there were no more free TPP1/POT1 complexes to interact with. Our data suggest the mechanism for TIN2 stimulation of telomerase is that TIN2 stabilizes the telomerase and processivity factor complexes by completing the heterotrimeric TPP1/POT1/TIN2 complex. POT1 is less stable in the absence of TPP1, which is consistent with their function as a heterodimer (Chen et al. 2017). TIN2 appears to cooperate with TPP1/POT1 function, suggesting they are actually a higher order heterotrimeric complex.

Previous work showed that TPP1/POT1 increases telomerase processivity (Wang et al. 2007), and we observed 10-20% stimulation on top of the TPP1/POT1 contribution when including TIN2. Our results are similar to recent observations of the telomerase processivity factors in *Tetrahymena*. *Tetrahymena* p50 and Teb1 were identified as telomerase processivity factors, just as TPP1/POT1 are known to stimulate human

telomerase (Min & Collins 2009). Subsequently it was found that additional factors from *Tetrahymena* further stimulate telomerase processivity and are part of the p50/Teb1 complex (Upton et al. 2017).

Based on a cryo-electron microscopy (cryo-EM) structure of the *Tetrahymena* telomerase holoenzyme, it was found that Teb1 forms an RPA-like complex, TEB, with two previously unknown proteins, Teb2 and Teb3 (Jiang et al. 2015). While p50-Teb1 contribute to the majority of the processivity stimulation, including the complete TEB complex in telomerase assays resulted in even further stimulation of telomerase processivity (Upton et al. 2017). Our findings with TIN2 and TPP1/POT1 are analogous to this observation.

Alterations in both telomerase activity and processivity are sufficient to cause disease in humans. We have shown here that TIN2 patient mutations have defects in the stimulation of telomerase through TPP1-POT1, suggesting that the mechanism of disease may be loss of telomerase processivity. Many TIN2 patients, however, experience rapid telomere shortening in one generation, which cannot be accounted for by loss of telomerase function alone. Given that TIN2/TPP1/POT1 form a single-stranded binding complex, we suggest they may also have roles in coupling telomere replication with telomerase activity. Uncoupling these processes may cause the rapid telomere loss that is seen in many TIN2 patients. In the next chapter we discuss how telomeric single-stranded binding proteins may coordinate telomere end protection, telomerase regulation, and telomere replication.

3.4 MATERIALS AND METHODS

3.4.1 Telomerase Expression Constructs

TPP1-POT1-TERT

Starting plasmids were a kind gift from the Cech Lab, p3x-Flag-POT1-cDNA6/Myc-HisC, p3x-Flag-TPP1-cDNA6/Myc-HisC, p3x-Flag-TERT-cDNA6/Myc-HisC. Note that TPP1 starts at Met87 (Nandakumar et al. 2012). We generated $TPP1^{TEL}$ by engineering the E169A/E171A mutation with site-directed mutagenesis primers A150/A151. We used the expression vector pcDNA5-Lox-Stop-Lox, which was generated by Jon Alder by adding an additional lox-bGH-lox after the bGH polyA signal in pcDNA5-FRT. This was initially chosen because we tried to express hTR from the same vector after TPP1-POT1-TERT cassette, but this alone did not produce sufficient hTR expression for telomerase activity.

Plasmids were designed with unique restriction sites BstBI and NotI flanking the polycistronic expression cassette for cloning into different vectors.

The cloning of the TPP1/POT1/TERT expression cassettes required a two-step approach because of the repetitive nature of the 3X-FLAG tags and 2A peptide sequences. In the first round of Gibson Assembly, POT1-2A-TERT was generated. POT1 was amplified with primers A76/A77, and TERT was amplified with A78/A71. The overlapping repetitive region with 3xFLAG-T2A-3XFLAG was synthesized as an IDT gBlock (A74, Appendix A). Because of the repetitive nature and GC-content of the codons in this region, we were required to engineer silent mutations, which are indicated in Appendix A. The pcDNA5-LSL vector was digested with AgeI/SbfI. Digested vector and POT1 and TERT amplicons were gel purified. 50ng vector was assembled with 3-fold molar excess of the POT1, gBlock, and TERT inserts using 2X Gibson Master Mix

according to the manufacturer protocol (NEB E2611). Reactions were transformed into NEB5α cells and colonies were screened for correct insertion of the fragments.

In the second round of Gibson Assembly, TPP1-P2A was incorporated into the POT1-2A-TERT cassette (Figure 3.6B). TPP1 or TPP1^{TEL} was amplified with primers A79/A80. The vector backbone from round one was opened with AgeI restriction digest. TPP1 amplicons and opened vector were gel purified. 50 ng backbone was assembled with 3-fold molar excess of TPP1 amplicon and 3X-FLAG-P2A gBlock.

PCR amplifications were performed with Phusion High-Fidelity DNA polymerase (NEB M0530) using the manufacturer protocols with the following changes. For all reactions, 5X GC buffer was used instead of HF buffer. TERT reactions were supplemented with 3.5 µl DMSO, and POT1 reactions were supplemented with 3.5 µl DMSO and 2.0 µl $MgCl_2$ that was supplied by the manufacturer. Reactions were performed in 50µl volumes. The PCR program was:

Denature	0:30	98°C
38 Cycles:	0:30	98°C
	0:15	48°C (POT1) or 55°C (TERT, TPP1)
	0:60	72°C
Final Extension	7:00	72°C

TPP1/POT1/TERT and TPP1^{TEL}/POT1/TERT were screened it by restriction digest and sequence verified using primers T7, bGH-Rev, and A87-A97. We found one T>C base change in TPP1/POT1/TERT, but it was a silent mutation that did not change the coding sequence. TERT only expression constructs were generated by PCR amplification of the 3XFLAG-TERT with A120/A121 and Gibson Assembly into pcDNA5-LSL. Sequence verified plasmids were used for generation of the telomerase assay cell lines.

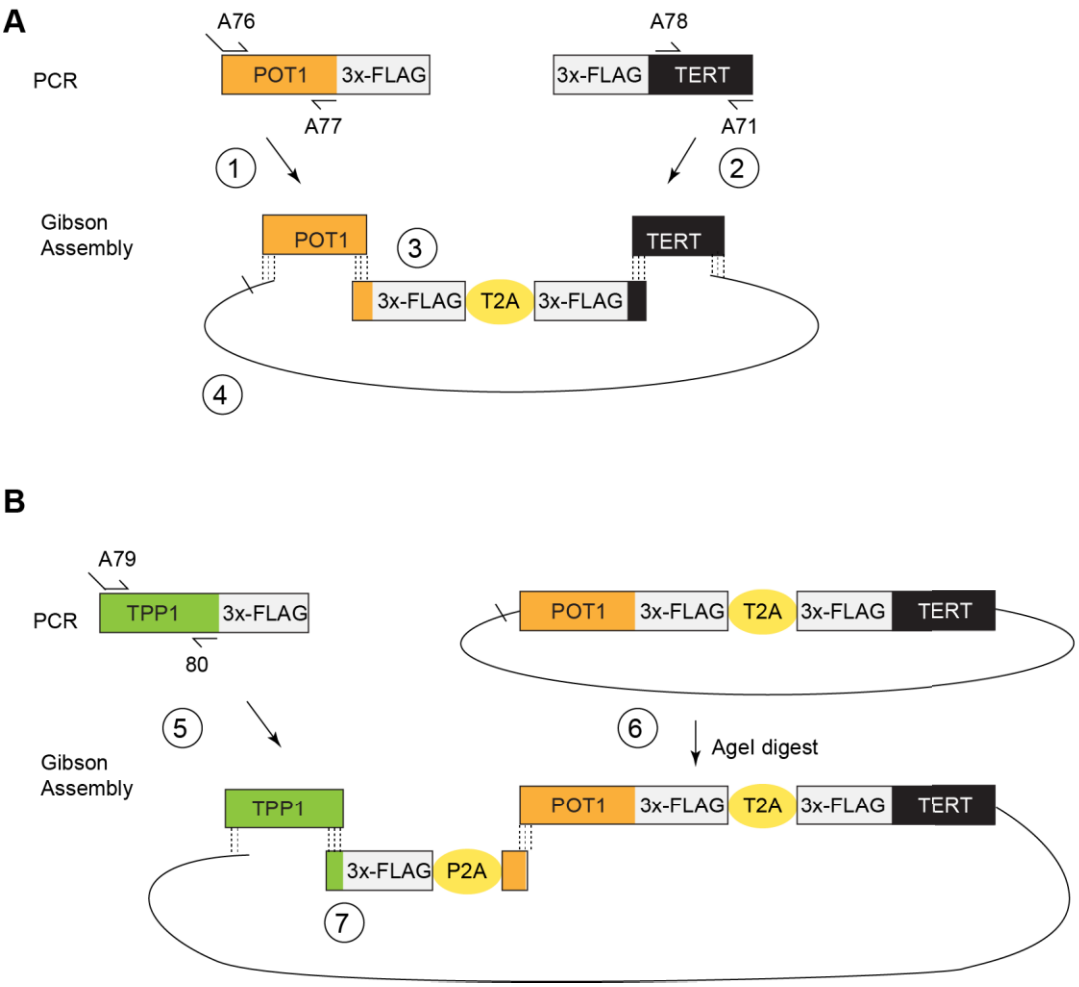

Figure 3.7 Cloning Scheme for TPP1-POT1-TERT construct.
(**A**) First Round 1 – POT1 amplification; 2-TERT amplification; 3- A74 gBlock; 4- pcDNA5-LSL vector
(**B**) Second Round. 5 – TPP1 amplification 6- AgeI digest of the product of Round 1; 7-A75 gBlock.

3.4.2 Telomerase Overexpression Cell lines

For stable hTR overexpression, pBluescript II SK(+)U1-hTR (Wang et al. 2007) was cloned into FUPW, a FUGW-derived lentiviral backbone where Puro was cloned into the GFP site with BamH1 and EcoR1. Virus was generated as described in Appendix E. 293TREx FLP-in cells were transduced with the FUPW-hTR lentivirus, selected with puromycin and cloned by limiting dilution. hTR expression of the resulting clones was measured by qRT-PCR. The TERT, TPP1-POT1-TERT, or TPP1^{TEL}-POT1-TERT

construct was subsequently flipped into a single genomic FRT site in one of the high hTR overexpressing clones using the Flp-in system (Invitrogen).

3.4.3 Quantitative RT-PCR of hTR

To measure hTR expression levels, RNA was isolated from FUPW-hTR transduced clones with the RNeasy Kit (Qiagen, 74104) following the manufacturer protocol with a 1 hour on-column DNase digestion using the RNase-free DNase kit (Qiagen, 79254) to remove any genomic DNA. 1 µg of RNA was reverse transcribed from with random hexamer primers using the SuperScript III First Strand Synthesis Kit (Qiagen, 18080-051). Quantitative RT-PCR was performed on a Bio-Rad CFX96 thermocycler with approximately 5ng cDNA, 1X IQ SYBR Green Supermix (Bio-Rad, 1708884BUN), and 5 µM primers. Samples were measured in triplicate. Every plate contains a no template control for background and a no-RT control for DNA contamination. hTR primers are GGAAGCTTGCTAGCGCACCGGGTTG and GTT TGCTCTAGAATGAACGGTGGAA. hTR levels were normalized to ARF3, which is measured with primers A21 and A22 (Cristofari & Lingner 2006) (Appendix A). Relative quantification (Δ(ΔCt) Method) was used to determine hTR expression level relative to non-transduced cells.

3.4.4 Preparation of telomerase assay lysates

Transfections

For TIN2 transfections, 5 x 10^5 cells of the respective telomerase assay cell line were plated in each well of a 6-well dish. The next day, the indicated TIN2 or GFP construct was transfected with Lipofectamine 2000 (Invitrogen 11668019) following the manufacturer protocol, using 8 µl Lipofectamine 2000 and 2.5 µg DNA per well diluted

in Opti-MEM (Gibco 31985088, 51985034). Transfected cells were incubated for 48 hours before harvesting.

Preparation of cell lysates

Cells were disrupted by pipetting and transferred to a conical tube, pelleted at 500xg for five minutes, washed once with PBS, then resuspended in 1ml 1X PBS and transferred to a microfuge tube. Cells were pelleted again with a quick spin in a benchtop centrifuge, all supernatant was removed, and pellets were resuspended in 100µl 1X CHAPS buffer (10mM Tris-HCl, pH 7.5, 1 mM $MgCl_2$, 1mM EGTA, pH 8.0, 0.1 mM Benzamidine, 5mM β-Mercaptoethanol, 0.5% CHAPS, 10% glycerol). Cells were either snap-frozen on dry ice until lysis or lysed immediately on ice for 30 minutes, with occasional vortexing. Lysates were clarified by a 10 minute spin at 8000xg at 4°C and transferred to a new tube. A western blot aliquot was taken and telomerase assays were either performed immediately or clarified lysates were snap frozen and stored at -80°C until use. Telomerase activity appears stable after storage at -80 and several freeze-thaw cycles, but freeze-thaw should be kept to a minimum.

3.4.5 Western Blotting

Western blot samples were made with 10 µl telomerase assay lysate, 10µl 4X LDS (Invitrogen, NP0008), 4 µl 500mM DTT, and 16 µl water and denatured at 65°C for 10 minutes. 10-15 µl prepared samples were separated by reducing, denaturing PAGE electrophoresis on a 4-12% Bis-Tris gel (NuPAGE, NP0323) in 1X MOPS buffer (Invitrogen, NP0001) and transferred to PVDF (Immobilon FL, IPFL00010) in 1X NuPAGE Transfer Buffer (Invitrogen, 00061) with 10% Methanol. 3 µl of the SeeBlue

Plus2 (Thermo, LC5925) prestained ladder are included to estimate molecular weight. Membranes are then blocked in 1X TBS + 0.1% Tween20 (TBST), 5% milk (Bio-Rad 170-6404) for 30 minutes at RT or overnight at 4°C. Primary antibody was diluted in blocking buffer and incubated with agitation at room temperature for 30 minutes to 2 hours. Primary antibodies and concentrations are as follows: mouse anti-myc 4A6 (Millipore 05-24), 1:2000; rabbit anti tubulin (Abcam, ab6046), 1:5000; mouse anti-FLAG M2 (Sigma F1804), 1:5000. Blots were washed 3 times with TBST and incubated with the appropriate secondary, anti-rabbit HRP or anti-mouse HRP (Cell Signaling), diluted 1:10,000 in TBST. After 3 washes with TBST, blots are developed with SuperSignal West chemiluminescence substrate (Thermo, PI34095) and imaged on an ImageQuant LAS4000 imager.

3.4.6 Co-Immunoprecipitation of TIN2 Complexes

Immunoprecipitations were carried out using either anti-FLAG M2 affinity gel (Sigma A2220) or anti myc resin, either anti-c-myc agarose (Pierce 20168) or anti-myc tag 4A6, agarose conjugate (Millipore 16-219). Beads were prepared for reactions by transferring 5-20 µl slurry per reaction into a microfuge tube, washing 3-5 times with 1X PBS, equilibrating in 1X CHAPS, and aliquoting to tubes for each sample. 45 µl lysate was added to each tube and brought up to suitable volume (~300-400µl) using 1X PBS. Samples were incubated in an end-over-end mixer at 4°C for two hours. Beads were pelleted with a quick spin, washed 4 times with 300 µl 1X CHAPS buffer, and either resuspended in either 1X LDS loading dye for western blot analysis or equilibrated in 1X telomerase assay buffer for telomerase assays.

3.4.7 Direct Telomerase Activity Assay

Lysates were prepared as described above. For recombinant TIN2L assays, telomerase assay lysates were prepared without transfection, and recombinant TIN2L was diluted in 1X telomerase assay buffer to the specified concentration. Recombinant TIN2L concentrations were measured using the Qubit Protein Assay Kit (Invitrogen Q33211).

Five microliters (5 µl) of the indicated lysate was incubated with a5 primer (49) and 0.5 mM dTTP, 0.5 mM dATP, 2.92 µM dGTP, and 0.33 µM α32P-dGTP (Perkin Elmer) in telomerase buffer (50 mM Tris-Cl, 30 mM KCl, 1 mM MgCl2, 1 mM spermidine). Reactions were incubated for the indicated time minutes at 30°C, terminated with 120 µl stop buffer (20mM EDTA, 10mM Tris), spiked with 500-750 cpm end-labeled 18-mer purification control per reaction.

Protein was removed by adding 140µl 1:1 phenol:chloroform, vortexing briefly, and spinning at max speed for 2 minutes. The upper aqueous layer was transferred to a new tube with 60µl 7.5M sodium acetate (NH_4OAC; Sigma A2706) and 5 mg glycogen (Life Technologies, AM9510) for ethanol precipitation. 540µl ethanol was added to the tubes and samples were allowed to precipitate on dry ice for one hour or at -80°C overnight. Tubes were spun at 4°C for 30 minutes at maximum speed to pellet the DNA and pellets were washed with 500µl 70% ethanol. After all residual ethanol was removed, telomerase products were resuspended in 4 µl water and 4 µl 2x formamide loading dye, denatured at 100°C for 5 minutes, and separated on a sequencing gel (10% acrylamide, 7 M urea 1x TBE), at 90 W for 1.5 hr. The gel was dried onto filter paper, exposed to a phosphor screen, and scanned on a Storm 825 scanner.

3.4.8 Quantitation of Direct Assays

Telomerase assays were analyzed with ImageQuantTL software using two different methods: the decay method and the 15+ method.

The Decay Method

Telomerase pause bands were quantified in the 1D gel analysis function of ImageQuantTL. After lane definition, detection of bands with a fixed with of 9 px, and background subtraction using the rolling circle method of correction, band intensities were exported to Excel. Because this method requires the ability to quantitate individual bands, it is only used here in assay run from 5 to 15 minutes.

The decay method calculation (Latrick & Cech 2010) is based on a probability p that telomerase will add repeat $n+1$ after adding repeat n, and a probability $(1-p)$ that it will stop adding repeats after n. Assuming p is constant for every value of n, the fraction of telomerases that add at least n repeats, $f(>n)$, in a single binding event is p^n. The step between two bands on the telomerase assay gel, $N_{n+1}-N_n$, directly correlates to the p. By plotting the relative activity of each band as $\ln(N_n>n)$ against repeat number n, the slope correlates to this step and therefore to the processivity. Processivity values are determined as the value of n for which half of the primers were elongated to n or more repeats, which equals $\ln(1/2)/\ln(p)$, or $\ln(1/2)/\text{slope}$. Thus, the value of processivity with plotting the relative activity for each repeat against repeat number is 0.693/slope. Slopes were determined by linear regression.

To generate this plot, the pixel intensities are first corrected for the number of radioactive guanosines incorporated. Total lane counts (TLC) are calculated by adding together intensities for all bands. The "fraction left behind" or FLB is then calculated for

each *n* by summing all intensities n_0 through *n* and dividing the sum by the TLC. Plotting ln(1-FLB) against repeat number *n* generates a line whose slope, *m*, corresponds to the processivity value of 0.693/*m*.

The 15+ Method

Processive telomerase generates many large products that are not resolved on the telomerase assay sequencing gels. To determine the processivity of telomerase in these samples, the scanned gels are loaded into ImageQuantTL Analysis Toolbox. Using the grid tool with the number of columns equaling the number of lanes in the gel, two boxes were generated: one covering bands 1 through 14 and a second covering bands 15+. Intensities were exported to Excel and the processivity was calculated as (15+ Intensity)/[(1-14 Intensity) + (15+ Intensity)] for each lane. The resulting value shows relative processivity for samples run on the same gel.

Replicate samples were plotted using GraphPad Prism software and we used a One-Way ANOVA with paired t-tests to determine if there were significant differences between the samples. Results from paired t-tests were only considered if the One-Way ANOVA showed that the samples had significantly different values ($p<0.05$).

Chapter 4. Implications of telomere-specific single-stranded binding complexes on replication and elongation of telomeres

4.1 Single-stranded DNA at the telomere

Telomeres have several sources of single-stranded DNA (ssDNA) and pose unique challenges that are addressed by specialized DNA binding complexes. The 3' overhang is a conserved feature of telomeres (Henderson & Blackburn 1989), but the length of the overhang is variable between organisms. While humans have 3' overhangs on the order of 100s of nucleotides (Makarov et al. 1997), the overhang in yeast is approximately 10 nucleotides (Wellinger et al. 1993) and only a few nucleotides in *Tetrahymena* and other ciliates (Roth & Prescott 1985; Jacob et al. 2001).

In all of these organisms, however, a much larger amount of telomeric ssDNA is exposed during DNA replication. Additionally, the repetitive and G-rich nature of telomere sequences poses a challenge to the replicative polymerases and there is evidence of telomeric replication fork stalling or collapse (Miller et al. 2006; Bosco & de Lange 2012). Replication Protein A (RPA) is the abundant, canonical single-stranded binding protein that carries out many functions in DNA replication and repair. However, there are also several single-stranded DNA binding complexes that perform specific functions at the telomere. These specialized complexes are much lower in abundance than RPA but have higher specificity for G-rich telomere sequences.

Telomere specific functions of these specialized complexes include telomere end protection, telomere replication, and telomerase regulation. Telomere end protection can be seen as the prevention of binding RPA from coating the telomeric ssDNA and triggering a DNA damage response. This is typically defined by cells displaying a telomeric DNA damage response when a telomere protein is absent or non-functional.

The telomeric DNA damage response is characterized by ATM or ATR signaling, telomeric localization of 53BP1 and/or γH2AX, or by chromosome fusions. While TRF2 deletion triggers an ATM-mediated DNA damage response (Karlseder et al. 1999; Karlseder et al. 2004), deletion of TRF1 or POT1 leads to an ATR-mediated DNA damage signal, which is reflective of RPA accumulation due to fork stalling (Bosco & de Lange 2012; Denchi & de Lange 2007).

Telomeric single stranded binding complexes (SSBs) also have a role in replication, specifically in coordinating the completion of telomere replication by the lagging strand replication machinery. This is necessary to normal complete lagging strand synthesis of the telomeric DNA. There is another process known as C-strand fill-in, which is the synthesis of new DNA complementary to *de novo* sequence added by telomerase, which is necessary for net elongation of both telomere strands. C-strand fill-in is also orchestrated by the lagging strand replication machinery. Disrupting complexes involved in telomere replication can result in excessive single-stranded telomeric DNA, ATR signaling, and a higher percentage of metaphase chromosomes with signal-free ends or a cytogenetic phenomenon known as "fragile telomeres".

Finally, there are also single-stranded DNA binding complexes that regulate telomerase activity. These proteins are required for telomerase localization to the telomere and have important roles in stimulating telomerase processivity. Defective telomerase processivity complexes have decreased telomerase processivity *in vitro* as well as decreased telomere length in cells.

These functions of single-stranded telomere DNA metabolism are managed by several different SSBs. Some of the telomere specific SSBs have overlapping roles and

may be redundant in cells. These telomere SSBs can be organized into two main classes. The first telomere specific SSB to be identified were the CST complexes, named for the *Saccharomyces cerevisiae* Cdc13-Stn1-Ten1 complex, or t-RPA. Both human and yeast CST share the conserved role of stimulating DNA polymerase alpha (pol α) at the telomere (Hughes et al. 2000; Qi & Zakian 2000; Wan et al. 2009). The second class is telomerase processivity complexes, which coordinate telomerase activity at the telomere. Across organisms, these two complexes vary in their contributions to telomere end protection, telomere replication, and telomerase recruitment.

4.2 RPA is the global SSB in eukaryotic cells

RPA is essential for DNA replication, replication fork progression, DNA damage response, and DNA repair (Wold et al. 1987; Wold 1997). RPA is a well conserved heterotrimeric protein complex. RPA binds ssDNA in a non-sequence specific manner and modulates enzymes involved in DNA metabolism.

The three subunits of RPA are RPA70, RPA32, and RPA14, also known as RPA1, RPA2, and RPA3, respectively. These proteins contain a total of six OB-fold domains, designated A-F, which contribute to DNA binding, protein interactions, and RPA heterotrimerization (Figure 4.1). RPA14 is the smallest subunit and consists of a single OB-fold, OB-E. The three proteins form a tight structurally conserved trimerization core with a helix just outside of OB-folds C, D, and E (Bochkareva et al. 2002).

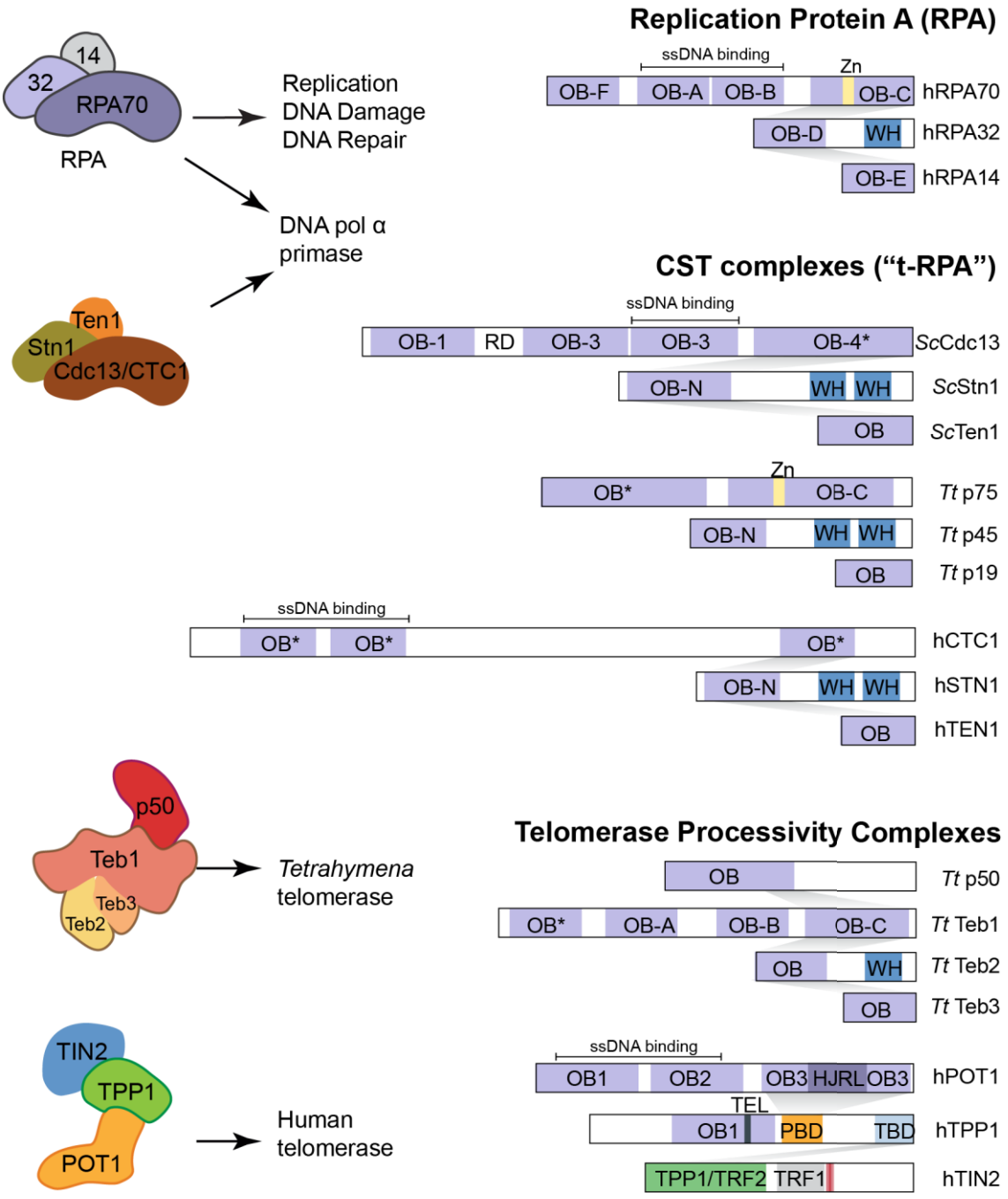

Figure 4.1 RPA and telomere SSB complexes.
Left, cartoons illustrating SSBs. *Right*, Schematic diagrams of RPA, CST, and telomerase processivity complexes from human (h), *Saccharomyces cerevisiae* (*Sc*), or *Tetrahymena thermophila* (*Tt*). Grey shadows mark interaction regions within the complex. ssDNA binding, Single-stranding DNA binding domains; OB, OB-fold; WH, winged helix-turn-helix; Zn, zinc ribbon; HJRL, Holliday junction resolvase-like; PBD, POT1 binding domain; TBD, TIN2 binding domain; *=putative domain.

RPA70 is a 70 kDa protein that contains four OB-fold domains and is the main DNA binding subunit. RPA70 uses OB-A and OB-B to bind an 8-nt footprint of DNA, and assembled RPA engages OB-C from RPA70 and OB-D from RPA32 to bind a 32nt DNA footprint with nanomolar to subnanomolar binding affinity (C. Kim et al. 1994). Dynamic association and dissociation of these OB folds with ssDNA contributes to different binding footprints and movement along the ssDNA (Fanning et al. 2006).

The N-terminal RPA70 OB-fold, OB-F, and the RPA32 winged-helix-turn-helix (wHTH) domain contribute to interactions with RPA-interacting proteins. OB-F interacts with a number of factors, including T-antigen, p53, DNA polymerase α, Rad52, ATRIP, Rad9, and Mre11 (Wold et al. 1989; Collins & Kelly 1991; Dornreiter et al. 1992; Han et al. 1999; Hicks et al. 2003; Prakash & Borgstahl 2012). The RPA32 wHTH interacts with UNG2, XPF, and Rad52 (Mer et al. 2000), among others.

Interestingly, RPA was first observed to stimulate DNA polymerase α processivity by Tsurimoto and Stillman in 1989. Including RPA in activity assays has also been found by others to stimulate processivity of polymerase α (Tsurimoto & Stillman 1989; Melendy & Stillman 1993). It was later shown that two distinct activities of RPA are required for stimulation of polymerase α: the interaction with ssDNA through the OB-A and OB-B DNA binding domain as well as the N-terminus of RPA70 (Dornreiter et al. 1992; Braun et al. 1997). The mechanism of RPA stimulation of other DNA maintenance enzymes is not as well understood, but likely requires both the ssDNA binding affinity of RPA and the protein-protein interactions.

4.3 CST complexes

CST complexes are conserved across many organisms but are best described in the budding yeast *Saccharomyces cerevisiae* where they were first identified. *Sc*CST is also known as a telomere-specific RPA, or t-RPA, because of its homology to the RPA trimer (Gao et al. 2007). It also functions as an end-binding complex and recruits telomerase in yeast (Evans & Lundblad 1999; Qi & Zakian 2000).

*Sc*CST, or t-RPA, consists of Cdc13, Stn1, and Ten1 (Figure 4.1). Cdc13 has a similar domain structure and organization to RPA70 (Gao et al. 2007), but the third OB-fold is the sole DNA binding domain of the complex (Mitton-Fry et al. 2004). Cdc13 also homodimerizes through its OB2 (Sun et al. 2011; Mason, Jennifer J Wanat, et al. 2013), and associates with Stn1/Ten1 with a heterotrimerization core homologous to that in RPA (Sun et al. 2009; Mason, Jennifer J. Wanat, et al. 2013). Stn1 is homologous to RPA32, but contains two rather than one wHTH domain.

While the overall domain structure of this t-RPA is very similar to that of RPA, the differences contribute to its unique functions. t-RPA binds an 11-nt footprint of the yeast telomere sequence, GTGTGGGTGTG, with picomolar affinity (Lewis et al. 2014; Altschuler et al. 2011; Anderson et al. 2002). Cdc13 recruits telomerase through protein interaction with EST1 (Evans & Lundblad 1999; Qi & Zakian 2000), and the interaction with Stn1-Ten1 is thought to bring in DNA polymerase α for C-strand fill in (Qi & Zakian 2000).

In other organisms that have CST, the Stn1-Ten1 subunits are highly conserved, but the large "C" subunit is very divergent (Rice & Skordalakes 2016; Price et al. 2010). Because it is the main DNA binding subunit, the divergence corresponds with varying

DNA binding affinities and changes in specificity. Still, the CST complexes share a role in recruiting and stimulating DNA polymerase α at lagging strand telomeres, which is important for telomere replication (Qi & Zakian 2000; Stewart et al. 2012).

The *Tetrahymena thermophila* proteins p75, p45, and p19 also form a CST complex (Wan et al. 2015). This CST complex binds a 24-nt footprint of sequence $(TTGGGG)_4$ (Wan et al. 2015). Not only is *Tetrahymena* CST important for telomere replication, it has also been recently found as part of the telomerase holoenzyme (Jiang et al. 2015), suggesting a possible mechanism for coupling telomerase activity with lagging strand telomere replication and/or C-strand fill-in.

Mammalian CST complexes have a more global role in DNA replication at G-rich DNA sequences. The main DNA binding component is CTC1, which does not bind telomeres specifically but instead shows a preference for G-rich DNA. Human Stn1/Ten1 was originally purified as a DNA polymerase α accessory factor and named AAF (Goulian et al. 1990; Goulian & Heard 1990), but was later found to be in a complex with CTC1 and shown to be homologous to CST proteins. CST can be found at G-rich sites across the genome and is thought to help with restart of stalled replication forks (Stewart et al. 2012; Wang et al. 2014). It has been suggested that because CST has a higher affinity for ssDNA than DNA polymerase α, forming a ternary complex enhances polymerase affinity for ssDNA and improves its activity (Goulian & Heard 1990). Mutations in CTC1 and STN1 have been identified in patients with the disease Coats Plus, which has many features of short telomere syndromes plus additional phenotypes that may be due to additional replication defects (Keller et al. 2012; Anderson et al. 2012; Gu & Chang 2013; Simon et al. 2016).

4.4 Other telomeric SSBs in telomere length maintenance

Unlike yeast CST, mammalian CST does not perform end protection functions in non-replicating cells (Stewart et al. 2012). Instead, this role is assumed by the POT1 protein in complex with TPP1 and TIN2. POT1 specifically binds telomeric ssDNA on the telomeric G-strand. Like RPA70, POT1 contacts the ssDNA with two OB-folds that comprise the DNA binding domain (Lei et al. 2004; Loayza et al. 2004). POT1 heterodimerizes with the TPP1 protein, and the heterodimer forms the telomerase processivity complex that is important for both recruitment and stimulation of telomerase at telomeric DNA (Figure 4.1).

We found that TIN2 cooperates with TPP1 and POT1 in stimulating telomerase. TIN2, TPP1, and POT1 appears to function as a heterotrimeric DNA binding complex that regulates telomerase activity. In addition to other evidence that TIN2 is important for TPP1/POT1 function *in vivo* (See Chapters 1.5.2 and 3.3), recent experiments that individually knocked out shelterin components found that POT1, TPP1, or TIN2 knockout affected localization of the other respective TIN2/TPP1/POT1 components more than other shelterin components as detected by ChIP and immunofluoresence (Kim et al. 2017). These results led the authors to propose that TIN2/TPP1/POT1 forms a subcomplex within shelterin.

TIN2 participation in this complex could improve the POT1-ssDNA interaction in a manner similar to the increased binding affinity of the complete RPA complex compared to RPA70 alone. Similarly, TIN2 participation in the complex may improve the TPP1-telomerase interaction, resulting in the observed increase in processivity. TIN2

is also important for localizaing the complex to telomeres through its interactions with TRF1 and TRF2.

While TIN2-TPP1-POT1 seem to function as a heterotrimeric complex like RPA, they are likely not a canonical RPA. Recent structural studies of the TPP1-POT1 interaction do not follow the canonical protein-protein interaction interface of RPA complexes (Rice et al. 2017; Chen et al. 2017). There is no structural information about TIN2 at this time. Additionally, TIN2 interacts with TPP1 but has not been shown to interact directly with POT1 (Houghtaling et al. 2004; Takai et al. 2011; David Frescas & de Lange 2014a). While it cannot be ruled out that the three proteins coexpressed may take on a different structure, it appears that TIN2-TPP1-POT1 is a divergent telomeric SSB.

Tetrahymena have homolous proteins to TPP1 and POT1, Tpt1 and Pot1, respectively. These proteins bind the single-stranded telomere overhang and are structurally analogous to TPP1/POT1, but do not appear to play a role in telomerase stimulation (Jacob et al. 2007; Linger et al. 2011; Premkumar et al. 2014). Instead, another set of homologous proteins, Teb1 and p50 are involved in stimulation of telomerase. Teb1 is a telomere-specific single-stranded binding protein with homology to POT1 and to RPA70 (Upton et al. 2017; Zeng et al. 2011) and stimulates telomerase processivity along with its binding partner p50 (Hong et al. 2013; Jiang et al. 2015). It has been argued that Tpt1/Pot1 and p50/Teb1 compete for the short 3' telomere overhang (Chan et al. 2017), but it could be that they have specialized roles in end protection and in regulation of the ssDNA generated during DNA replication. Interesting advances in the

Tetrahymena telomerase holoenzyme structure revealed that Teb1 is actually part of a larger complex, TEB, which is described below (Jiang et al. 2015; Upton et al. 2017).

4.5 *Tetrahymena* telomerase holoenzyme structure

Recent advances in studying the *Tetrahymena thermophila* telomerase holoenzyme structure by cryo EM have led to some interesting discoveries. First, that the telomerase holoenzyme contains both the CST complex (p75, p45, and p19) and the telomerase processivity complex (p50/Teb1) (Jiang et al. 2015). Second, the telomerase processivity factor Teb1 actually forms a complex with previously unidentified components Teb2 and Teb3, which form the RPA-like complex TEB (Jiang et al. 2015; Upton et al. 2017).

Tetrahymena Teb1/p50 had been previously identified as a telomerase processivity complex (Witkin & Collins 2004; Witkin et al. 2007; Min & Collins 2009), where Teb1 stimulates telomerase in a p50 dependent manner. The p50 protein is thought to be analogous to TPP1, as it interacts directly with telomerase analogous to the TPP1 TEL-patch interaction with the telomerase TEN domain (Schmidt et al. 2014; Jiang et al. 2015). Teb1 is an OB-fold containing telomere-specific single-stranded binding protein with similarities to POT1 and RPA70 (Zeng et al. 2011; Upton et al. 2017). Once the Teb2 and Teb3 components of TEB were identified, however, the full TEB complex was shown to stimulate processivity more than Teb1 alone (Upton et al. 2017)

Including the complete TEB complex with Teb2 and Teb3 appears to favor stability of the fully assembled telomerase holoenzyme (Upton et al. 2017). The contribution of Teb2/Teb3 to telomerase stimulation above the known processivity factor is similar to what we have observed with TIN2 and TPP1/POT1 (see Chapter 3). By

analogy to *Tetrahymena*, the contribution of TIN2 to stimulation of telomerase may act through complete assembly of the processive holoenzyme.

The most intriguing part of the *Tetrahymena* telomerase holoenzyme structure, however, is that the enzyme contains both CST and the telomerase-stimulating SSB complex (Jiang et al. 2015) (Figure 4.2). Having these two SSB complexes in the telomerase holoenzyme presents a potential mechanism for coupling lagging strand replication with telomerase. The path of the single-stranded DNA was mapped across the Teb1 OB-folds and into the telomerase active site (Jiang et al. 2015). Considering both the processivity complex and the CST complex, we propose a mechanism that physically

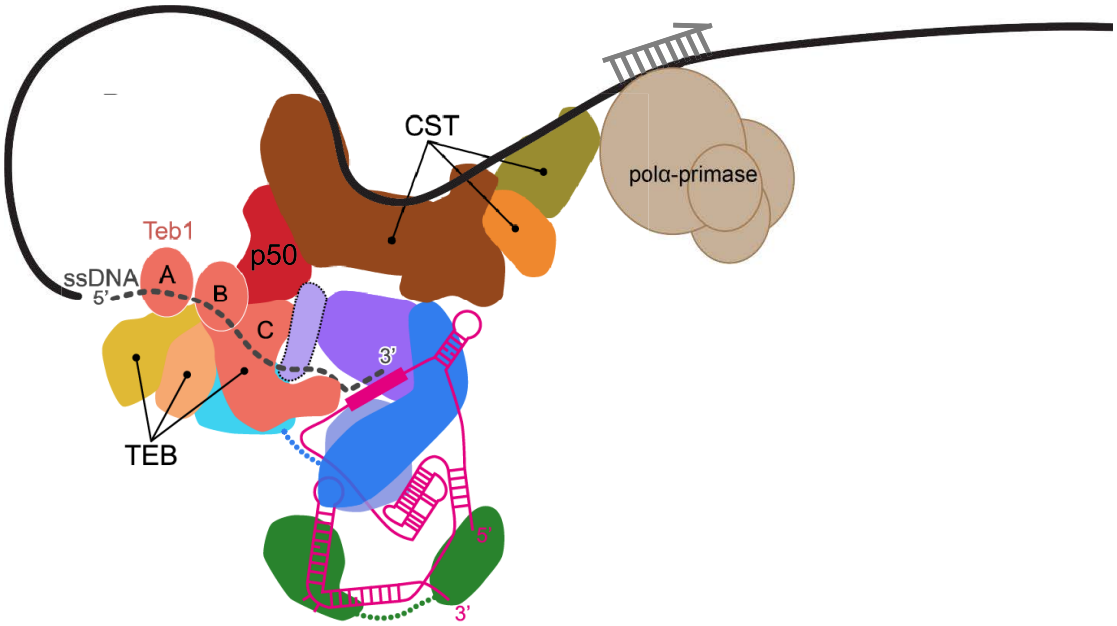

Figure 4.2 *Tetrahymena thermophila* telomerase holoenzyme.
The components of the telomerase holoenzyme and mapping of the ssDNA (ssDNA) path across Teb1 and into the telomerase active site (TERT=blue/purple; TR=pink) together allude to a possible mechanism of physical coupling of telomerase activity with telomere replication. The black line is an illustration of the single-stranded DNA, either during replication or after being synthesized by telomerase, looping back over to CST, which coordinates polymerase α-primase synthesis of Okazaki fragments. Image is adapted from Jiang et al (Jiang et al. 2015).

couples telomerase activity with lagging strand replication (Figure 4.2). We have illustrated how the DNA, either during replication or after being synthesized by telomerase, could concurrently interact with CST to coordinate lagging strand replication and telomerase to coordinate elongation.

4.6 Coupling of telomere replication and telomerase activity

It has been known for many years that there is a relationship between telomerase elongation of telomeres and the lagging strand replication machinery. Deletion of lagging strand DNA polymerases α or δ, but not the leading strand polymerase ε, prevented de novo telomere addition by telomerase in cells (Diede & Gottschling 1999). Mutations in lagging strand polymerases or other factors involved in Okazaki fragment maturation lead to excessive telomeric single-stranded DNA, but also to increased telomere lengths (Carson & Hartwell 1985; Parenteau & Wellinger 1999; Grossi et al. 2004; Budd et al. 2006). Evidence connecting telomerase elongation of the telomeres and DNA replication is reviewed in (Greider 2016). Also, the telomere specific SSBs are specific for the G-strand, which is replicated by the lagging strand replication machinery, rather than the C-strand (Sections 4.3 and 4.4).

Given their high affinity for telomeric DNA, telomere-specific SSBs will likely compete with canonical RPA as a replication fork progresses into telomere sequence. Additionally, we know that the two classes of telomere-specific SSB are involved in both DNA replication and in telomerase elongation of telomeres, which are two processes that are known to be coupled. Coupling of lagging strand replication and telomere elongation is important in two circumstances. First, C-strand fill-in must be coordinated by CST for net elongation of telomeres where the G-strand was elongated by telomerase. Second, if

replication fork stalling leads to telomeric fork collapse, or when a replication fork terminates before reaching the end of the chromosome, mechanisms need to exist that ensure the complete lagging strand replication of the DNA end to prevent telomere truncations caused by unreplicated DNA (Figure 4.3).

When a replication fork reaches the end of a chromosome, the leading strand replicative polymerase may be able to continue synthesizing DNA to the end of its template, but the discontinuous lagging strand cannot continue (Figure 4.3). Thus, the

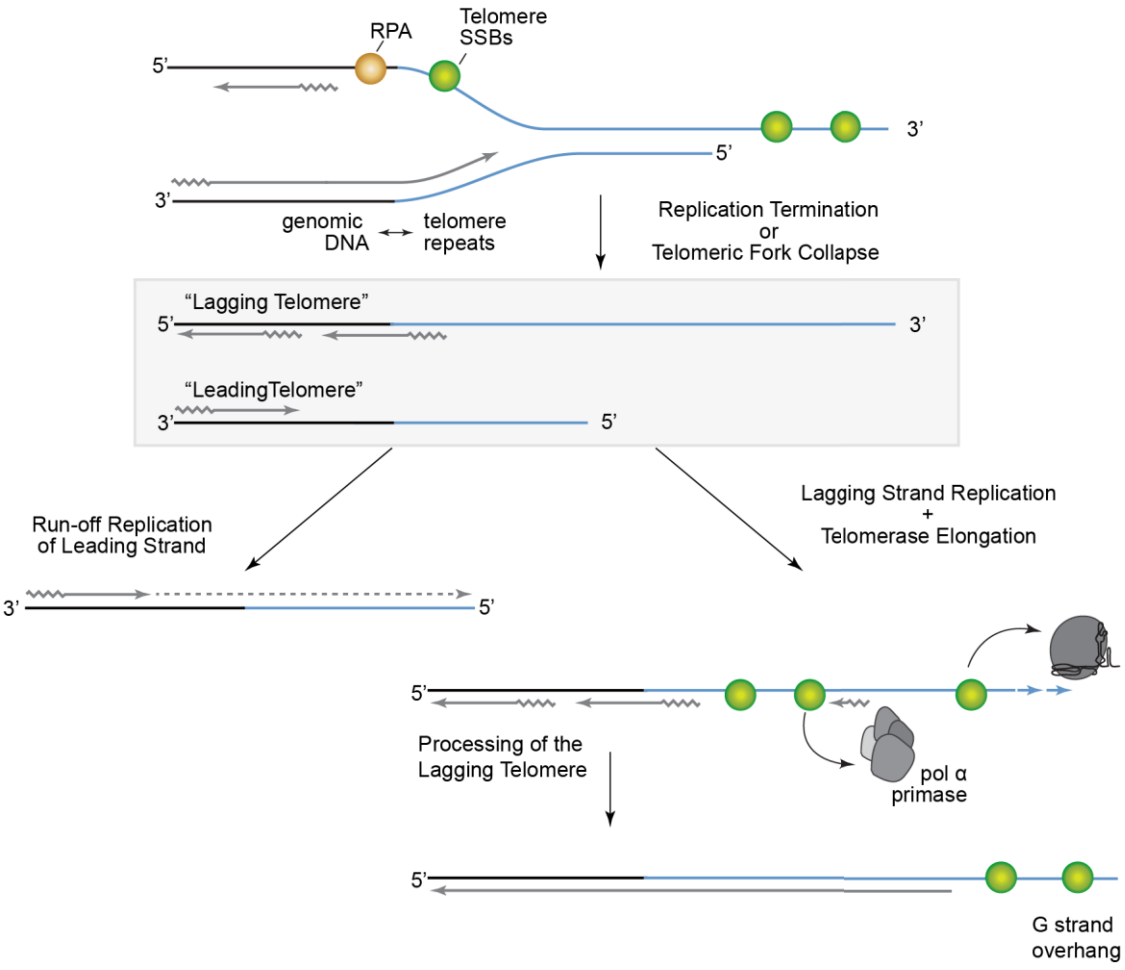

Figure 4.3 Coupling of telomerase and the lagging strand machinery.
As the replication fork enters the telomere, either termination or collapse leaves unreplicated telomeric DNA. The leading strand (left) may be able to complete replication upon fork uncoupling. Telomere-specific SSBs help complete telomere replication of the lagging strand (right) by stimulating DNA polymerase α and telomerase.

telomere SSB complexes may be required to help continue Okazaki fragment synthesis as well as to stimulate telomerase. The implication of the *Tetrahymena* holoenzyme structure is that these two processes are physically coupled, and this may be conserved across organisms.

Considering telomerase and lagging strand machinery as coupled, there may be multiple ways to disrupt the telomere length equilibrium. The simplest way is loss of telomerase function, which may not affect telomere replication, but will result in a gradual telomere shortening over time due to insufficient or absent telomere elongation. This type of telomere shortening is what is observed in families with telomerase mutations who experience progressive telomere shortening over multiple generations (Figure 4.4A).

Defective telomere SSBs could cause uncoupling of telomerase and replication, however, leading to two distinct scenarios. Defective or uncoupled lagging strand replication machinery may allow unregulated telomere elongation (Figure 4.4B). This leads to excessive ssDNA and DNA damage signaling as well as increased telomere lengths without effective C-strand fill-in. This is a phenotype observed with POT1 deletion or POT1 mutants that cannot bind DNA (Takai et al. 2011; Takai et al. 2016). Similarly, mutations in many components of the lagging strand replication machinery cause telomere elongation and increased telomeric single-stranded DNA (Greider 2016).

Complete uncoupling of telomere replication from telomerase activity could result in more drastic effects at the telomere. This uncoupling could cause both defective lagging strand replication and a failure to recover from telomeric replication fork collapse or early replication fork termination. Without a mechanism to elongate these telomeres

or complete DNA replication, much larger amounts of telomere DNA could be lost compared to in the absence of telomerase alone (Figure 4.4C). This could result in not only drastic telomere shortening but also DNA damage response and excess single-stranded DNA at the telomere. TIN2's role as part of a telomeric SSB suggests it could also function in coupling telomere replication with telomerase activity.

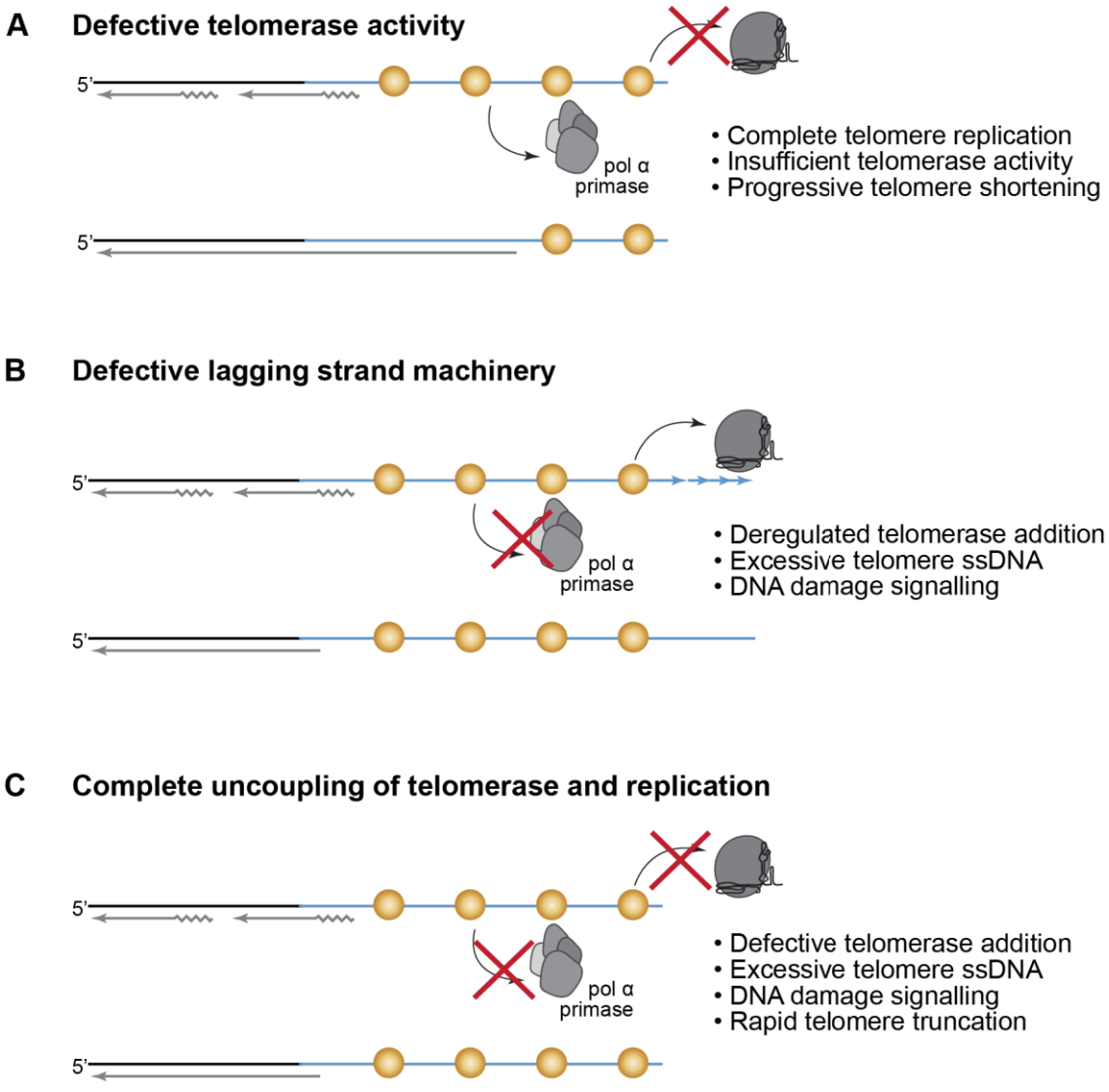

Figure 4.4 Several routes to telomere dysfunction.
(**A**) Loss of telomerase function eliminates telomere elongation but does not affect telomere replication (**B**) Defective lagging strand machinery can uncouple telomerase activity from replication, allowing excessive telomerase elongation of telomeres without C-strand fill in (**C**) Complete uncoupling of telomerase and replication is marked by lack of telomerase addition and incomplete telomere replication, leading to telomere loss.

4.7 Replication fork collapse as a possible mechanism of telomere shortening with TIN2 mutants

The degree of telomere shortening in patients with de novo TIN2 mutations is severe and cannot be explained by loss of telomerase processivity alone (Mary Armanios & Blackburn 2012; Savage et al. 2008). Indeed, the telomere length of these patients compared to their unaffected parents and siblings suggests there must be a mechanism of telomere truncation in these patients. Unrepaired replication fork collapse in the telomere could explain this drastic telomere loss.

There is evidence of the POT1 complex having a role in replication fork progression. Certain POT1 mutants that cannot bind DNA cause an ATR-mediated DNA damage response, fragile telomeres, and increased telomere replication fork stalling detected by DNA combing (Pinzaru et al. 2016). Interestingly, cells expressing these POT1 mutants also have a decreased association of CST at telomeres detected by ChIP. Evidence in studies of TIN2 also point toward possible roles in replication. Mouse cells carrying the TIN2 K267E allele, analogous to the human K280E mutation, have increased ATR signaling, signal-free ends (SFEs), and fragile telomeres. Finally, disruption of TIN2 interaction with HP1γ has been proposed to cause defects in sister telomere cohesion. This is observed in FISH as an increase in the distance between sister telomeres before cell division (Canudas et al. 2011). This apparent defect in cohesion may actually be a reflection of uncoupling of telomere replication fork movement and telomerase activity.

We propose that there are multiple pathways to short telomeres. The first pathway is decreased telomerase activity or processivity that prevents telomere elongation. When telomere replication is unaffected, this leads to a progressive telomere shortening over time, which manifests as short telomere syndromes with genetic anticipation in families. The second pathway is that uncoupling of telomerase from lagging strand replication machinery leads to unrepaired replication fork collapse. Fork collapse, even in the presence of telomerase, can result in drastic telomere loss by failure

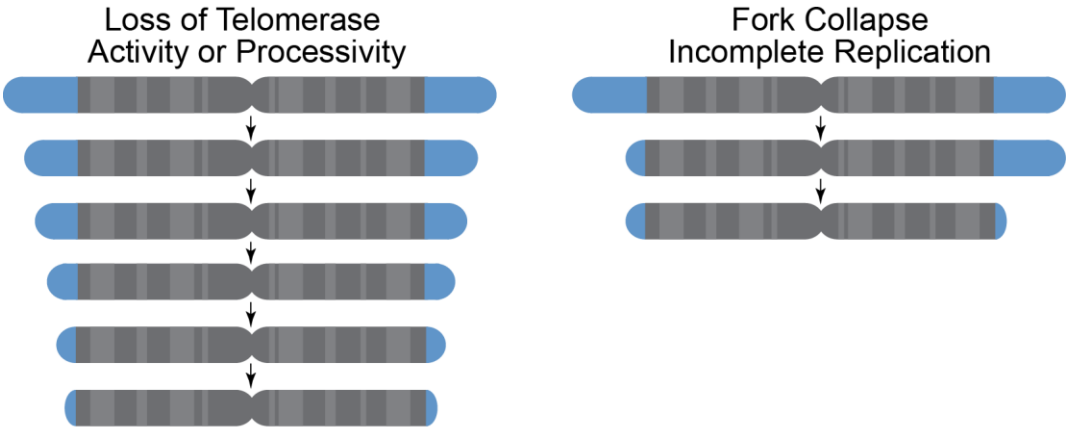

Figure 4.5 Two pathways to short telomeres.
Left, Loss of telomerase activity or processivity leads to progressive telomere shortening over many rounds of replication. Right, Replication fork collapse or incomplete replication causes rapid telomere loss.

to complete replicating the telomeric C-strand (Figure 4.5). We would expect these cells to have excessive single-stranded DNA, and extremely short telomeres at the next round of DNA replication.

4.8 Future Directions

Whether TIN2 does indeed function in telomere replication remains to be tested. Ongoing assays in the TIN2 overexpressing cultured cells (Chapter 2) are being tested to

investigate replication defects. Using quantitative fluorescence in situ hybridization (q-FISH) on metaphase chromosomes from the TIN2 isoform overexpression cell lines, we will determine whether there are abnormal telomere maintenance events that would not be visible by Southern blot. By probing telomeres and scoring metaphases for chromosome fusions, fragile telomeres, and signal-free ends, we can learn about the telomere dysfunction in TIN2 and TIN2-K280E cells expressing the different isoforms. Telomere truncations might be seen as uneven sister telomere lengths, if the truncation is large enough to detect within the sensitivity of this method.

The ability of TIN2 mutants to cause telomeric replication fork collapse will also be tested using the ADDIT (*ad*dition of *d*e novo *i*nitiated *t*elomeres) assay (Lee et al. 2015). While we may observe a lower percentage of *de novo* telomeres elongated or shorter tracts of new telomere sequence in TIN2 mutant-expressing cells compared to wild-type, it may also be possible to observe fork collapse events as large deletions in the telomere seed sequence. Comparison to the results in mTR knockout cells is an important control to determine if any changes observed are due to something other than the lack of telomerase. Fork collapse has not been tested before in this assay, so a positive control such as hydroxyurea or other damage agents that cause fork collapse will also be important for interpreting the data. It is important to note that the ADD-IT assay is set up in mouse cells, which only express one isoform of TIN2.

Another way telomeric DNA replication has been studied is by single-molecule analysis of replicating DNA (SMARD) by DNA fiber combing (Norio & Schildkraut 2001). This method can follow the progression of replication origins through the telomere, and has been used to identify replication fork stalling in telomeres in TRF1 and

POT1 knockout conditions (Sfeir et al. 2009; Pinzaru et al. 2016). This is a technique we can employ with our HeLa cell lines expressing TIN2 isoforms and mutants or with CRISPR knock-in cell lines carrying TIN2 patient mutations.

It has been nearly a decade since TIN2 mutations were first identified in short telomere patients with Dyskeratosis Congenita. While there remain many unanswered questions about the endogenous functions of TIN2 and the mechanism of telomere shortening in the TIN2 patients, our findings of multiple TIN2 isoforms in human cells and the cooperation of TIN2 with the TPP1/POT1 processivity complex provide a new approach to understanding the role of TIN2 in telomere length regulation.

APPENDIX

Appendix A. Primers used in this project

#	Name	Purpose	sequence
A1	V5_C (-)	sequencing	accgaggagagggttagggat
A2	M13 (+)	sequencing	gtaaaacgacggccag
A3	M13 (-)	sequencing	caggaaacagctatgac
A4	TIN2 stop>Ser (+)	SDM	cacagagcaaaaggagtcgaacccagctttcttg
A5	TIN2 stop>Ser (-)	SDM	caagaaagctgggttcgactccttttgctctgtg
A6	TIN2 K280E (+)	SDM	ctaggggaggccatgaggagcgccccacag
A7	TIN2 K280E (-)	SDM	ctgtggggcgctcctcatggcctccctag
A8	Tin2 R282S (+)	SDM	ggaggccataaggagagccccacagtcatg
A9	Tin2 R282S (-)	SDM	catgactgtggggctctccttatggcctcc
A10	Tin2 R282H (+)	SDM	gaggccataaggagcaccccacagtcatgctg
A11	Tin2 R282H (-)	SDM	cagcatgactgtggggtgctccttatggcctc
A14	trunc_tin2_A	overlap extension	cgttgtaaaacgacggccag
A17	trunc_tin2_D	overlap extension	attttgagacacgggccaga
A18	Ub (+)	sequencing	tcagtgttagactagtaaattg
A19	trunc_TIN2_B2	overlap extension	agctgggttcttatggcctcccctagt
A20	trunc_TIN2_C2	overlap extension	ggccataagaacccagctttcttgtac
A21	ARF3 +	qRT-PCR	tcaccaccatccctaccatt
A22	ARF3 -	qRT-PCR	aggtggcctgaatgtaccag
A23	ins_tin2L_B	overlap extension	caagcaattctccttttgctctgtggc
A24	ins_tin2L_C	overlap extension	caaaaggagaattgcttggattgctac
A25	ins_tin2L_D	overlap extension	tgctgggttcaaaggtctagaactgtc
A26	ins_tin2L_E	overlap extension	agacctttgaacccagctttcttgtac
A27	TS	TRAP	aatccgtcgagcagagtt
A28	RP	TRAP	cccttacccttacccttacccctta
A29	TSK1	TRAP	aatccgtcgagcagagttaaaaggccgagaagcgat
A30	K1	TRAP	atcgcttctcggcctttt
A31	primer a5	Direct Assay	ttagggttagcgttaggg
A32	TIN2 qPCR+	qRT-PCR	gtcagaggctcctgtggatt
A33	TIN2 qPCR-	qRT-PCR	cagtgctttctccagctgac
A34	GMPR-proximal Homology Arm (+)	gibson assembly	cgaattcctgcagcccgggggacagtggaagttccttttaaaggagatg
A35	GMPR-proximal Homology Arm (-)	gibson assembly	tcgtttgttcctaagtgttgttcagctgtgcc
A36	NeoR (+)	gibson assembly	caacacttaggaacaaacgacccaacaccg
A37	NeoR (-)	gibson assembly	tacgaagttattgcatctcaattagtcagcaaccatag
A38	TINF2-proximal Homol Arm (+)	gibson assembly	ttgagatgcaataacttcgtataggatactttatacgaagttatcaaggaagtaaaaaaaggcaaaggg

A39	TINF2-proximal Homol Arm (-)	gibson assembly	tggagctccaccgcggtggccaaaaggagtgagtggaacagagttg
A40	US-homology arm 1 (+)	gibson assembly	cgaattcctgcagcccggggaaataaaatacaggctgggcgtggtg
A41	US-homology arm 1 (-)	gibson assembly	ttgagatgcaccggggcggagacaaggatg
A42	sv40 ori (+)	gibson assembly	tccgccccggtgcatctcaattagtcagcaaccatag
A43	sv40 ori (-)	gibson assembly	ggctgcaggttttgcaaaagcctaggcctcc
A44	PuroDTK(+)	gibson assembly	cttttgcaaaacctgcagccaacgccac
A45	PuroDTK (-)	gibson assembly	atgcttcaataccatagagcccaccgcatc
A46	US-distal homology arm (+)	gibson assembly	ggctctatggtattgaagcatattacatacgatatgcttcaataatcagtctcagctgatccgc
A47	US-distal homology arm (-)	gibson assembly	tggagctccaccgcggtggcaaaacatatttttctttttttttttttttgtagagtcagggtc
A48	V5 qPCR Reverse	qRT-PCR	agagggttagggataggcttac
A49	TIN2 V5 F	qRT-PCR	ctgaaggagaacccagttgac
A50	280X-V5-F	qRT-PCR	acgaagagttcagtcccaatg
A51	open pENTR F	TIN2L	ctccttttgctctgtggcag
A52	open pENTR R	TIN2L	aacccagctttcttgtacaaagttggcattataagaaagc
A53	genomic TINF2 promoter		
A54	genomic TINF2 promoter		
A55	TPP1 F1	gibson assembly	ccggactctagcgtttaaactaatacgactcactatagggag
A56	TPP1 R1	gibson assembly	ctgcttcagcaggctgaagttggtggccttgtcatcgtcatccttg
A57	POT1 F1	gibson assembly	cgatgacaaggccaccaacttcagcctgctgaagcaggccggcgacgtggaggagaaccccggccccgagatgtctttggttccagcaac
A58	POT1 R1	gibson assembly	gcaggtcagcaggctgcccctgcccttgtcatcgtcatccttg
A59	TERT F1(shortened to be 90bp)	gibson assembly	ggcaggggcagcctgctgacctgcggcgacgtggaggagaacccccggccccgactacaaagaccatgacggtgattataaagatcatgat
A60	TERT R2	gibson assembly	gtatgctatacgaagttatctcagtccaggatggtcttg
A61	oligo-dT adapter	cDNA synthesis	caggaaacagctatgacttttttttttttttttttt
A62	clone seq primer F	screening	ctaggaagtcgagcctcacg
A63	PAC sequence F		gagtacaagcccacggtgc
A64	PAC sequence R		cttgcgggtcatgcaccag
A65	u1hTR with Acc65I sites	cloning	gatcggtacctcgaggtcgacggtatcgataagc
A66	u1hTR rev with NOT1	cloning	gcggtggcggccgctctag
A67	u1hTR F with Not1	cloning	gatcgcggccgcaacctcgaggtcgacggtatcgataagc
A68	u1hTR Rev with Acc65I	cloning	gatcggtaccggaccagcttctttgggagagaac
A69	TPP1 F2-AgeI	gibson assembly	attctgcagcccgggactaaccggtcgatggcaggttcggggagctgg

A70	TPP1 R2 AgeI opened	gibson assembly	gctgaagttggtggccttgtcatcgtcatccttg
A71	TERT R-NheI site	gibson assembly	gcggcatgtctagcctgcaggaacaccgctagctcagtccaggatggtcttg
A72	PAC Crispr Top		caccgggcggggtagtcggcgaacg
A73	PAC Crispr Bottom		aaaccgttcgccgactaccccgccc
A74	Pot1FLAG-T2a-FLAG-tert	gibson assembly Notes: Gray highlight = T2A sequence Lowercase = Silent mutations made to reduce GC content and repetitiveness for gBlock synthesis	AGGAGTACTAGAAGCCTATCTCATGGAT TCTGACAAATTCTTCCAGATTCCAGCAT CAGAAGTTCTGATGGATGATGACCTTCA GAAAAGTGTGGATATGATCATGGATAT GTTTTGTCCTCCAGGAATAAAAATTGAT GCATATCCGTGGTTGGAATGCTTCATCA AGTCATACAATGTCACAAATGGAACAG ATAATCAAATTTGCTATCAGATTTTTGA CACCACAGTTGCAGAAGATGTAATCTcA GACTACAAgGAtCATGAtGGTGAcTATAA AGATCATGACATCGACTACAAGGATGA CGATGACAAGGGCAGGGGCAGCCTGCT GACCTGCGGCGACGTGGAGGAGAACCC CGGCCCCGACTACAAAGACCATGACGG TGATTATAAAGATCATGATATCGATTAC AAGGATGACGATGACAAGATGCCGaGaG CTCCCaGaTGCCGAGCCGTGaGaTCCCTG CTGaGaAGCCACTACaGaGAGGTGCTGCC GCTGGCCACGTTCGTGaGaaGaCTGGGGC CCCAGGGCTGGaGaCTGGTGCAGaGaGGG GACCCGGCGGCTTTCaGaGCGCTGGTGG CCCAGTGCCTGGTGTGCGTGCCCTGGGA CGCAaGaCCtCCaCCtGCaGCtCCaTCCTTCa GaCAGGTGTCtTGCCTGAAGGAGCTGGT GGCCaGAGT
A74-F		gibson assembly	agg agt act aga agc cta tct cat gga ttc tg
A74-R		gibson assembly	ggc cac cag ctc ctt cag gc
A75	tpp1FLAG-p2a-pot1	gibson assembly See note for A74	AGGAGTACTAGAAGCCTATCTCATGGAT TCTGACAAATTCTTCCAGATTCCAGCAT CAGAAGTTCTGATGGATGATGACCTTCA GAAAAGTGTGGATATGATCATGGATAT GTTTTGTCCTCCAGGAATAAAAATTGAT GCATATCCGTGGTTGGAATGCTTCATCA AGTCATACAATGTCACAAATGGAACAG ATAATCAAATTTGCTATCAGATTTTTGA CACCACAGTTGCAGAAGATGTAATCTcA GACTACAAgGAtCATGAtGGTGAcTATAA AGATCATGACATCGACTACAAGGATGA CGATGACAAGGGCAGGGGCAGCCTGCT GACCTGCGGCGACGTGGAGGAGAACCC CGGCCCCGACTACAAAGACCATGACGG TGATTATAAAGATCATGATATCGATTAC AAGGATGACGATGACAAGATGCCGaGaG CTCCCaGaTGCCGAGCCGTGaGaTCCCTG CTGaGaAGCCACTACaGaGAGGTGCTGCC GCTGGCCACGTTCGTGaGaaGaCTGGGGC CCCAGGGCTGGaGaCTGGTGCAGaGaGGG

			GACCCGGCGGCTTTCaGaGCGCTGGTGG CCCAGTGCCTGGTGTGCGTGCCCTGGGA CGCAaGaCCtCCaCCtGCaGCtCCaTCCTTCa GaCAGGTGTCtTGCCTGAAGGAGCTGGT GGCCaGAGT
a75-F		gibson assembly	gca ctt tct gat gga tgc aca gc
a75-R		gibson assembly	tgt tgc tgg aac caa aga cat acc g
A76	POT1 F age1	gibson assembly	attctgcagcccgggactaaccggtatgtctttggttccagcaaca
A77	POT1 R gblock	gibson assembly	ccatgagataggcttctagtactcctg
A78	Tert F gblock	gibson assembly	gcctgaaggagctggtggcccgag
A79	TPP1 F BstBI	gibson assembly	gacggtatcgattctgcagcccgggactaattcgaagccaccatg gcaggttcggggagg
A80	TPP1R gblock	gibson assembly	gacatcggagttggctcagaccctggc
A81	upstream CRISPR top		caccgcgccaccaggggcgtagcca
A82	upstream CRISPR bottom		aaactggctacgcccctggtggcgc
A83	downstream #1 top		caccgctgtgcctaaaagggttagc
A84	downstream #1 bottom		aaacgctaacccttttaggcacagc
A85	downstream #2 top		caccgtcaaccctgctaacccttt
A86	downstream #2 bottom		aaacaaaagggttagcagggttgac
A87	FOR_1	sequencing	gaggaccaggagcatcagg
A88	FOR_2	sequencing	tagggttgccctgcaagaat
A89	FOR_3	sequencing	tggagatattgttcgctttca
A90	FOR-4	sequencing	ggggaatcagggtcttacca
A91	FOR-5	sequencing	tgtgagatctggccacgaag
A92	REV-6	sequencing	agatgccgagagctcccag
A93	REV-7	sequencing	aaccatagcgtcagggagg
A94	REV-9	sequencing	ctgtcggaagcagaggtca
A95	REV-9 FOR	sequencing	tgacctctgcttccgacag
A96	REV_10	sequencing	gcctcttcgacgtcttccta
A97	REV_11	sequencing	tacaagatcctcctgctgca
A98	hU6	sequencing	gag ggc cta ttt ccc atg att cc
A99	Primer A	making TINF2 downstream	gtaggaatgaagtggaagtccagg
A100	Primer B	making TINF2 downstream	gcgaagcttataacttcgtataatgtatgctatacgaagttataacc cttttaggcacagctg
A101	Primer C	making TINF2 downstream	aaaagggttataacttcgtatagcatacattatacgaagttataagc ttcgccgaccatgg
A102	Primer D	making TINF2 downstream	aaccctgctccatagagcccaccgcat
A103	Primer E	making TINF2 downstream	gctctatggagcagggttgaaagcctg
A104	Primer F	making TINF2 downstream	taaagagatgctggggctttctg
A105			cattcctactaaactacttgcagagct
A106			cagcctcgactgtgccttctagttg

A107			
A108			
A109	TINF2_CRSP_scn_L3	TINF2 myc tag screen	aggtacccagagccgacag
A110	TINF2_CRSP_scn_R3	TINF2 myc tag screen	gcagagatcgcagaaactcc
A111	JA Homology Arm 1		cggcgacgtttaaagctga
A112	JA Homology Arm 2		atcccgccccttttctttct
A113	HA Seq Primer R		agcgtaatctggaacatcgt
A114	TPP1 del F	0611 deletion	agcccgggactaagtctttggttcca
A115	TPP1 DEL R	0611 deletion	tggaaccaaagacttagtcccgggct
A116	TPP1-FLAG-Rev	0611 minus POT1	cttgtcatcgtcatccttgtagtcgatgtcatgatcttta
A117	TERT-2A-Fwd	0611 minus POT1	tacaaggatgacgatgacaagggcaggggcagcctgctg
A118	K280R +	SDM	ctaggggaggccatagggagcgccccacag
A119	K280R -	SDM	ctgtggggcgctccctatggcctccctag
A120	TERT fwd	gibson	gcagcccgggactaagactacaaagaccatgacgg
A121	TERT rev	gibson	gcatgtctagcctgcatcagtccaggatggtcttg
A122	myc fwd		caaaaacttatttctgaagaagatctg
A123	RACE Adapter	3' RACE	gactcgagtcgacatcg
A124	RACE-oligodT	3'RACE	gactcgagtcgacatcgttttttttttttttttttt
A125	100bp arm F1		acagggagttgccagaagcc
A126	100bp arm R1		cggaaaatgttccacgcagc
A127	30bp arms F2		aacccggagggaccgcct
A128	30bp arms R2		agcgtagagctgcgggacc
A129	HindIII-myc		gcgtttaaacttaagcttcgccgaccatggaacaaaaacttatttctg
A130	TIN2M+Not1 rev		gactcgagcggccgcctacccatccccttcc
A131	K280X+		ctaggggaggccattaggagcgccccacag
A132	K280X -		ctgtggggcgctcctaatggcctccctag
A133	eGFP-2a-TERT F1		ctcggcatggacgagctgtacaagggcaggggcagcctgctgac
A134	eGFP-2a-TERT R1		cagctcctcgcccttgctcaccatggtggcttcgaattagtccc
A135	eGFP F2		agcccgggactaattcgaagccaccatggtgagcaagggcgag
A136	eGFP R2		cgcaggtcagcaggctgcccctgccttgtacagctcgtccat
A137	TIN2M overlap Forward	gibson	tgtacaaaaaagcaggcaccgctacgcccctggtggcg
A138	TIN2M Overlap Reverse	gibson	tgtacaagaaagctgggtttgagtgcagagaaacacaggctcc
A139	pcDEST40 open		aacccagctttcttgtaca
A140	pcDEST open rev		ggtgcctgctttttttgtacaaac
A141	#1 5'UTR_TIN2_1	PacBio mouseTIN2	gtg cag atg aga gaa gcg
A142	#1 5'UTR_TIN2_2	PacBio mouseTIN2	tgg gtt gaa cga aag gag
A143	Exon1_Tin2_1	PacBio mouseTIN2	agt ttc tgc agt cct tgc

A144	pcDNA-DEST40R_TIN2M	TIN2M cloning	ggt gcc tgc ttt ttt gta caa ac
A145	pcDNA-DEST40F_TIN2M		tcg aac cca gct ttc ttg
A146	TIN2MF_pcDNA-DEST40		tgt aca aaa aag cag gca cca tgg cta cgc ccc tgg tg
A147	TIN2MR_pcDNA-DEST40		tac aag aaa gct ggg ttc gag tgc aga gaa aca cag gct cc
A148	c-V5 Fwd	insert Cterm tag	cctaaccctcctcggtctcgattctacgtgatagaactaaaatgc tctc
A149	c-V5-Rev	insert Cterm tag	accgaggagagggttagggataggcttacccaaaggtctagaa ctgtctc
A150	TEL patch Fwd		cggaagccgaacgccttcgcctcccagtccg
A151	Tel Patch Rev		cggactgggaggcgaaggcgttcggcttccg
A152	mTIN2_F	amp from cDNA	atggccccacctccaggg
A513	mTIN2_R1	amp from cDNA	ggacactacgggatgtagtcaca
A154	mTIN2_R2	amp from cDNA	ctacgggatgtagtcacaaaacatgggg
A155	pcDNA5_open_F	gibson clone	agcggccgctcgagtctag
A156	pcDNA5_open_R	gibson clon	ccagatcttcttcagaaataag
A157	mTIN2 gib F	gibson	tatttctgaagaagatctggatggccccacctccaggg
A158	mTIN2 gib R	gibson	tctagactcgagcggccgctctacgggatgtagtcacaaaacatg g
A159	K267E fwd	SDM	tcggcaaaggcgtgccatgaagagcggccca
A160	K267E rev	SDM	tgggccgctcttcatggcacgcctttgccga
A161	K267X fwd	SDM	caaaggcgtgccattaagagcggcccac
A162	K267X rev	SDM	gtgggccgctcttaatggcacgcctttg
A163	R269S fwd	SDM	ggcgtgccataaagagagccccacagtcatgctac
A164	R269S rev	SDM	gtagcatgactgtggggctctctttatggcacgcc
A165	R269H fwd	SDM	ggcgtgccataaagagcaccccacagtcatgctac
A166	R269H rev	SDM	gtagcatgactgtggggtgctctttatggcacgcc
A167	TPP1 ΔC22 Open F	TPP1 ΔC22	aagctgccaggcttcctcccgactacaaagaccatgacgg
A168	TPP1 ΔC22 open R	TPP1 ΔC22	accgtcatggtctttgtagtcgggaggaagcctggcagc
A169	FLAG-TPP1 + overlap		gctgaagttggtggccctaggcttgtcatcgtcatccttg
A170	TPP1 ΔC22 F2		gggaggaagcctggcagc
A171	TPP1 ΔC22 R2		tcagactacaaagaccatgacgg
A172	overlap		gctgccaggcttcctccctcagactacaaagaccatgacgg

Appendix B. TIN2 Multiple Sequence Alignments

List of organisms used in the Praline Multiple Sequence Alignment:

Homo_sapiens NP_001092744.1
Pan_troglodytes NP_001233535.1
Pan_paniscus XP_003809126.1
Pongo_abelii NP_001124653.1
Chlorocebus_sabaeus XP_007984509.1
Macaca_fascicularis XP_005561020.1
Macaca_mulatta XP_014998924.1
Callithrix_jacchus XP_002807259.1
Cricetulus_griseus EGW11547.1
Ictidomys_tridecemlineatus XP_005338777.1
Saimiri_boliviensis XP_010333305.1
Heterocephalus_glaber EHB03391.1
Oryctolagus_cuniculus XP_008267657.1
Ochotona_princeps XP_012782354.1
Sus_scrofa XP_001927960.1
Ovis_aries XP_012036332.1
Tursiops_truncates XP_004311674.1
Vicugna_pacos XP_006217349.1
Canis_lupus XP_005623322.1
Bos_taurus NP_001091583.1
Equus_caballus XP_005603304.1
Mustela_putorius_furo XP_004755289.1
Felis_catus XP_006932836.1
Mus_musculus NP_663751.2
Mus_spretus AAN77121.1
Rattus_norvegicus NP_001006963.1
Myotis_brandtii EPQ11041.1
Loxodonta_africana XP_003421012.2
Sarcophilus_harrisii XP_012400471.1
Alligator_sinensis XP_006036607.1
Xenopus_laevis AAI26059.1
Xenopus_tropicalis ACC76751.1
Danio_rerio XP_005172357.1
Monodelphis_domestica XP_007479934.1
Anolis_carolinensis XP_008117770.1

Appendix C. Mouse TIN2 Isoform Sequencing

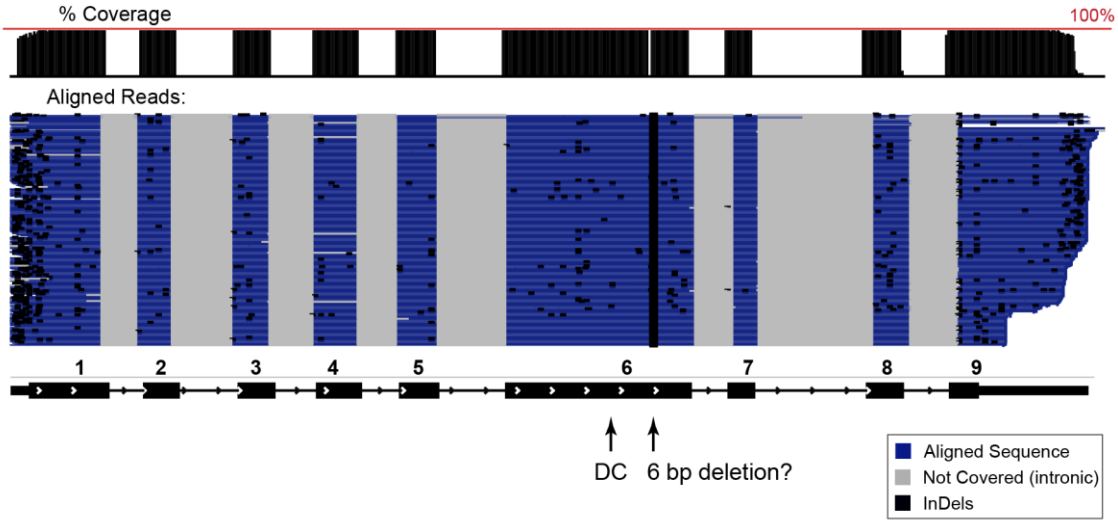

Appendix C. TIN2 isoform sequencing results. See also Figure 2.3.
The coverage track shows the coverage of TIN2 exons (labeled at bottom). There is one predominant isoform expressed. The aligned reads are shown in blue and gray. One line represents a single read. Blue = aligned sequence; Gray = not covered; Black=InDels. Note the frequency of Indels from pacbio sequencing. InDels were not included in Figure 2.3 but were left in this figure to highlight one recurrent deletion in exon 6. We found a previously unknown 6bp deletion in exon 6, downstream of the mutation cluster. This mutation would delete E307-P308 but is in frame with the rest of the protein. This deletion was not observed in CAST/EiJ mouse sequencing. It is unclear at this time if this is a CJ57BL/6 mutation or a specific mutation in the mouse sequenced.

Appendix E. TIN2 Knock-down and Overexpression Constructs and Methods

Before using stable FLP-in cell lines and CRISPR/Cas9 genomic editing, we performed studies on TIN2 using the following lentiviral overexpression and shRNA knockdown techniques. Protocols are listed here for future reference.

Lentiviral Production and Transduction

Lentivirus was produced for pGIPZ shRNA and pLenti6/UbC-TIN2-V5 constructs using a standard protocol. To generate virus, $8x10^6$ 293FT cells were plated in a 15-cm plate coated with poly-D-Lysine (Sigma, P1024; 100µg/ml in water) in complete medium (DMEM, 10% FBS, 1% PSG). The next day, the medium was changed to DMEM with 1% FBS and no PSG. Cells were transfected with 9µg of the respective construct, 12 µg pCMVΔ8.91 (containing lentiviral *gag* and *pol* genes), and 3 µg pMD.G (containing lentiviral *env* gene) using Lipofectamine 2000 (Invitrogen, 11668) and Opti-MEM (Gibco) according to manufacturer protocol. Cells were incubated at 37°C, 5% CO_2 for 72h. The cell medium was then harvested into a 50 mL conical tube, spun at 1000rpm to clear debris, and filtered through a 0.45µm filter prewetted with 1%FBS DMEM. Virus was concentrated in Amicon Ultra-15 Centrifugal Filters by spinning at 4000xg in 5-minute increments until the final volume is <0.5ml. Virus aliquots are stored at -80°C. pGIPZ lentivirus was titered by adding a series of dilutions of concentrated and unconcentrated virus to wells in a 24-well dish according to the pGIPZ manual. 48 hours post-transduction, cells were disrupted and inspected for GFP expression using flow cytometry. Viruses were transduced with an MOI of 0.3.

Suspension cells were transduced using a spinoculation protocol, where K562 cells in media were spun at 800xg for 1 hour at 32°C with the appropriate amount of virus. The supernatant was then removed and cells were grown in IMDM media until selection.

shRNA Constructs

Lentiviral shRNA constructs were ordered from OpenBiosystems to target the TIN2 3'UTR (pGIPZ V3LHS_395331; pGIPZ V3LHS_401958) and a non-targeting shRNA used as a control (pGIPZ RHS4346 D0709). Expression constructs of the TIN2S and TIN2M isoforms are shRNA resistant because they have exogenous UTR sequence. Silent shRNA resistance mutations which were designed when cloning TIN2L, which contains some UTR sequence as coding sequence.

Quantitative RT-PCR

To measure relative amounts of TIN2 knock-down, RNA was isolated and reverse transcribed from TIN2 shRNA or scrambled shRNA cell lines. Quantitative RT-PCR was performed on a Bio-Rad CFX96 thermocycler. Approximately 5ng cDNA was mixed with 1X IQ SYBR Green Supermix (Bio-Rad, 1708884BUN) and 5 μM primers. TIN2 primers are A32 and A33. TIN2 expression levels were calculated relative to ARF3, which is measured with primers A21 and A22. Samples were measured in triplicate. Every plate contains a no template control for background and a no-RT control for DNA contamination.

Appendix F. Design for RCME at *TINF2* locus

We designed two approaches to cassette exchange at the endogenous *TINF2* locus. The first simply flanks the gene with heterologous loxP sites and selectable markers. The heterologous loxP sites make it possible to transfect an exogenous expression cassette with matching loxP sites for homologous recombination mediated by Cre recombinase (Toledo et al. 2006). The second approach was to add TIN2 cassettes downstream of the *TINF2* gene as a lox-stop-lox cassette, where the endogenous gene could be removed and the downstream cassette could be simultaneously expressed.

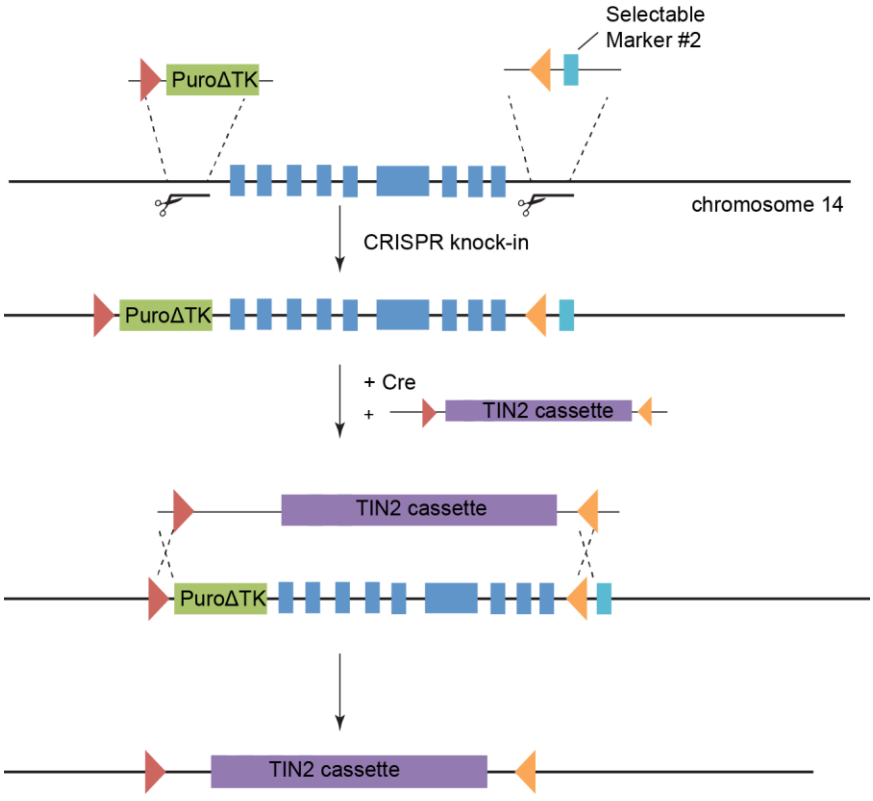

Appendix F.1. The first step of editing inserts the upstream loxP with a PuroΔTK gene which has a minimal sequence of puromycin resistance gene fused with thymidine kinase, so it can be used with both positive and negative selection. The second step incorporates the heterologous LoxP site with a second selectable marker downstream of *TINF2*. Transfection with the recombination cassette and Cre recominase will replace the endogenous gene with the TIN2 construct of interest. Counter selection with Ganciclovir will remove cells that have not undergone cassette exchange and retain the PuroΔTK gene.

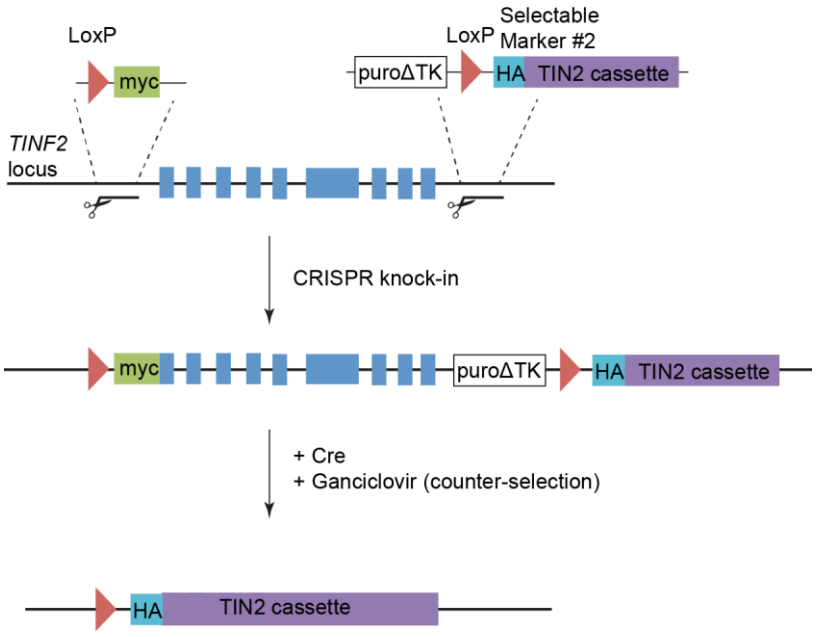

Appendix F.2. The second approach to cassette exchange at the endogenous locus is to make the *TINF2* gene into a Lox-Stop-Lox cassette with a downstream TIN2 coding sequence that will be expressed after Cre-mediated removal of the endogenous cassette. Endogenous and downstream cassettes are differentially epitope tagged for quality control of the Lox-Stop-Lox and for efficiency of Cre-mediated removal of the endogenous gene. Puro-delta-TK serves both positive selection for puromycin resistance and negative selection by thymidine kinase expression.

These approaches can be used to ask specific questions that require removal of endogenous TIN2 expression, such as whether one specific TIN2 isoform is sufficient for telomere length maintenance, or if the TIN2 patient mutations have different effects depending on which isoform is expressed. Because TIN2 knockout is lethal, this simultaneous exchange of endogenous for the expression construct of interest will be beneficial. Technical challenges may arise, considering that the TIN2-DC mutation was lethal when homozygous (D Frescas & de Lange 2014), so both homozygous and heterozygous edits may be necessary for studying patient mutation effects.

Appendix G. Higher TERT expression in polycistronic expression cassette cannot be explained by polycistronic transcript context

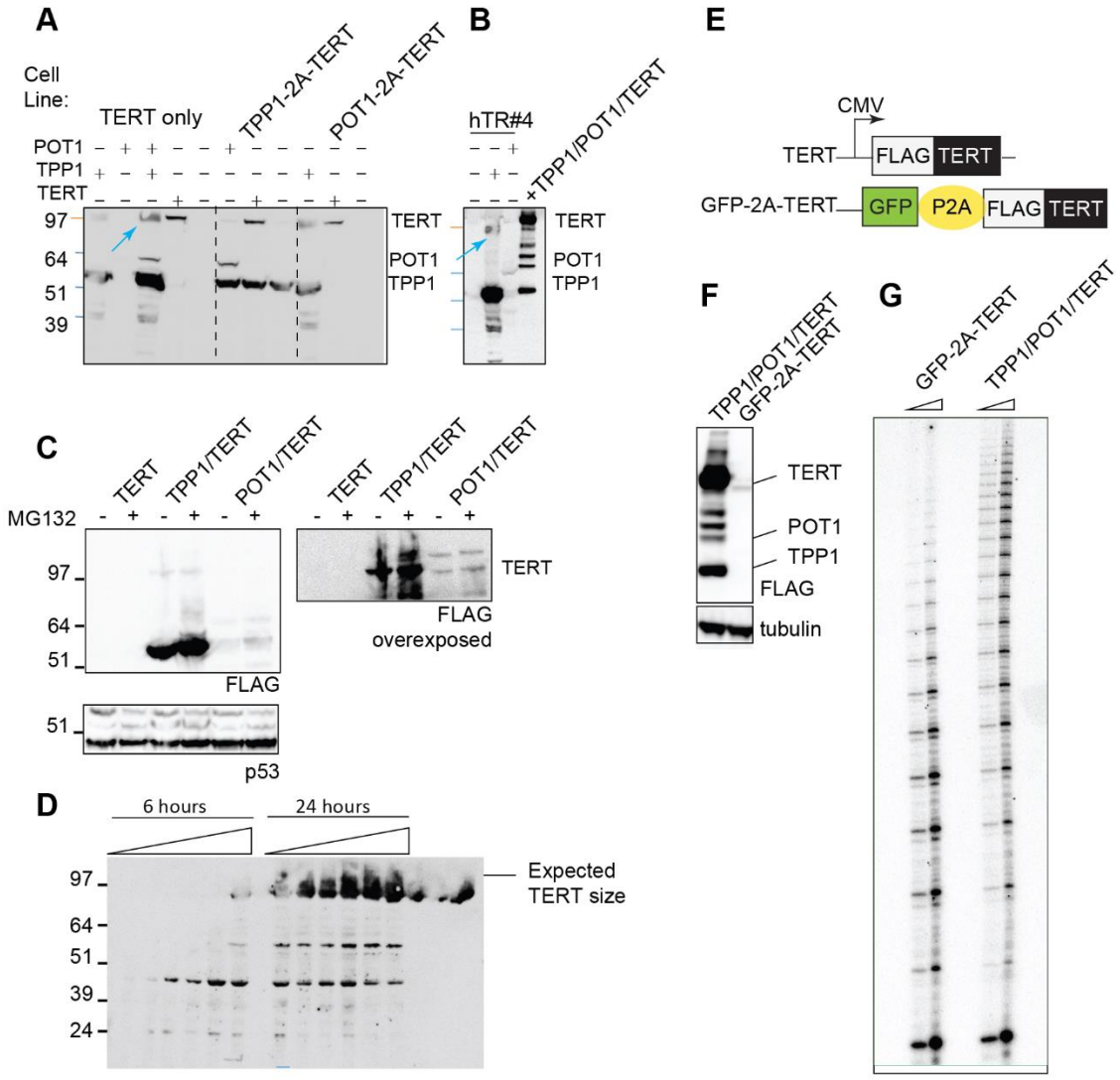

Appendix G. (**A**) We transfected TPP1 and POT1 plasmids to see if TPP1/POT1 stabilized telomerase expression. We observed a smear near the expected TERT molecular weight with TPP1 or TPP1/POT1 transfection (arrow). This band shape not match TERT expression bands observed in TERT expression (lane next to arrow). Also shown are TPP1-2a-TERT and POT1-2a-TERT cell lines, generated to test dependence of TIN2 on TPP1/POT1. (**B**) Transfection of TPP1 into hTR parent cell line with no FLAG-TERT also produces the smeary band around TERT MW observed in *A*, so we conclude that this is a background band caused by TPP1 overexpression and not stabilization of TERT. (**C**) MG132 was added to the indicated cell lines (same cell lines as in *A*) for overnight at a1:1000 dilution (10mg/ml stock). No appreciable difference between treatment was observed in the TERT cell lines. (**D**) MG132 treatment either 6 or 24 hours where indicated. Concentrations were 0-200 µM. An increase in bands was apparent at 24 hr but they did not correspond to the expected TERT size ad were also found in the no MG132 lane. P53 blot (not shown) showed no difference. Results are inconclusive. (**E**) GFP-2A-TERT construct (**F**) Polycistronic transcript does not stabilize TERT, as TERT levels are still well below those in TPP1/POT1/TERT (see alsoTPP1/TERT and POT1/TERT in *A, C*) (**G**) GFP-2A-TERT has telomerase activity. Shown are assays with 2 or 6 µl lysate.

Appendix H. Reciprocal FLAG co-immunopreciptiation of TIN2

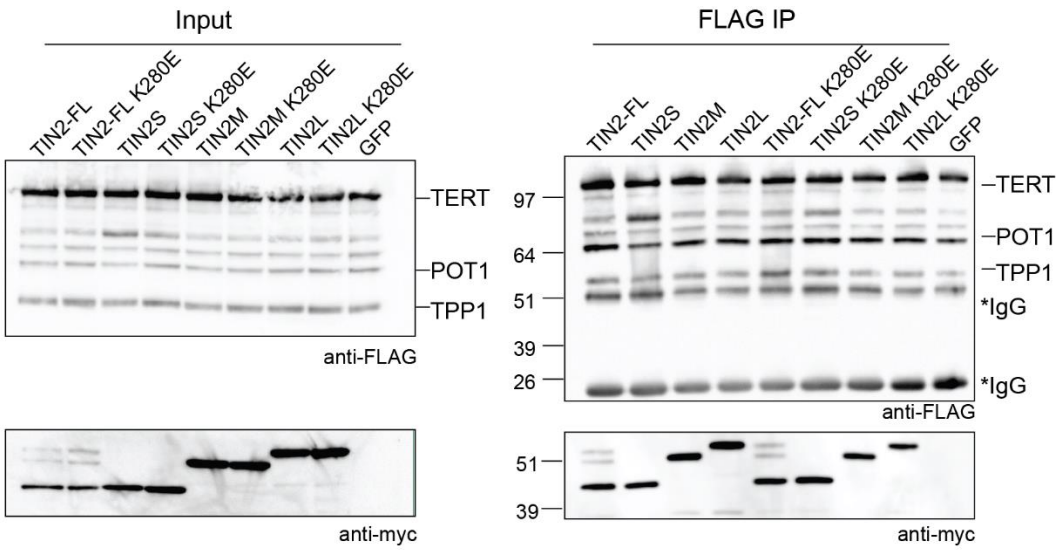

Appendix H. FLAG immunoprecipitation pulls down myc-TIN2. *Left*, input samples. *Right*, IP samples. (Note the different loading order between input and IP). Data goes with Figure 3.2.

Appendix I. C-terminally tagged TIN2S, TIN2L do not stimulate telomerase

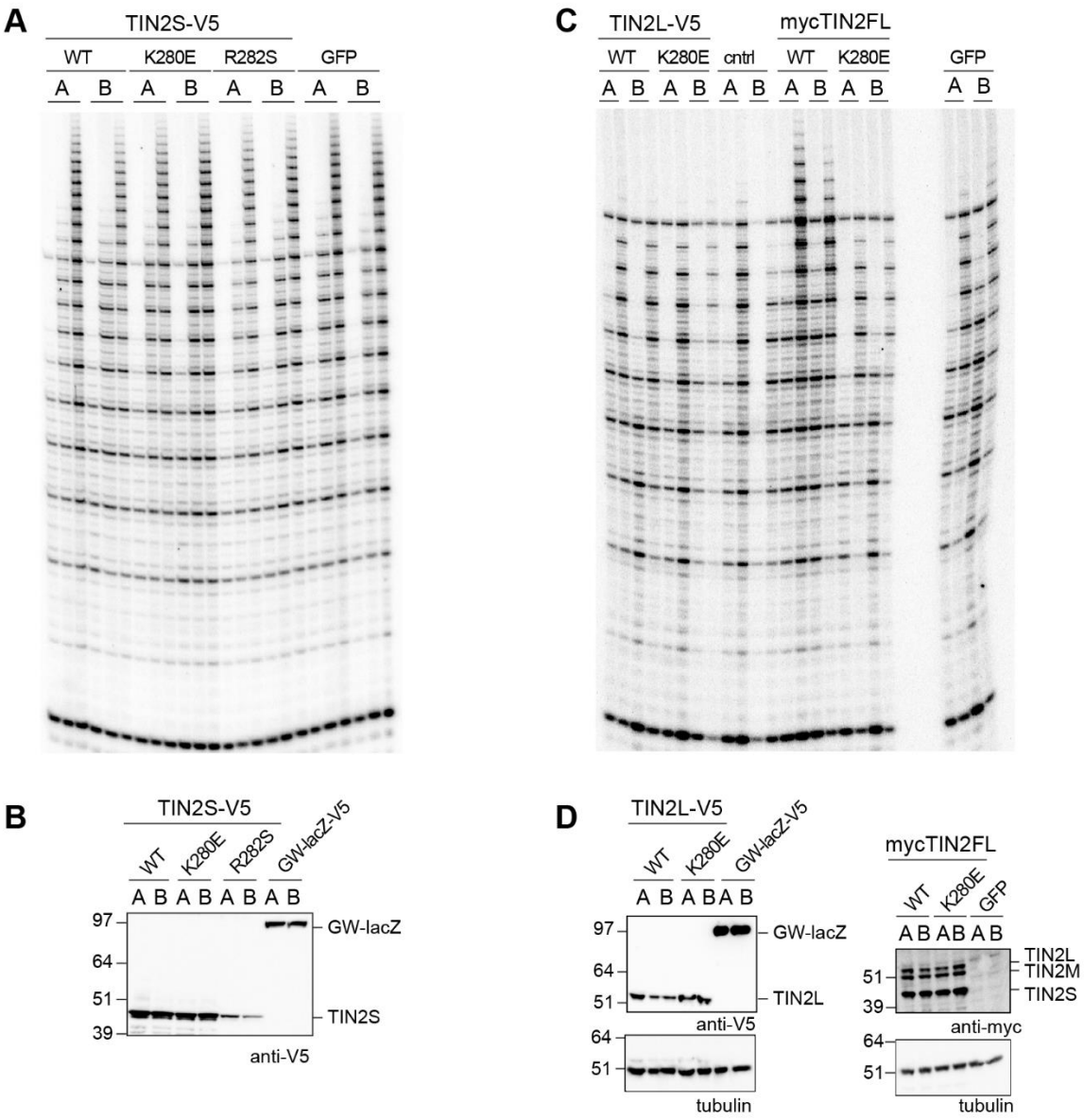

Appendix I. No observed stimulation of telomerase processivity with C-terminally tagged TIN2 constructs. (**A**) Direct telomerase assays. TIN2S-V5 WT, K280E, and R282S or GW-lacZ-V5 control were transfected into TPP1/POT1/TERT cell lines. Assays were stopped at 2.5, 5, or 10 minutes. A &B, duplicate transfections. (**B**) V5 western blots of lysates used in *A*. (**C**) Direct telomerase assays of TIN2L-V5 WT or K280E mutation, GW-lacZ-V5 and of mycTIN2-FL WT or K280E or GFP. Assays were stopped at 5 or 10 minutes. A&B, duplicate transfections (**D**) V5 and myc western blots of lysates in *C*. See also Figure 3.3.

REFERENCES

Abreu, E. et al., 2010. TIN2-tethered TPP1 recruits human telomerase to telomeres in vivo. *Molecular and Cellular Biology*, 30(12), pp.2971–2982.

Alder, J.K. et al., 2011. Ancestral mutation in telomerase causes defects in repeat addition processivity and manifests as familial pulmonary fibrosis. *PLoS Genetics*, 7(3), pp.1–9.

Alder, J.K. et al., 2015. Exome sequencing identifies mutant TINF2 in a family with pulmonary fibrosis. *Chest*, 147(5), pp.1361–1368.

Altschuler, S.E., Dickey, T.H. & Wuttke, D.S., 2011. Schizosaccharomyces pombe protection of telomeres 1 utilizes alternate binding modes to accommodate different telomeric sequences. *Biochemistry*, 50(35), pp.7503–13.

Anderson, B.H. et al., 2012. Mutations in CTC1, encoding conserved telomere maintenance component 1, cause Coats plus. *Nature Genetics*, 44(3), pp.338–342.

Anderson, E.M., Halsey, W.A. & Wuttke, D.S., 2002. Delineation of the high-affinity single-stranded telomeric DNA-binding domain of Saccharomyces cerevisiae Cdc13. *Nucleic Acids Research*, 30(19), pp.4305–13.

Aoude, L.G. et al., 2015. Nonsense mutations in the shelterin complex genes ACD and TERF2IP in familial melanoma. *Journal of the National Cancer Institute*, 107(2).

Armanios, M. et al., 2005. Haploinsufficiency of telomerase reverse transcriptase leads to anticipation in autosomal dominant dyskeratosis congenita. *Proceedings of the National Academy of Sciences*, 102(44), pp.15960–15964.

Armanios, M. & Blackburn, E.H., 2012. The telomere syndromes. *Nature Reviews Genetics*, 13(10), pp.693–704.

Armbruster, B.N. et al., 2001. N-terminal domains of the human telomerase catalytic subunit required for enzyme activity in vivo. *Molecular and cellular biology*, 21(22), pp.7775–86.

Autexier, C. & Greider, C.W., 1995. Boundary elements of the Tetrahymena telomerase RNA template and alignment domains. *Genes & Development*, 9(18), pp.2227–39.

Baumann, P. & Cech, T.R., 2001. Pot1, the Putative Telomere End-Binding Protein in Fission Yeast and Humans. *Science*, 292(5519), pp.1171–1175.

Baumann, P., Podell, E. & Cech, T.R., 2002. Human Pot1 (protection of telomeres) protein: cytolocalization, gene structure, and alternative splicing. *Molecular and Cellular Biology*, 22(22), pp.8079–87.

Bhanot, M. & Smith, S., 2012. TIN2 stability is regulated by the E3 ligase Siah2. *Molecular and Cellular Biology l*, 32(2), pp.376–384.

Bianchi, A. et al., 1999. TRF1 binds a bipartite telomeric site with extreme spatial flexibility. *EMBO J*, 18(20), pp.5735–5744.

Bianchi, A. et al., 1997. TRF1 is a dimer and bends telomeric DNA. *The EMBO Journal*, 16(7), pp.1785–1794.

Bilaud, T. et al., 1997. Telomeric localization of TRF2, a novel human telobox protein. *Nature Genetics*, 17(2), pp.236–9.

Bisht, K. et al., 2016. Structural and functional consequences of a disease mutation in the telomere protein TPP1. *Proceedings of the National Academy of Sciences*, p.201605685.

Blackburn, E.H., 1990. Telomeres and their synthesis. *Science*, 249(4968), pp.489–90.

Bochkareva, E. et al., 2002. Structure of the RPA trimerization core and its role in the multistep DNA-binding mechanism of RPA. *The EMBO Journal*, 21(7), pp.1855–1863.
Bosco, N. & de Lange, T., 2012. A TRF1-controlled common fragile site containing interstitial telomeric sequences. *Chromosoma*, 121(5), pp.465–474.
Braun, K.A. et al., 1997. Role of Protein - Protein Interactions in the Function of Replication Protein A (RPA): RPA Modulates the Activity of DNA Polymerase R by Multiple Mechanisms. *Biochemistry*, 2960(97), pp.8443–8454.
Broccoli, D. et al., 1997. Human telomeres contain two distinct Myb-related proteins, TRF1 and TRF2. *Nature Genetics*, 17(2), pp.231–235.
Budd, M.E. et al., 2006. Evidence Suggesting that Pif1 Helicase Functions in DNA Replication with the Dna2 Helicase/Nuclease and DNA Polymerase. *Molecular and Cellular Biology*, 26(7), pp.2490–2500.
Canudas, S. et al., 2011. A role for heterochromatin protein 1gamma at human telomeres. *Genes Development*, 25(17), pp.1807–1819.
Carey, B.W. et al., 2009. Reprogramming of murine and human somatic cells using a single polycistronic vector. *Proceedings of the National Academy of Sciences*, 106(1), pp.157–162.
Carneiro, M.O. et al., 2012. Pacific biosciences sequencing technology for genotyping and variation discovery in human data. *BMC Genomics*, 13(1), p.375.
Carson, M.J. & Hartwell, L., 1985. CDC17: An essential gene that prevents telomere elongation in yeast. *Cell*, 42(1), pp.249–257.
Casacuberta, E., 2017. Drosophila: Retrotransposons Making up Telomeres. *Viruses*, 9(7), p.192.
Chan, H., Wang, Y. & Feigon, J., 2017. Progress in Human and Tetrahymena Telomerase Structure. *Annual Review of Biophyiscs.* 46:199-225.
Chen, C. et al., 2017. Structural insights into POT1-TPP1 interaction and POT1 C-terminal mutations in human cancer. *Nature Communications*, 8, p.14929.
Chen, J.-L. & Greider, C.W., 2003. Determinants in mammalian telomerase RNA that mediate enzyme processivity and cross-species incompatibility. *The EMBO Journal*, 22(2), pp.304–14.
Chen, Y. et al., 2008. A shared docking motif in TRF1 and TRF2 used for differential recruitment of telomeric proteins. *Science*, 319(5866), pp.1092–1096.
Chiang, Y.J. et al., 2004. Telomere-associated protein TIN2 is essential for early embryonic development through a telomerase-independent pathway. *Molecular and Cellular Biology*, 24(15), pp.6631–6634.
Chiba, K. et al., 2017. Endogenous Telomerase Reverse Transcriptase N-Terminal Tagging Affects Human Telomerase Function at Telomeres In Vivo. *Molecular and Cellular Biology*, 37(3), pp.e00541-16.
Collins, K.L. & Kelly, T.J., 1991. Effects of T antigen and replication protein A on the initiation of DNA synthesis by DNA polymerase alpha-primase. *Molecular and Cellular Biology*, 11(4), pp.2108–15.
Counter, C.M. et al., 1998. Dissociation among in vitro telomerase activity, telomere maintenance, and cellular immortalization. *Proceedings of the National Academy of Sciences*, 95(25), pp.14723–8.

Cristofari, G. & Lingner, J., 2006. Telomere length homeostasis requires that telomerase levels are limiting. *EMBO J*, 25(3), pp.565–574.
Denchi, E.L. & de Lange, T., 2007. Protection of telomeres through independent control of ATM and ATR by TRF2 and POT1. *Nature*, 448(7157), pp.1068–1071.
Diede, S.J. & Gottschling, D.E., 1999. Telomerase-mediated telomere addition in vivo requires DNA primase and DNA polymerases alpha and delta. *Cell*, 99(7), pp.723–33.
Dornreiter, I. et al., 1992. Interaction of DNA polymerase a primase with cellular replication protein A and SV40 T antigen. *The EMBO Journal*, 11(2), pp.769–776.
Doronina, V.A. et al., 2008. Site-specific release of nascent chains from ribosomes at a sense codon. *Molecular and Cellular Biology*, 28(13), pp.4227–39.
Evans, S.K. & Lundblad, V., 1999. Est1 and Cdc13 as comediators of telomerase access. *Science*, 286(5437), pp.117–20.
Fairall, L. et al., 2001. Structure of the TRFH dimerization domain of the human telomeric proteins TRF1 and TRF2. *Molecular Cell*, 8(2), pp.351–361.
Fanning, E., Klimovich, V. & Nager, A.R., 2006. A dynamic model for replication protein A (RPA) function in DNA processing pathways. *Nucleic Acids Research*, 34(15), pp.4126–37.
Frank, A.K. et al., 2015. The Shelterin TIN2 Subunit Mediates Recruitment of Telomerase to Telomeres. *PLoS Genetics*, 11(7), pp.1–19.
Frescas, D. & de Lange, T., 2014. A TIN2 dyskeratosis congenita mutation causes telomerase-independent telomere shortening in mice. *Genes & Development*, 28(2), pp.153–166.
Frescas, D. & de Lange, T., 2014a. TRF2-tethered TIN2 can mediate telomere protection by TPP1/POT1. *Molecular and Cellular Biology*, 34(7), pp.1349–1362.
Frescas, D. & De Lange, T., 2014. Binding of TPP1 protein to TIN2 protein is required for POT1a,b protein-mediated telomere protection. *Journal of Biological Chemistry*, 289(35), pp.24180–24187.
Frohman, M.A., 1993. Rapid amplification of complementary DNA ends for generation of full-length complementary DNAs: Thermal race. *Methods in* Enzymology. 218, pp.340–356.
Frohman, M.A., Dush, M.K. & Martin, G.R., 1988. Rapid production of full-length cDNAs from rare transcripts: amplification using a single gene-specific oligonucleotide primer. *Proceedings of the National Academy of Sciences*, 85(23), pp.8998–9002.
Gao, H. et al., 2007. RPA-like proteins mediate yeast telomere function. *Nature Structural & Molecular Biology*, 14(3), pp.208–214.
Gillis, A.J., Schuller, A.P. & Skordalakes, E., 2008. Structure of the Tribolium castaneum telomerase catalytic subunit TERT. *Nature*, 455(7213), pp.633–637.
Gordon, S.P. et al., 2015. Widespread Polycistronic Transcripts in Fungi Revealed by Single-Molecule mRNA Sequencing. D. Zheng, ed. *PloS one*, 10(7), p.e0132628.
Goulian, M. & Heard, C.J., 1990. The mechanism of action of an accessory protein for DNA polymerase alpha/primase. *Journal of Biological Chemistry*, 265(22), pp.13231–13239.

Goulian, M., Heard, C.J. & Grimm, S.L., 1990. Purification and Properties of an Accessory Protein for DNA Polymerase a/Primase. *Journal of Biological Chemistry*, 265(22), pp.13221–13230.
Gramatges, M.M. et al., 2013. A homozygous telomerase T-motif variant resulting in markedly reduced repeat addition processivity in siblings with Hoyeraal Hreidarsson syndrome. *Blood*, 121(18), pp.3586–3593.
Greider, C.W., 2016. Regulating telomere length from the inside out: the replication fork model. *Genes & Development*, 30(13), pp.1483–91.
Greider, C.W., 1991. Telomerase is processive. *Molecular and Cellular Biology*, 11(9), pp.4572–80.
Greider, C.W. & Blackburn, E.H., 1989. A telomeric sequence in the RNA of Tetrahymena telomerase required for telomere repeat synthesis. *Nature*, 337(6205), pp.331–337.
Greider, C.W. & Blackburn, E.H., 1985. Identification of a specific telomere terminal transferase activity in Tetrahymena extracts. *Cell*, 43(2 Pt 1), pp.405–13.
Grossi, S. et al., 2004. Pol12, the B subunit of DNA polymerase alpha, functions in both telomere capping and length regulation. *Genes and Development*, 18(9), pp.992–1006.
Gu, P. & Chang, S., 2013. Functional characterization of human CTC1 mutations reveals novel mechanisms responsible for the pathogenesis of the telomere disease Coats plus. *Aging Cell*, 12(6), pp.1100–1109.
Guo, Y. et al., 2014. Inherited bone marrow failure associated with germline mutation of ACD, the gene encoding telomere protein TPP1. *Blood*, 124(18), pp.2767–74.
Han, Y. et al., 1999. Interactions of the Papovavirus DNA Replication Initiator Proteins , Bovine Papillomavirus Type 1 E1 and Simian Virus 40 Large T Antigen with Human Replication Protein A. *Journal of Virology*, 73(6), pp.4899–4907.
Hao, L.-Y. et al., 2005. Short telomeres, even in the presence of telomerase, limit tissue renewal capacity. *Cell*, 123(6), pp.1121–31.
Harley, C.B., Futcher, A.B. & Greider, C.W., 1990. Telomeres shorten during ageing of human fibroblasts. *Nature*, 345(6274), pp.458–460.
Hemann, M.T. et al., 2001. The shortest telomere, not average telomere length, is critical for cell viability and chromosome stability. *Cell*, 107(1), pp.67–77.
Henderson, E.R. & Blackburn, E.H., 1989. An overhanging 3' terminus is a conserved feature of telomeres. *Molecular and Cellular Biology*, 9(1), pp.345–8.
Hicks, B.B. et al., 2003. Sensing DNA Damage Through ATRIP Recognition of RPA-ssDNA. , 300(June), pp.1542–1549.
Hockemeyer, D. et al., 2005. POT1 protects telomeres from a transient DNA damage response and determines how human chromosomes end. *EMBO J*, 24(14), pp.2667–2678.
Hockemeyer, D. et al., 2006. Recent expansion of the telomeric complex in rodents: Two distinct POT1 proteins protect mouse telomeres. *Cell*, 126(1), pp.63–77.
Hong, K. et al., 2013. Tetrahymena telomerase holoenzyme assembly, activation, and inhibition by domains of the p50 central hub. *Molecular and Cellular Biology*, 33(19), pp.3962–71.

Houghtaling, B.R. et al., 2004. A dynamic molecular link between the telomere length regulator TRF1 and the chromosome end protector TRF2. *Current Biology*, 14(18), pp.1621–1631.
Hughes, T.R. et al., 2000. Identification of the single-strand telomeric DNA binding domain of the Saccharomyces cerevisiae Cdc13 protein. *Proceedings of the National Academy of Sciences*, 97(12), pp.6457–62.
IJpma, A.S. & Greider, C.W., 2003. Short telomeres induce a DNA damage response in Saccharomyces cerevisiae. *Molecular Biology of the Cell*, 14(3), pp.987–1001.
Ishdorj, G. et al., 2017. A novel spliced variant of the TIN2 shelterin is present in chronic lymphocytic leukemia. *Leukemia Research*, 59(March), pp.66–74.
Jacob, N.K. et al., 2007. Tetrahymena POT1a regulates telomere length and prevents activation of a cell cycle checkpoint. *Molecular and Cellular Biology*, 27(5), pp.1592–601.
Jacob, N.K., Skopp, R. & Price, C.M., 2001. G-overhang dynamics at Tetrahymena telomeres. *The EMBO Journal*, 20(15), pp.4299–4308.
Jiang, J. et al., 2015. Structure of Tetrahymena telomerase reveals previously unknown subunits, functions, and interactions. *Science*, 350(6260).
Jinek, M. et al., 2012. A programmable dual-RNA-guided DNA endonuclease in adaptive bacterial immunity. *Science*, 337(6096), pp.816–821.
Jinek, M. et al., 2013. RNA-programmed genome editing in human cells. *Elife*, 2, p.e00471.
Kabir, S., Hockemeyer, D. & de Lange, T., 2014. TALEN gene knockouts reveal no requirement for the conserved human shelterin protein Rap1 in telomere protection and length regulation. *Cell Reports*, 9(4), pp.1273–1280.
Kaminker, P.G. et al., 2009. A novel form of the telomere-associated protein TIN2 localizes to the nuclear matrix. *Cell Cycle*, 8(6), pp.931–939.
Karlseder, J. et al., 1999. p53- and ATM-dependent apoptosis induced by telomeres lacking TRF2. *Science*, 283(5406), pp.1321–1325.
Karlseder, J. et al., 2004. The telomeric protein TRF2 binds the ATM kinase and can inhibit the ATM-dependent DNA damage response. *PLoS Biology*, 2(8), p.E240.
Keller, R.B. et al., 2012. CTC1 Mutations in a patient with dyskeratosis congenita. *Pediatric Blood & Cancer*, 59(2), pp.311–314.
Kim, C., Paulus, B.F. & Wold, M.S., 1994. Interactions of human replication protein A with oligonucleotides. *Biochemistry*, 33(47), pp.14197–14206.
Kim, D., Langmead, B. & Salzberg, S.L., 2015. HISAT: a fast spliced aligner with low memory requirements. *Nature Methods*, 12(4), pp.357–360.
Kim, H. et al., 2017. Systematic analysis of human telomeric dysfunction using inducible telosome/shelterin CRISPR/Cas9 knockout cells. *Cell Discovery*, 3, p.17034.
Kim, N.W. et al., 1994. Specific association of human telomerase activity with immortal cells and cancer. *Science.* 266(5193), pp.2011–5.
Kim, S.H. et al., 2003. Mus musculus and Mus spretus homologues of the human telomere-associated protein TIN2. *Genomics*, 81(4), pp.422–432.
Kim, S.H. et al., 2008. Telomere dysfunction and cell survival: Roles for distinct TIN2-containing complexes. *Journal of Cell Biology*, 181(3), pp.447–460.
Kim, S.H. et al., 2004. TIN2 mediates functions of TRF2 at human telomeres. *Journal of Biological Chemistry*, 279(42), pp.43799–43804.

Kim, S.H., Kaminker, P. & Campisi, J., 1999. TIN2, a new regulator of telomere length in human cells. *Nat Genet*, 23(4), pp.405–412.
Kirsch, R.D. & Joly, E., 1998. An improved PCR-mutagenesis strategy for two-site mutagenesis or sequence swapping between related genes. *Nucleic Acids Research*, 26(7), pp.1848–50.
Kocak, H. et al., 2014. Hoyeraal-Hreidarsson syndrome caused by a germline mutation in the TEL patch of the telomere protein TPP1. *Genes & Development*, 28(19), pp.2090–102.
Latrick, C.M. & Cech, T.R., 2010. POT1-TPP1 enhances telomerase processivity by slowing primer dissociation and aiding translocation. *The EMBO Journal*, 29(5), pp.924–33.
Lee, S.S. et al., 2015. ATM Kinase Is Required for Telomere Elongation in Mouse and Human Cells. *Cell Reports*, 13(8), pp.1623–1632.
Lei, M. et al., 2005. Switching human telomerase on and off with hPOT1 protein in vitro. *The Journal of Biological Chemistry*, 280(21), pp.20449–56.
Lei, M., Podell, E.R. & Cech, T.R., 2004. Structure of human POT1 bound to telomeric single-stranded DNA provides a model for chromosome end-protection. *Nature Structural & Molecular Biology*, 11(12), pp.1223–9.
Lewis, K.A. et al., 2014. The tenacious recognition of yeast telomere sequence by Cdc13 is fully exerted by a single OB-fold domain. *Nucleic Acids Research*, 42(1), pp.475–484.
Li, B. & de Lange, T., 2003. Rap1 affects the length and heterogeneity of human telomeres. *Molecular Biology of the Cell*, 14(12), pp.5060–5068.
Li, B., Oestreich, S. & de Lange, T., 2000. Identification of human Rap1: implications for telomere evolution. *Cell*, 101(5), pp.471–483.
Linger, B.R., Morin, G.B. & Price, C.M., 2011. The Pot1a-associated proteins Tpt1 and Pat1 coordinate telomere protection and length regulation in Tetrahymena. *Molecular Biology of the Cell*, 22(21).
Liu, D., Safari, A., et al., 2004. PTOP interacts with POT1 and regulates its localization to telomeres. *Nature Cell Biology*, 6(7), pp.673–680.
Liu, D., O'Connor, M.S., et al., 2004. Telosome, a mammalian telomere-associated complex formed by multiple telomeric proteins. *Journal of Biological Chemistry*, 279(49), pp.51338–51342.
Loayza, D. et al., 2004. DNA binding features of human POT1: a nonamer 5'-TAGGGTTAG-3' minimal binding site, sequence specificity, and internal binding to multimeric sites. *Journal of Biological Chemistry*, 279(13), pp.13241–13248.
Loayza, D. & de Lange, T., 2003. POT1 as a terminal transducer of TRF1 telomere length control. *Nature*, 423(6943), pp.1013–1018.
Makarov, V.L., Hirose, Y. & Langmore, J.P., 1997. Long G tails at both ends of human chromosomes suggest a C strand degradation mechanism for telomere shortening. *Cell*, 88(5), pp.657–66.
Mason, M., Wanat, J.J., et al., 2013. Cdc13 OB2 Dimerization Required for Productive Stn1 Binding and Efficient Telomere Maintenance. *Structure*, 21(1), pp.109–120.
McClintock, B., 1941. The Stability of Broken Ends of Chromosomes in Zea Mays. *Genetics*, 26(2), pp.234–82.

Melendy, T. & Stillman, B., 1993. An interaction between replication protein A and SV40 T antigen appears essential for primosome assembly during SV40 DNA replication. *The Journal of Biological Chemistry*, 268(5), pp.3389–95.
Mer, G. et al., 2000. Structural Basis for the Recognition of DNA Repair Proteins UNG2, XPA, and RAD52 by Replication Factor RPA. *Cell*. 103(3), pp.449–456.
Michel, A.M. et al., 2014. GWIPS-viz: development of a ribo-seq genome browser. *Nucleic Acids Research*, 42(D1), pp.D859–D864.
Miller, K.M., Rog, O. & Cooper, J.P., 2006. Semi-conservative DNA replication through telomeres requires Taz1. *Nature*, 440(7085), pp.824–828.
Min, B. & Collins, K., 2009. An RPA-Related Sequence-Specific DNA-Binding Subunit of Telomerase Holoenzyme Is Required for Elongation Processivity and Telomere Maintenance. *Molecular Cell*, 36(4), pp.609–619.
Mitton-Fry, R.M. et al., 2004. Structural Basis for Telomeric Single-stranded DNA Recognition by Yeast Cdc13. *Journal of Molecular Biology*, 338(2), pp.241–255.
Muller, H.J., 1938. The remaking of chromosomes. *Collecting Net*, 13, pp.181–198.
Nandakumar, J. et al., 2012. The TEL patch of telomere protein TPP1 mediates telomerase recruitment and processivity. *Nature*, 492(7428), pp.285–289.
Nelson, N.D. & Bertuch, A.A., 2012. Dyskeratosis congenita as a disorder of telomere maintenance. *Mutation Research*, 730(1–2), pp.43–51.
Norio, P. & Schildkraut, C.L., 2001. Visualization of DNA Replication on Individual Epstein-Barr Virus Episomes. *Science*, 294(5550), pp.2361–2364.
O'Connor, M.S. et al., 2006. A critical role for TPP1 and TIN2 interaction in high-order telomeric complex assembly. *Proceedings of the National Academy of Science*, 103(32), pp.11874–11879.
Olovnikov, A.M., 1973. A theory of marginotomy: The incomplete copying of template margin in enzymic synthesis of polynucleotides and biological significance of the phenomenon. *Journal of Theoretical Biology*, 41(1), pp.181–190.
Pacific Biosciences, 2015. Human MCF-7 Transcriptome. Available at: http://www.pacb.com/blog/data-release-human-mcf-7-transcriptome/ [Accessed January 1, 2017].
Palm, W. & de Lange, T., 2008. How Shelterin Protects Mammalian Telomeres. *Annual Review of Genetics*, 42(1), pp.301–334.
Pan, Q. et al., 2008. Deep surveying of alternative splicing complexity in the human transcriptome by high-throughput sequencing. *Nature Genetics*, 40(12), pp.1413–1415.
Parenteau, J. & Wellinger, R.J., 1999. Accumulation of single-stranded DNA and destabilization of telomeric repeats in yeast mutant strains carrying a deletion of RAD27. *Molecular and Cellular Biology*, 19(6), pp.4143–52.
Pertea, M. et al., 2015. StringTie enables improved reconstruction of a transcriptome from RNA-seq reads. *Nature Biotechnology*, 33(3), pp.290–295.
Pertea, M. et al., 2016. Transcript-level expression analysis of RNA-seq experiments with HISAT, StringTie and Ballgown. *Nature Protocols*, 11(9), pp.1650–1667.
Pinzaru, A.M. et al., 2016. Telomere Replication Stress Induced by POT1 Inactivation Accelerates Tumorigenesis. *Cell Reports*, 15(10), pp.2170–2184.

Prakash, A. & Borgstahl, G.E.O., 2012. The Structure and Function of Replication Protein A in DNA Replication. *The Eukaryotic Replisome: A Guide to Protein Structure and Function*, pp.171–196.
Premkumar, V.L. et al., 2014. The 3' overhangs at Tetrahymena thermophila telomeres are packaged by four proteins, Pot1a, Tpt1, Pat1, and Pat2. *Eukaryotic Cell*, 13(2), pp.240–5.
Price, C.M. et al., 2010. Evolution of CST function in telomere maintenance. *Cell Cycle* 9(16), pp.3157–3165.
Qi, H. & Zakian, V.A., 2000. The Saccharomyces telomere-binding protein Cdc13p interacts with both the catalytic subunit of DNA polymerase alpha and the telomerase-associated Est1 protein. *Genes and Development*, 14(14), pp.1777–1788.
Ran, F.A. et al., 2013. Genome engineering using the CRISPR-Cas9 system. *Nature Protocols*, 8(11), pp.2281–2308.
Rice, C. et al., 2017. Structural and functional analysis of the human POT1-TPP1 telomeric complex. *Nature Communications*, 8, p.14928.
Rice, C. & Skordalakes, E., 2016. Structure and function of the telomeric CST complex. *Computational and structural biotechnology journal*, 14, pp.161–7.
Robinson, J.T. et al., 2011. Integrative genomics viewer. *Nature Biotechnology*, 29(1), pp.24–26.
Robles-Espinoza, C.D. et al., 2014. POT1 loss-of-function variants predispose to familial melanoma. *Nature Genetics*, 46(5), pp.478–481.
Roth, M. & Prescott, D.M., 1985. DNA intermediates and telomere addition during genome reorganization in Euplotes crassus. *Cell*, 41(2), pp.411–7.
Ryan, M. & Drew, J., 1994. Foot-and-mouth disease virus 2A oligopeptide mediated cleavage of an artificial polyprotein. *The EMBO journal*.
Ryan, M.D., King, A.M. & Thomas, G.P., 1991. Cleavage of foot-and-mouth disease virus polyprotein is mediated by residues located within a 19 amino acid sequence. *The Journal of General Virology*, 72(11), pp.2727–32.
Sanger, F. & Coulson, A.R., 1975. A rapid method for determining sequences in DNA by primed synthesis with DNA polymerase. *Journal of Molecular Biology*, 94(3), pp.441–8.
Sarkar, G. & Sommer, S.S., 1990. The "megaprimer" method of site-directed mutagenesis. *BioTechniques*, 8(4), pp.404–7.
Sasa, G.S. et al., 2012. Three novel truncating TINF2 mutations causing severe dyskeratosis congenita in early childhood. *Clinical Genetics*, 81(5), pp.470–478.
Savage, S.A. et al., 2008. TINF2, a component of the shelterin telomere protection complex, is mutated in dyskeratosis congenita. *Am J Hum Genet*, 82(2), pp.501–509.
Savage, S.A. & Bertuch, A.A., 2010. The genetics and clinical manifestations of telomere biology disorders. *Genet Med*, 12(12), pp.753–764.
Schmidt, J.C., Dalby, A.B. & Cech, T.R., 2014. Identification of human TERT elements necessary for telomerase recruitment to telomeres. *eLife*, 3.
Scotto–Lavino, E., Du, G. & Frohman, M.A., 2007. 3′ End cDNA amplification using classic RACE. *Nature Protocols*, 1(6), pp.2742–2745.
Sexton, A.N. et al., 2014. Genetic and molecular identification of three human TPP1 functions in telomerase action: recruitment, activation, and homeostasis set point regulation. *Genes and Development*, 28(17), pp.1885–1899.

Sexton, A.N., Youmans, D.T. & Collins, K., 2012. Specificity requirements for human telomere protein interaction with telomerase holoenzyme. *Journal of Biological Chemistry*, 287(41), pp.34455–34464.
Sfeir, A. et al., 2009. Mammalian telomeres resemble fragile sites and require TRF1 for efficient replication. *Cell*, 138(1), pp.90–103.
Shi, J. et al., 2014. Rare missense variants in POT1 predispose to familial cutaneous malignant melanoma. *Nature Genetics*, 46(5), pp.482–6.
Simon, A.J. et al., 2016. Mutations in STN1 cause Coats plus syndrome and are associated with genomic and telomere defects. *The Journal of Experimental Medicine*, 213(8), pp.1429–1440.
Simossis, V.A. & Heringa, J., 2005. PRALINE: a multiple sequence alignment toolbox that integrates homology-extended and secondary structure information. *Nucleic Acids Research*, 33(Web Server), pp.W289–W294.
Simossis, V.A. & Heringa, J., 2003. The PRALINE online server: optimising progressive multiple alignment on the web. *Computational Biology and Chemistry*, 27(4–5), pp.511–9.
Smogorzewska, A. et al., 2000. Control of Human Telomere Length by TRF1 and TRF2. *Molecular and Cellular Biology*, 20(5), pp.1659–1668.
Stanley, S.E. & Armanios, M., 2015. The short and long telomere syndromes: paired paradigms for molecular medicine. *Current Opinion in Genetics & Development*, 33, pp.1–9.
van Steensel, B. & de Lange, T., 1997. Control of telomere length by the human telomeric protein TRF1. *Nature*, 385(6618), pp.740–743.
Steijger, T. et al., 2013. Assessment of transcript reconstruction methods for RNA-seq. *Nature Methods*, 10(12), pp.1177–1184.
Stewart, J.A. et al., 2012. Human CST promotes telomere duplex replication and general replication restart after fork stalling. *The EMBO Journal*, 31(17), pp.3537–3549.
Sun, D. et al., 1999. Regulation of Catalytic Activity and Processivity of Human Telomerase. *Biochemistry*, 38(13), pp.4037–4044.
Sun, J. et al., 2009. Stn1-Ten1 is an Rpa2-Rpa3-like complex at telomeres. *Genes & Development*, 23(24), pp.2900–14.
Sun, J. et al., 2011. Structural bases of dimerization of yeast telomere protein Cdc13 and its interaction with the catalytic subunit of DNA polymerase α. *Cell Research*, 21(2), pp.258–274.
Szymczak, A.L. et al., 2004. Correction of multi-gene deficiency in vivo using a single "self-cleaving" 2A peptide–based retroviral vector. *Nature Biotechnology*, 22(5), pp.589–594.
Takai, H. et al., 2016. A POT1 mutation implicates defective telomere end fill-in and telomere truncations in Coats plus. *Genes and Development*, 30(7), pp.812–826.
Takai, K.K. et al., 2011. Telomere protection by TPP1/POT1 requires tethering to TIN2. *Molecular Cell*, 44(4), pp.647–659.
Thorvaldsdottir, H., Robinson, J.T. & Mesirov, J.P., 2013. Integrative Genomics Viewer (IGV): high-performance genomics data visualization and exploration. *Briefings in Bioinformatics*, 14(2), pp.178–192.
Toledo, F. et al., 2006. RMCE-ASAP: a gene targeting method for ES and somatic cells to accelerate phenotype analyses. *Nucleic Acids Research*, 34(13), p.e92.

Tong, A.S. et al., 2015. ATM and ATR Signaling Regulate the Recruitment of Human Telomerase to Telomeres. *Cell Reports*, 13(8), pp.1633–1646.
Trigueros-Motos, L., 2014. Mutations in POT1 predispose to familial cutaneous malignant melanoma. *Clinical Genetics*, 86(3), pp.217–8.
Tsurimoto, T. & Stillman, B., 1989. Multiple replication factors augment DNA synthesis by the two eukaryotic DNA polymerases, a and d. *The EMBO Journal*, 8(1), pp.3883–3889.
Upton, H.E. et al., 2017. Shared Subunits of Tetrahymena Telomerase Holoenzyme and Replication Protein A Have Different Functions in Different Cellular Complexes. *Journal of Biological Chemistry*, 292(1), pp.217–228.
Veldman, T., Etheridge, K.T. & Counter, C.M., 2004. Loss of hPot1 Function Leads to Telomere Instability and a cut-like Phenotype. *Current Biology*, 14(24), pp.2264–2270.
Vogan, J.M. & Collins, K., 2015. Dynamics of human telomerase holoenzyme assembly and subunit exchange across the cell cycle. *Journal of Biological Chemistry*, 290(35), pp.21320–21335.
Walne, A.J. et al., 2008. TINF2 mutations result in very short telomeres: analysis of a large cohort of patients with dyskeratosis congenita and related bone marrow failure syndromes. *Blood*, 112(9), pp.3594–3600.
Wan, B. et al., 2015. The Tetrahymena telomerase p75–p45–p19 subcomplex is a unique CST complex. *Nature Structural & Molecular Biology*, 22(12), pp.1023–1026.
Wan, M. et al., 2009. OB fold-containing protein 1 (OBFC1), a human homolog of yeast Stn1, associates with TPP1 and is implicated in telomere length regulation. *Journal of Biological Chemistry*, 284(39), pp.26725–26731.
Wang, F. et al., 2007. The POT1-TPP1 telomere complex is a telomerase processivity factor. *Nature*, 445(7127), pp.506–10.
Wang, F., Stewart, J. & Price, C.M., 2014. Human CST abundance determines recovery from diverse forms of DNA damage and replication stress. *Cell Cycle*, 13(22), pp.3488–3498.
Watson, J.D., 1972. Origin of Concatemeric T7DNA. *Nature New Biology*, 239(94), pp.197–201.
Wellinger, R.J., Wolf, A.J. & Zakian, V.A., 1993. Origin activation and formation of single-strand TG1-3 tails occur sequentially in late S phase on a yeast linear plasmid. *Molecular and Cellular Biology*, 13(7), pp.4057–65.
Witkin, K.L. & Collins, K., 2004. Holoenzyme proteins required for the physiological assembly and activity of telomerase. *Genes & Development*, 18(10), pp.1107–18.
Witkin, K.L., Prathapam, R. & Collins, K., 2007. Positive and negative regulation of Tetrahymena telomerase holoenzyme. *Molecular and Cellular Biology*, 27(6), pp.2074–83.
Wold, M.S. et al., 1989. Identification of cellular proteins required for simian virus 40 DNA replication. *The Journal of Biological Chemistry*, 264(5), pp.2801–9.
Wold, M.S., 1997. REPLICATION PROTEIN A : A Heterotrimeric, Single-Stranded DNA-Binding Protein Required for Eukaryotic DNA Metabolism. *Annual Review of Biochemistry*, 66, pp.61–92.

Wold, M.S., Li, J.J. & Kelly, T.J., 1987. Initiation of simian virus 40 DNA replication in vitro: large-tumor-antigen- and origin-dependent unwinding of the template. *Proceedings of the National Academy of Sciences*, 84(11), pp.3643–7.

Xi, L. & Cech, T.R., 2014. Inventory of telomerase components in human cells reveals multiple subpopulations of hTR and hTERT. *Nucleic Acids Research*, 42(13), pp.8565–8577.

Xin, H. et al., 2007. TPP1 is a homologue of ciliate TEBP-beta and interacts with POT1 to recruit telomerase. *Nature*, 445(7127), pp.559–562.

Xin, Z.T. & Ly, H., 2012. Characterization of interactions between naturally mutated forms of the TIN2 protein and its known protein partners of the shelterin complex. *Clinical Genetics*, 81(3), pp.301–302.

Yang, D. et al., 2011. TIN2 protein dyskeratosis congenita missense mutants are defective in association with telomerase. *Journal of Biological Chemistry*, 286(26), pp.23022–23030.

Yang, S. & Counter, C.M., 2013. Cell cycle regulated phosphorylation of the telomere-associated protein TIN2. *PLoS One*, 8(8), p.e71697.

Ye, J.Z., Hockemeyer, D., et al., 2004. POT1-interacting protein PIP1: a telomere length regulator that recruits POT1 to the TIN2/TRF1 complex. *Genes & Development*, 18(14), pp.1649–1654.

Ye, J.Z., Donigian, J.R., et al., 2004. TIN2 binds TRF1 and TRF2 simultaneously and stabilizes the TRF2 complex on telomeres. *Journal of Biological Chemistry*, 279(45), pp.47264–47271.

Ye, J.Z. & de Lange, T., 2004. TIN2 is a tankyrase 1 PARP modulator in the TRF1 telomere length control complex. *Nature Genetics*, 36(6), pp.618–623.

Zeng, Z. et al., 2011. Structural basis for Tetrahymena telomerase processivity factor Teb1 binding to single-stranded telomeric-repeat DNA. *Proceedings of the National Academy of Sciences*, 108(51), pp.20357–61.

Zhang, Y. et al., 2013. Phosphorylation of TPP1 regulates cell cycle-dependent telomerase recruitment. *Proceedings of the National Academy of Sciences*, 110(14), pp.5457–62.

Zhong, F.L. et al., 2012. TPP1 OB-fold domain controls telomere maintenance by recruiting telomerase to chromosome ends. *Cell*, 150(3), pp.481–494.

Zhong, Z. et al., 1992. A mammalian factor that binds telomeric TTAGGG repeats in vitro. *Molecular Cell Biology*, 12(11), pp.4834–4843.

CURRICULUM VITAE

Alexandra Joanna Mims Pike

Biographical Information

Alexandra was born in 1989 in Memphis, TN where she attended St. Mary's Episcopal School. She moved to Bloomington, IN 2007 for her undergraduate studies, where she began research with Dr. Martha Oakley. She went on to pursue her doctorate at Johns Hopkins University after graduating from IU in 2011 with honors.

Educational History

2017	Ph.D. expected	Program in Cellular and Molecular Medicine Mentor: Dr. Carol Greider, PhD	Johns Hopkins University School of Medicine
2011	B.S.	Biochemistry Minor: Biology, Studio Art	Indiana University

Other Professional Experience

2012	Research Rotation	Lab of Dr. Fred Bunz, Johns Hopkins
2012	Research Rotation	Lab of Dr. Andrew Feinberg, Johns Hopkins
2009-2011	Undergraduate Research	Lab of Dr. Martha Oakley, Indiana University

Scholarships, Fellowships or other external funding

2016-present Turock Scholar - Stipend support for graduate research students in the Institute for Basic Biomedical Sciences (IBBS)

Honors and Awards

2017	Student Group Leader of the Year	Johns Hopkins Graduate Student Association
2017	Above and Beyond Award	Johns Hopkins Office of Sustainability
2014	Spider Plant Award	Johns Hopkins Office of Sustainbility
2012	Pollard Scholar for Genetics	Johns Hopkins Cellular & Molecular Medicine
2011	Phi Beta Kappa, Elected member	Indiana University
2011	Merck Index Award	Indiana University Department of Chemistry
2010	Harry G. Day Summer Scholarship	Indiana University Department of Chemistry
2010	Summer Research Grant	Indiana University Hutton Honors College

Publications

Pike, A.M., Strong, M.A., Ouyang, J.P., Connelly, C.J., Greider, C.W. TIN2 has multiple expressed isoforms that differentially affect telomere length. *In preparation*.

Pike, A.M., Greider, C.W. TIN2 cooperates with TPP1/POT1 to stimulate telomerase processivity. *In preparation.*

Wang, S., **Pike, A.M**., Lee, S.S., Strong, M.A., Connelly, C. J., Greider, C.W. (2017) BRD4 inhibitors block telomere elongation. *Nucleic Acids Res*. 45(14):8403-8410.

Lee, S.L., Bohrson, C., **Pike, A.M.,** Wheelan, S.J., and Greider, C.W. (2015) ATM kinase is required for telomere elongation in mouse and human cells. *Cell Rep*. 3(8):1623-1632.

Waldman, V. M., Stanage, T. H., **Mims, A.,** Norden, I. S. and Oakley, M. G. (2015) Structural mapping of the coiled-coil domain of a bacterial condensin and comparative analyses across all domains of life suggest conserved features of SMC proteins. *Proteins*. 83:1027–1045.

Harris, D. R., **Mims, A.,** and Bunz, F. (2012) Genetic disruption of USP9X sensitizes colorectal cancer cells to 5-fluorouracil. *Cancer Biol Ther*. 13(13):1319-1324.

Posters and Presentations

Pike,A. M., Strong, M.A., Glustrom, L.W., Wuttke, D.S, and Greider, C.W. Characterization of multiple TIN2 isoforms and their effect on telomerase activity. Nucleic Acids Gordon Conference, Biddeford, ME. 4-8 June 2017 *(Poster)*

Pike,A. M., Strong, M.A., Glustrom, L.W., Wuttke, D.S, and Greider, C.W. Characterization of multiple TIN2 isoforms and their effect on telomerase activity. Telomeres and Telomerase meeting at Cold Spring Harbor Laboratory, Cold Spring Harbor, NY. 2-6 May 2017 *(Talk)*

Mims, A. and C.W. Greider. Testing the Role of TIN2 in Telomerase Activity and Processivity. Telomeres and Telomerase meeting at Cold Spring Harbor Laboratory, Cold Spring Harbor, NY. 28 April-2May 2015 *(Poster)*

Service and Leadership

2011-present	Hopkins Leadership Initiative for the Environment President, 2015-2017 Secretary, 2014-2015 Member, 2011-present
2012-present	Baltimore Washington Eagles Australian Rules Football Club, 501(c)(3) Secretary, 2014-present Member, 2012-present